

Table of Contents

Part I GFAS	4
Part II Contents	5
Part III Introduction	7
1 Overview	7
2 Analysis capabilities	9
Part IV Mesh generation	10
1 Introduction	10
2 Structured mesh generation	12
The Quadrilateral Region	12
Mapping technique	13
Automatic meshing	14
Quadrilateral division	15
Delaunay triangulation	15
Region connectivity	16
3 Unstructured mesh generation	19
4 Mesh editing	20
Mesh refinement	21
Local mesh refinement.....	21
Global mesh refinement.....	21
Deleting meshes	23
Nodes renumbering	23
Transforming meshes (p-refinement)	23
Part V Formulation of the element matrices and vectors for elasticity problem	24
1 Equilibrium equations	26
2 Boundary conditions	26
3 Strain-Displacement Relations	27
4 A General Formula for the Stiffness Matrix	28
Plane strain	30
Plane stress	31
Axisymmetric case	31
5 Finite element types	32
Constant strain triangle (T3)	34
Linear Strain Triangle (T6)	35
Linear Quadrilateral Element (Q4)	37
Quadratic Quadrilateral Element (Q8)	38
6 Numerical integration in finite elements	39
7 Stress calculation	41

8	Consistent element nodal loads	45
	Body forces	45
	Distributed forces	47
	Initial stress/strain loads	47
	Pore pressure loads	48
	Excavation loads	49
	Gravity loading	50
9	Assembly and storage strategy	51
10	Incorporation of boundary conditions	51
	Explicit specification of BC's	52
	Imposing prescribed displacements (Penalty method)	52
	Elastic supports	52
11	Solution of equilibrium equations	53
Part VI Formulation of the beam-column elements		53
1	Bar or truss elements	53
2	Two-noded beam-column element	55
3	Joining beam-column elements to plane elements. Dissimilar elements.	59
	Beam-column element connected to a plane element	60
	Truss element connected to a plane element	61
	Bolts elements	65
	End anchored bolts	65
	Fully bonded bolts	68
	Liner elements	70
	Geogrid elements	71
Part VII Nonlinear analysis formulation		72
1	Inelastic stress-strain behavior	72
	Yield criterion	72
	Flow rule	73
	Hardening rule	74
2	Incremental stress-strain relations	75
3	Failure criteria	76
	The Von-Misses criterion	76
	Mohr-Coulomb and Tresca criterions	77
4	Elastic-plastic procedures	78
	Constant-stiffness method	79
	Generation of self-equilibrating body loads	80
	Initial strain method	81
	Initial stress method	84
	Solution procedure	84
	Tangent (variable)-stiffness method	85
	Integration of the constitutive relations. Consistent tangent matrix	87
	Solution procedure	89
Part VIII Steady state analysis		90
Part IX Initial conditions		91

1 Initial groundwater conditions	92
2 Initial geostatic stresses	94
Part X Dynamic and seismic analysis	95
Part XI Staged constructions	97
Part XII Analysis types	98
1 Slope stability analysis	98
Factor of Safety (FOS) and Strength reduction factor (SRF)	98
Material properties	99
Slope collapse	99
Computational example	100
2 Bearing capacity analysis	102
3 Staged construction analysis	105
Part XIII Bibliography	110
Part XIV Contact	110
Index	0

1 GFAS

GFAS **Geotechnical and Finite Element Analysis System**

Version 2.0 Theoretical Manual

GEOSTRU SOFTWARE

2009

2 Contents

Contents

Introduction

[Overview](#)

[Analysis capabilities](#)

Mesh generation

[Introduction](#)

Structured mesh generation

[The Quadrilateral Region](#)

[Mapping technique](#)

[Automatic meshing](#)

[Region connectivity](#)

Unstructured mesh generation

Mesh editing

[Mesh refinement](#)

[Deletion meshes](#)

[Nodes renumbering](#)

[Transforming meshes \(p-refinement\)](#)

Formulation of the element matrices and vectors for elasticity problem

[Equilibrium equations](#)

[Boundary conditions](#)

[Strain-displacement relations](#)

A general formula for the stiffness matrix

[Plane strain case](#)

[Plan stress case](#)

[Axisymmetric elements](#)

Finite elements types

[Constant strain triangle \(CST-T3\)](#)

[Linear strain triangle \(LST-T6\)](#)

[Linear quadrilateral element \(Q4\)](#)

[Quadratic quadrilateral element \(Q8\)](#)

Numerical integration in finite elements

Stress calculation

Consistent element nodal loads

- Body forces
- Distributed forces
- Initial stress/strain loads
- Pore pressure loads
- Excavation loads
- Gravity loading

Assembly and storage strategyIncorporation of boundary conditions

- Explicit specification of BC's
- Imposing prescribed displacements (Penalty method)
- Elastic supports

Solution of equilibrium equations**Formulation of beam-column elements**Bar or truss elementsTwo-noded beam-column elementJoining beam-column elements to plane elements. Dissimilar elements.Beam-column element connected to a plane elementTruss element connected to a plane elementBolts elementsEnd anchored boltsFully bonded boltsLiner elementsGeogrid elementsNonlinear analysis formulationInelastic stress-strain behaviorYield criterionFlow ruleHardening ruleIncremental stress-strain relationsFailure criteriaThe Von-Mises yielding criteriaMohr-Coulomb and Tresca yielding criteriaElastic-plastic proceduresConstant-stiffness methodGeneration of self-equilibrating body loadsInitial strain methodInitial stress methodSolution procedureTangent (variable) stiffness methodIntegration of the constitutive relations. Consistent tangent matrixSolution procedure

Steady state analysis

Initial conditions

Initial ground
conditions

Initial geostatic stresses

Dynamic and seismic analysis

Staged constructions

Analysis types

Slope stability analysis

Bearing capacity analysis

Staged construction analysis.

Bibliography

3 Introduction

3.1 Overview

GFAS is a finite element package that has been developed specifically for the analysis of deformation and stability analysis in geotechnical engineering problems. GFAS is an easy-to-use yet powerful geotechnical-engineering tool for the linear and nonlinear analysis of homogenous or non-homogenous structures in which soil models are used to simulate the soil behavior. It features a full graphical interface for pre-processing or post-processing and uses the Finite Element Method (FEM) for 2D solids for its analysis purposes. The graphical interface enable a quick generation of complex finite element models, and the enhanced output facilities provide a detailed presentation of computational results. The analysis procedures are fully automated and based on robust numerical procedures.

The basic program features include:

- **Graphical input of geometry models:** The input of soil layers, structures, loads and boundary conditions is based on convenient CAD drawing procedures, which allows for a detailed modeling of the geometry contour. From this geometry model, a 2D finite element mesh is easily generated.

- **Automatic mesh generation:** GFAS allows for automatic generation of structured and unstructured 2D finite element meshes with options for global mesh refinement. The program contains a built-in automatic mesh generator that considerably simplifies construction of the finite element model. Both triangular (3-noded or 6-noded) and quadrilateral (4-noded or 8-noded) elements are available.
- **Higher-order elements:** Quadratic 8-node and 6-node triangular elements are available to model the deformations and stresses in the soil.
- **Optimization of the matrix bandwidth** to reduce the computer storage and calculation time can be performed by the program using internal re-numbering of the system equations.
- **Staged constructions:** Complex multi-stage models can be created and analyzed such as: tunnels, excavations, embankments, soil reinforcement, etc.
- **Beam-column elements:** The program offers a wide range of support modelling options such as liners, anchors and geotextile. The beam -column elements in either Bernoulli or Timoshenko theory are incorporated in the code and enabled the user to create complex finite element models in which both plane and line elements interact each other. Liner elements can be used in the modelling of tunnel lining or sheeting structures. Bolt types include end anchored or fully bonded. These elements can be assigned anywhere in the mesh.
- **Steady state flow analysis:** The program includes the steady state flow analysis built right into the general program. Water pore pressures are determined as well as flow and gradient based on user defined hydraulic boundary conditions and material permeability. The water pore pressures are automatically incorporated into the finite element stress analysis.
- **Dynamic and seismic analysis:** The program allows the users to carry out a dynamic analysis for determining the eigen values and eigen mode for construction and consequently to determine the seismic forces according with Eurocode 8.
- **Elasto-plastic material models:** The present release offers the following models: Mohr-Coulomb and Von-Misses models for elasto-plastic behavior of plane elements. Both models are robust and simple non-linear models and are based on soil parameters that are well known in engineering practice. Both anchored and geotextile elements could have either a linear elastic or elasto-plastic behaviour.

3.2 Analysis capabilities

The general objective of GFAS is to provide analytical tools for deformation and stress assessment of plane structures in direct support of geotechnical analysis.

The program provides three basic analysis tools:

The **Linear Elastic Analysis** tool can be used to perform a finite element analysis of a membrane of any general geometry subjected to *plane stress*, *plane strain* or *axisymmetric stress and strains*. The conditions of *plane stress* and *plane strain* are two similar two-dimensional states of stress. When forces are applied to a thin two-dimensional plate in its own plane, the state of stress and deformation in the plate is called *plane stress*. A typical example would be a shear wall that, due to it being a thin plate, will experience mainly in-plane stresses. No restraint is provided for out-of-plane deformation. On the other hand, a prismatic solid subjected to a constant loading normal to its axis can be analyzed as an infinite length of two-dimensional slices of unit thickness experiencing *plane strain*. A dam wall, for example, would typically be subjected to hydrostatic and soil pressures normal to its surface. A slice is taken from the wall will be restrained from deforming out-of-plane.

The **Bearing Capacity Analysis** tool can be used to compute the response to loading of a nonlinear material. Plane strain conditions are enforced and in order to monitor the elasto-plastic behavior, the loads are applied incrementally. The method uses constant stiffness iterations, thus the relatively time consuming stiffness matrix factorization process is called just once, while the backward substitution phase is called at each iteration. Several failure criteria have been implemented for representing the strength of soils as engineering materials. For soils with both frictional and cohesive components of shear strength *Mohr-Coulomb* failure criteria is appropriate. For undrained clays, which behave in a "frictionless" manner, *Von-Misses* failure criteria may be used.

The **Slope Stability Analysis** tool can be used to carry out the slope stability analysis of a given structure. During the analysis the program gradually reduces the basic strength characteristics of the soil mass until failure occurs. The factor of safety (*FS*) is to be assessed, and this quantity is defined as the proportion by which $\tan \Phi$ (friction angle) and *c* (cohesion) must be reduced in order to cause failure with the gravity loading kept constant. This is in contrast to the bearing capacity analysis in which failure is induced by increasing the loads with the material properties remaining constant. The program can give information about the deformations at working stress levels and is able to monitor progressive failure including overall shear failure. The present release can be applied only for two-dimensional plain-strain problems. Either the *Mohr-Coulomb* or *Von-Misses* constitutive models can be used to describe the soil or rock material properties. Gravity loads are generated automatically and applied to the slope in a single increment. A trial strength reduction factor loop gradually weakens the soil parameters until the algorithm fails to converge. The factored soil strength parameters that go into the elasto-plastic analysis are obtained from:

$$\Phi_f = \arctan(\tan\Phi / SRF)$$

$$c_f = c / SRF$$

where SRF is strength reduction factor. Several increasing values of the SRF factor are attempted until the algorithm fails to converge, at which point SRF is then interpreted as the factor of safety FS . This actually means that no stress distribution can be achieved to satisfy the failure criterion and global equilibrium. Non-convergence within a user-specified number of iterations in finite element program is taken as a suitable indicator of slope failure and is joined by an increase in the displacements. Usually the value of the maximum nodal displacement just after slope failure has a big jump compared to the one before failure.

The **Staged Analysis** option can be used to carry out staged construction analysis. During the Staged construction analysis, the loads are increased from 0 to 1, for each stage of construction. As soon as the load parameter reaches the value of 1.0, the constructions stage is completed and the analysis of the current phase is completed, and go the the next phase of the construction. If a staged construction calculations finishes while the load factor is smaller than 1.0, the program will stop the analysis. The most likely reason for not finishing a construction stage is that a failure mechanism has occurred.

4 Mesh generation

4.1 Introduction

The finite element method requires dividing the analysis region into several sub-regions. These small regions are the elements, which are connected with adjacent elements at their nodes. Mesh generation is a procedure of generating the geometric data of the elements and their nodes, and involves computing the coordinates of nodes, defining their connectivity and thus constructing the elements. Here, mesh designates aggregates of elements, nodes and lines representing their connectivity. Capability and convenience of modeling the analysis domain are dominated by the mesh generation procedure. The geometric characteristics of generated elements affect the overall performance and accuracy of the finite element analysis. Therefore, mesh generation is one of the most important procedures in finite element modeling.

A mesh of isoparametric quadrilateral or triangular is automatically generated and optimized during analysis. You can specify the grid spacing in the X and Y -directions as part of the analysis parameters. A finer grid will often improve accuracy. However, the time taken to perform an analysis is a function of the number of finite elements – the finer the grid, the longer the analysis time.

GFAS uses two types for finite element mesh generation: *block mesh generator* (structured mesh) that requires some initial form of gross partitioning and *unstructured mesh generator* (constraint automatic triangulation). In the first approach the solution domain is partitioned in some relatively small number of blocks. Each block should have eight-node quadrilateral form. Mapping technique generates the mesh inside the block. In the second approach the mesh is generated for an arbitrarily shaped region. The mesh is generated simply by designating the curves of the mesh boundary and issuing a mesh generation command. A curved surface as well as a plane may be meshed by this method. Also you can generate a coarse mesh (i.e. the gross geometry of the model) that can be refined later using the tools provided by GFAS specifically for this purpose. Removal of elements and renumbering of the mesh options are also allowed through the GFAS processors. During the mesh generation phase it is not required to make a decision on the element type to be used. Only the element class is important at this stage (triangular or quadrilateral). For instance: 3-noded triangular elements can be used to generate the mesh and then the entire mesh can be converted to the higher-order 6-noded triangle elements. In the phase of the analysis definition it has to be decided if the element is *axisymmetric*, *plane stress* or *plane strain*.

The basic mesh generator features include:

- Automatic mesh generation: T3, T6, Q4, Q8.
- Nodes renumbering: Reverse Cuthill-McKee algorithm implemented for T3, T6, Q4, Q8 finite elements meshing.
- Transform simple (T3, Q4) to higher order finite elements (T6, Q8).
- Regions and Material data recognition: after mesh generation, properties such as material type (for each finite element) and region subdivision can be revealed in the framework of the further mesh manipulation.
- Mesh refinements: automatic mesh refinement for all of the above finite elements types (T3, Q4, T6, Q8).
- Mask finite elements: Allowed to cut selected elements in order to create complex geometry.

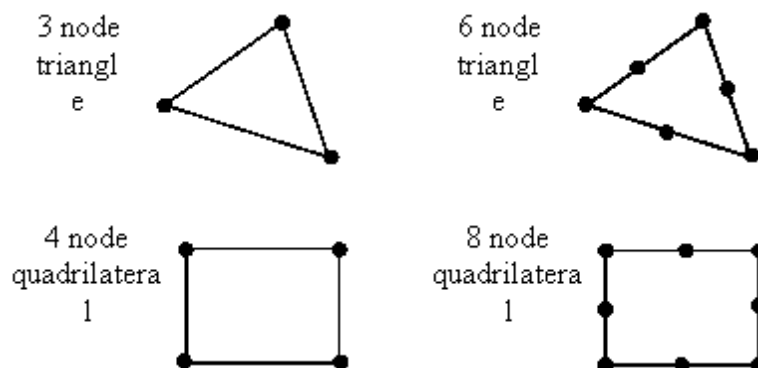


Fig.1. Element types in mesh generation.

4.2 Structured mesh generation

4.2.1 The Quadrilateral Region

The mesh generation for any two-dimensional domain into elements should start with the division of the body in consideration into quadrilateral or triangular regions. These regions are then subdivided either into triangle or quadrilateral finite elements. The subdivision between regions should be located where there is a change in geometry or material properties. **GFAS** uses a group of eight-node (quadratic) quadrilateral regions to define the body under consideration, being capable of modeling two-dimensional domains that are composed of rectangles and triangles having second-order curved boundaries. The element nodes are numbered and optimization of the matrix bandwidth to reduce the computer storage and calculation time can be performed by the program using internal re-numbering of the system equations.

The region available in **GFAS** is the quadratic quadrilateral. This element is quite versatile, it can be used as a *rectangle*, *general quadrilateral*, or as a *triangle* as shown in Figure 2. Two sides of the quadrilateral are used to define one side of the triangular region. The eight nodes that define the region must be numbered as shown in the Figure 2. Node 1 is always at the coordinate location $\xi=\eta=-1$. Note that one of the corner nodes (node 5 in Figure 2) will always be on the hypotenuse of the triangular region. The region is then subdivided either in triangular elements or quadrilateral elements using the mapping technique.

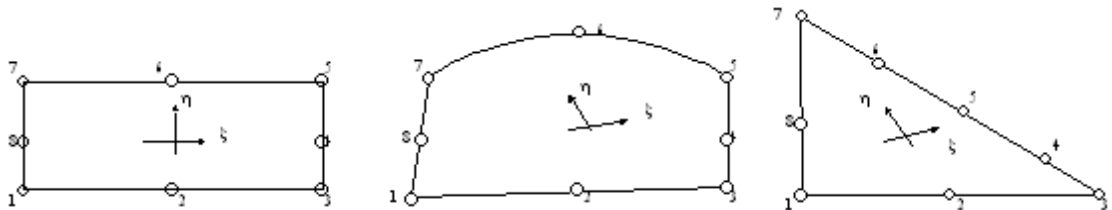


Fig. 2. Possible regions for the quadrilateral. Nodes numbering.

4.2.2 Mapping technique

Mapping techniques transform a parent region with regular grid spacing to a more arbitrarily shaped region. For a unit square, the region being mapped should have four logical sides and four rather natural corners (Fig.3).

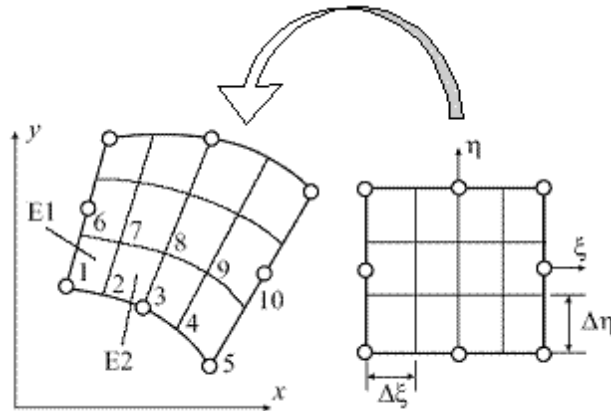


Fig.3. Mesh generation with mapping technique.

Suppose we want to generate a quadrilateral mesh inside a domain that has the shape of second-order quadrilateral. Mapping technique shown in Fig.3 can be used for this purpose. If each side of the curvilinear quadrilateral domain can be approximated by parabola then the domain looks like 8-node isoparametric element. The domain is mapped to a square in the local coordinate system ξ, η . The square in coordinates ξ, η is divided into rectangular elements then nodal coordinates are transformed back to the global coordinate system x, y . The algorithm of coordinate computation for the nodes inside the domain is given below:

$$\begin{aligned}
 R &= \frac{i-1}{n_{\xi} + 1} + 1 \\
 C &= \text{mod}((i-1)(n_{\xi} + 1)) + 1 \\
 \Delta\xi &= \frac{2}{n_{\xi}}; \quad \Delta\eta = \frac{2}{n_{\eta}} \\
 \xi &= -1 + \Delta\xi(C-1) \\
 \eta &= -1 + \Delta\eta(R-1) \\
 x &= \sum N_k(\xi, \eta)x_k \\
 y &= \sum N_k(\xi, \eta)y_k
 \end{aligned} \tag{1}$$

where n_{ξ} and n_{η} represents the number of elements in ξ and η direction respectively and where the

shape functions N_k defined in local coordinates ξ, η ($-1 \leq \xi \leq 1$; $-1 \leq \eta \leq 1$) are:

(a) for bi-linear elements:

$$N_k(\xi, \eta) = \frac{1}{4} (1 - \xi_k \xi)(1 - \eta_k \eta) \quad (\xi_k, \eta_k) = (\pm 1, \pm 1) \quad (2)$$

$$k=1,2,3,4$$

(b) for quadratic elements:

$$N_1(\xi, \eta) = -\frac{1}{4} (1 - \xi)(1 - \eta)(\xi + \eta + 1)$$

$$N_2(\xi, \eta) = \frac{1}{2} (1 - \xi^2)(1 - \eta)$$

$$N_3(\xi, \eta) = \frac{1}{4} (1 + \xi)(1 - \eta)(\xi - \eta - 1)$$

$$N_4(\xi, \eta) = \frac{1}{2} (1 + \xi)(1 - \eta^2)$$

$$N_5(\xi, \eta) = \frac{1}{4} (1 + \xi)(1 + \eta)(\xi + \eta - 1) \quad (3)$$

$$N_6(\xi, \eta) = \frac{1}{2} (1 - \xi^2)(1 + \eta)$$

$$N_7(\xi, \eta) = \frac{1}{4} (1 - \xi)(1 + \eta)(\xi - \eta - 1)$$

$$N_8(\xi, \eta) = \frac{1}{2} (1 - \xi)(1 - \eta^2)$$

4.2.3 Automatic meshing

The region can be subdivided into triangular or quadrilateral elements by considering four nodes that form a quadrilateral such as the area in Fig.4. There are two types of automatic triangulation for mesh generation, i.e. *quadrilateral division* and *Delaunay technique*. Either linear or quadratic order can be selected: linear elements (3-node triangle or 4-node quadrilateral); quadratic elements (6-node triangle or 8-node quadrilateral). When the mesh has been generated, this plan grid then serves as the reference for the assignment of all material properties, supports and loadings that are placed on the grid using the mouse.

4.2.4 Quadrilateral division

When the nodes of the model have been generated, the next step is to define the elements. The region is subdivided into triangular elements by considering four nodes that form a quadrilateral such as the area in Fig. 4. The interior *quadrilaterals* can be left as elements or they may be further divided into *triangular* elements by inserting the shortest diagonal into each interior quadrilateral. The length of the two diagonals are calculated and compared. The elementary quadrilateral is then subdivided into two triangular elements using the shortest diagonal. This procedure is repeated until all sets of four nodes have been analysed. Division using the shortest diagonal is preferable because elements close to an equilateral shape produce more accurate results than long narrow triangles.

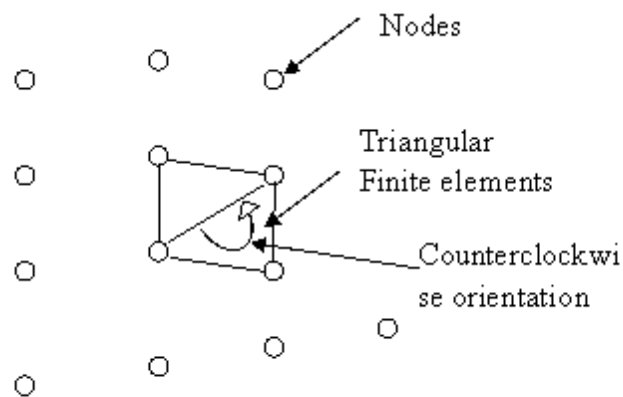


Fig. 4. A set of four nodes divided into two triangular finite elements.

4.2.5 Delaunay triangulation

Having generated the sample points inside the regions, using the mapping technique, the finite element mesh could be generated also using the well-known Delaunay triangulation technique.

A counterclockwise numbering is used for local element nodes as shown in Figure 5.

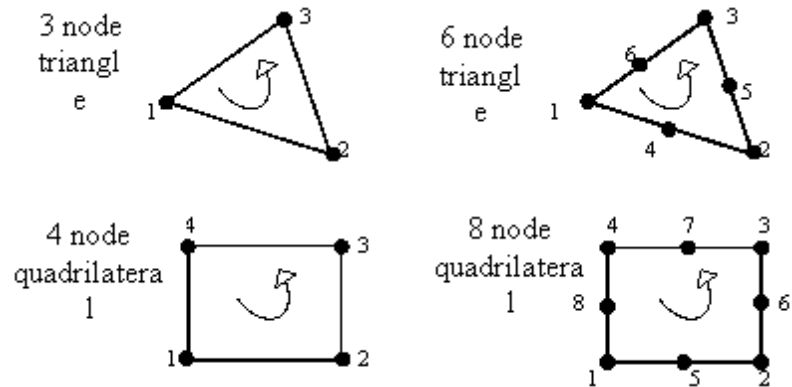


Fig. 5. A counterclockwise numbering of finite element nodes.

4.2.6 Region connectivity

A body or domain is generally modeled using several quadrilateral regions connected to one another along one or more sides. The possibility of a common boundary between two regions requires that certain information be provided to insure that the nodes on this common boundary have the same numbers regardless of which region is being considered. The number of nodes on this boundary must be identical in number and must occupy the same relative position. This property is necessary to insure continuity across the element boundary.

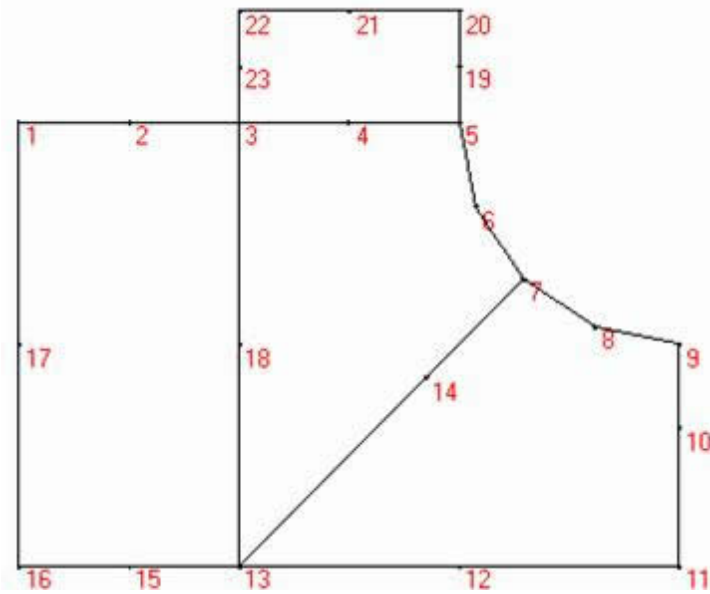


Fig. 6. A connected set of four quadrilateral regions.

The determination of the connectivity data is probably best illustrated through an example such as the four-region body as shown in Fig.6. The boundary nodes coordinates are shown in Table 1 while the region's data (the number of divisions, the quadrilateral nodes numbering) is shown in table 2.

Table 1. Coordinates of boundary nodes.

Node	X[m]	Y[m]
1	0	0
2	10	0
3	20	0
4	30	0
5	40	0
6	41.52	-7.65
7	45.86	-14.14
8	52.35	-18.48
9	60	-20
10	60	-27.5
11	60	-40
12	40	-40
13	20	-40
14	37	-23
15	10	-40
16	0	-40
17	0	-20
18	20	-20
19	40	5

20	40	10
21	30	10
22	20	10
23	20	5

Table 2. Region's data.

Region	NRows	Ncols	Node 1	Node 2	Node 3	Node 4	Node 5	Node 6	Node 7	Node 8
1	25	15	16	15	13	18	3	2	1	17
2	25	25	13	14	7	6	5	4	3	18
3	25	25	13	12	11	10	9	8	7	14
4	15	25	3	4	5	19	20	21	22	23

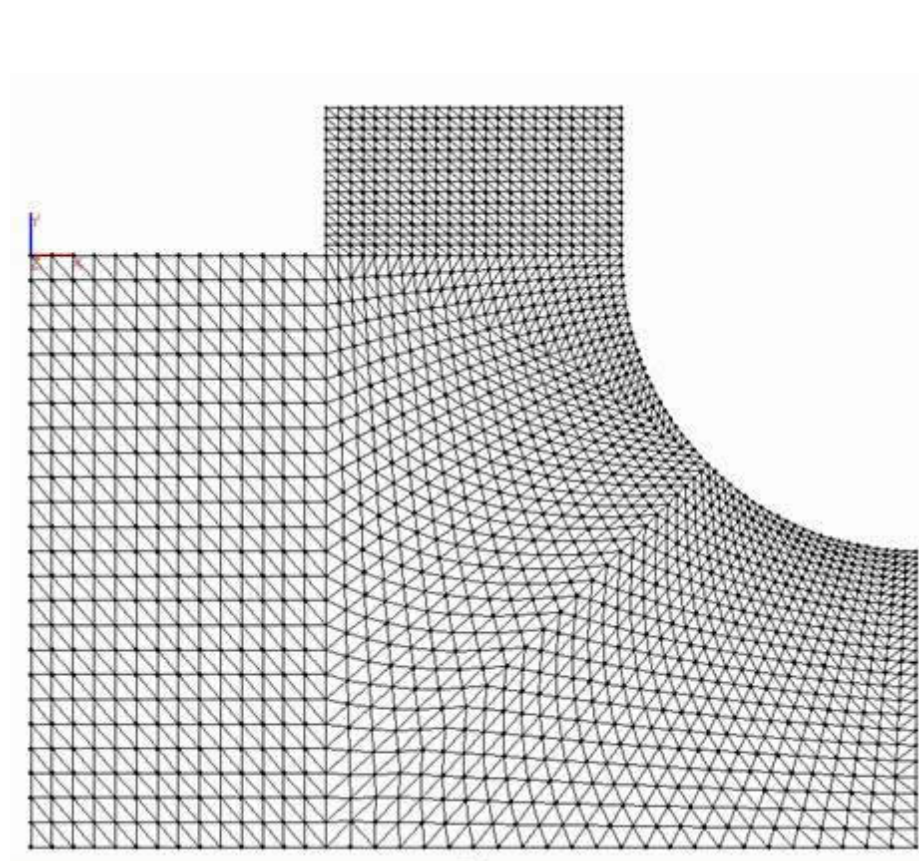


Fig. 7. The mesh. Delaunay triangulation.

4.3 Unstructured mesh generation

The easiest way of generating mesh on a plane is unstructured mesh generation with Delaunay constraint triangulation. For an arbitrarily shaped region or connected regions the mesh is generated automatically by designating the interfaces or the holes of that domain. You can easily fill an arbitrarily shaped region with triangular elements using automatic triangulation as described below. For successful automatic triangulation, curves or polylines should be selected so that they may form a region compatible for mesh generation as described below.

- A region is formed from one or multiple interfaces.
- The outer boundary of the region should be enclosed by serially connected lines or curves.
- The region boundary may be either convex or concave.
- The region may contain holes or control curves inside the boundary.

The following examples illustrate mesh regions compatible and incompatible for automatic triangulation.

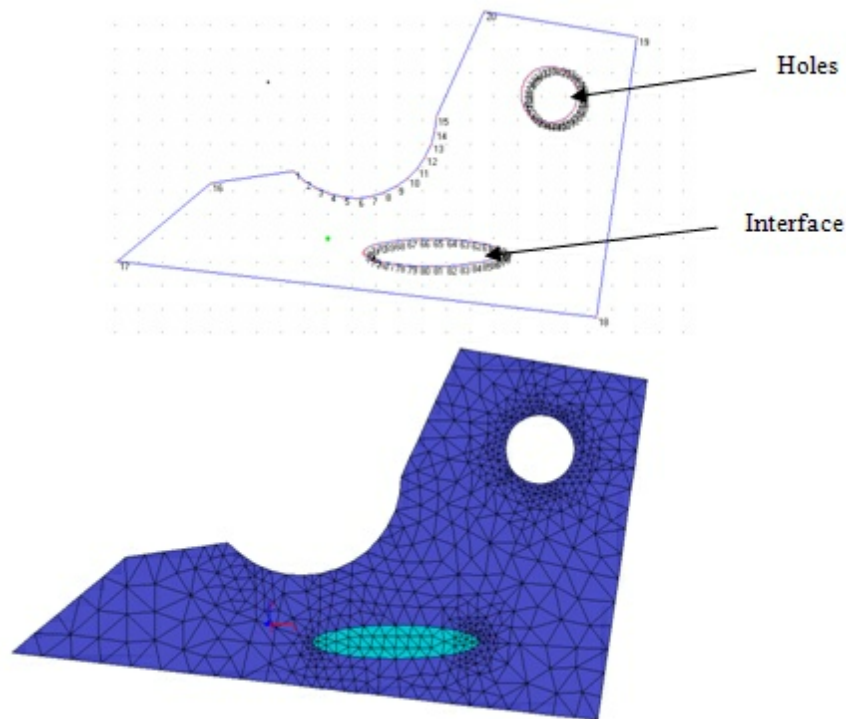
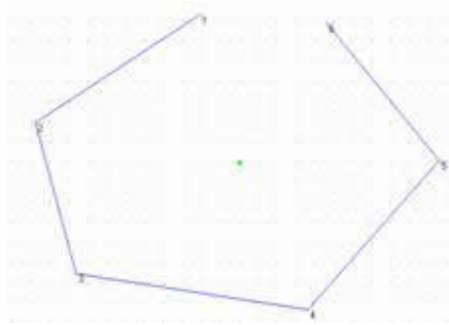
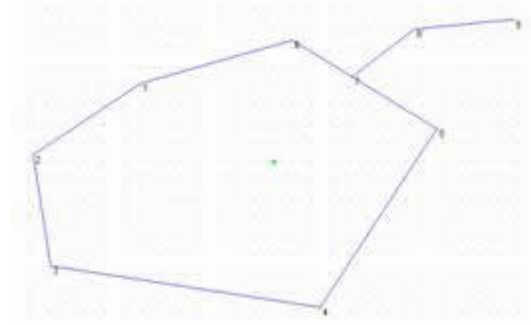


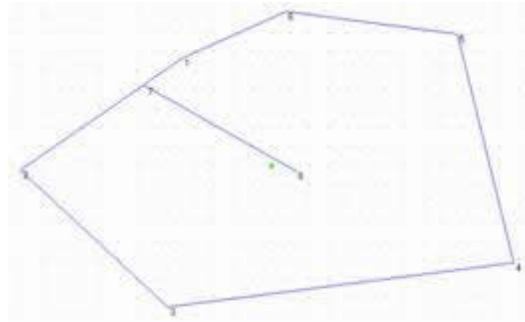
Figure 8. Compatible region for automatic triangulation.



(a) *The lines do not form a closed boundary*



(b) *The lines are not contained within the boundary of the region*



(c) *Two curves are containing at point which is not a common node*

Figure 9. Incompatible regions for automatic triangulation.

4.4 Mesh editing

GFAS allows editing or modifying the mesh. The current release has several functions of mesh editing.

4.4.1 Mesh refinement

4.4.1.1 Local mesh refinement

A regular mesh, all elements the same size and shape, usually is not practical because of stress concentrations. Shifting of mid-side nodes closer to some corner of the domain helps to refine (make smaller elements) mesh near this corner. The size of the elements can be varied by placing nodes 2, 4, 6, or 8 at some point other than the center of the side. Movement of these nodes shifts the origin of the coordinate system and produces a pattern similar to the one in Fig.10. These mid side nodes must remain within the interval:

$$\begin{aligned} -\frac{1}{2} < \xi < \frac{1}{2} \\ -\frac{1}{2} < \eta < \frac{1}{2} \end{aligned} \quad (4)$$

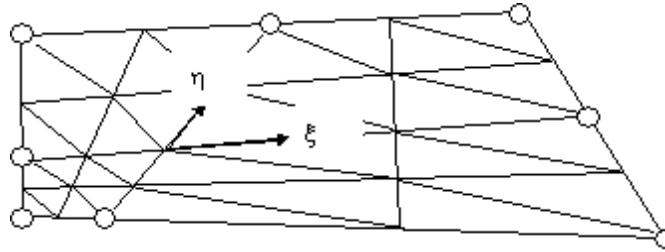


Fig. 10. A region with a change in element size.

4.4.1.2 Global mesh refinement

In order to reduce the size of the initial finite element mesh, global mesh refinement can be done at run time. Once you have generated a coarse model, you can refine it to the desired level. It allows much smaller input data files and adds the flexibility of increasing the mesh resolution without re-meshing the model with a mesh generator. The global refinement scheme is very simple, because it just splits up every finite element into four "children" (Fig.11). If this scheme is applied to the whole finite element mesh, its structure remains consistent (Fig.12). The quality of the mesh is preserved. This feature is implemented for all finite element types supported by the code.

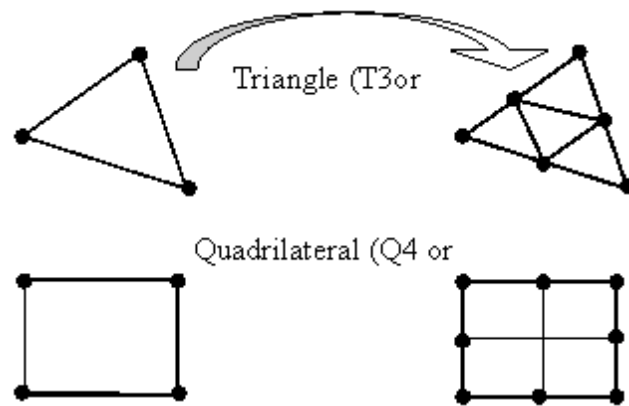


Fig.11 Global refinement of a "parent" finite element into four "children".

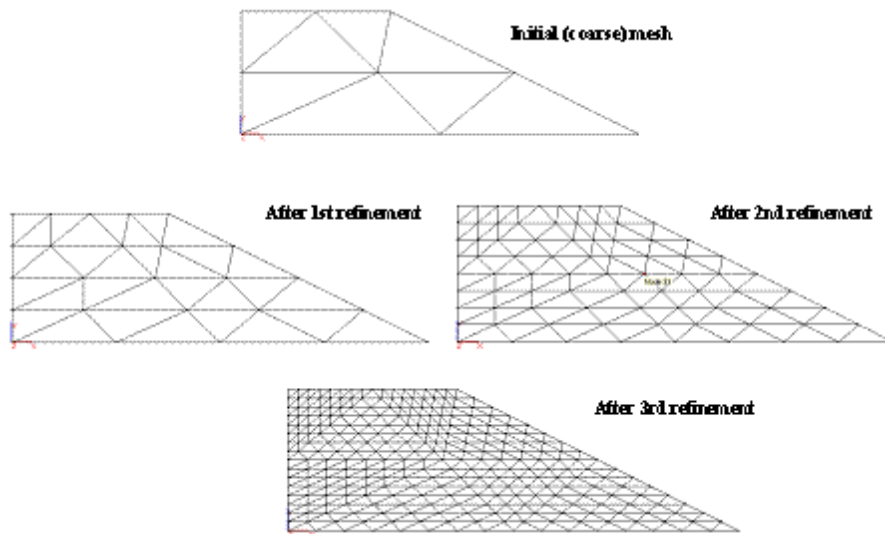


Fig.12 Automatic mesh refinement (*h*-refinement).

As a result, the input data files and especially the file containing the mesh geometry are much smaller. Even more important, the mesh generator does not have to generate a very fine and therefore large mesh, even though it has to be fine enough to resolve the details of the geometrical model and should give finite elements of good quality. Moreover, convergence of the results can be easily checked with a refined finite element mesh (Fig.12).

4.4.2 Deleting meshes

The finite element model options allow convenient addition or deletion of elements in order to create complex geometry. After deleting a portion from the model all the properties assigned to the rest of model are preserved (i.e. region number, material properties). Also renumbering of the nodes is automatically run in order to reduce the bandwidth of the resulted system of equations.

4.4.3 Nodes renumbering

Numbering of nodes has a definite influence on the bandwidth of the coefficient matrix associated with the mesh. The smaller the bandwidth the less storage and amount of computation required. The method used, for this purpose, is nodes renumbering by the RCM (Reverse Cuthill-McKee) method. With this method the formed matrix will be sparse and regularly banded, so that it can be solved economically.

4.4.4 Transforming meshes (p-refinement)

After mesh generation of the body with simple finite elements either triangular (T3) or quadrilateral (Q4) GFAS allows to transform the generated elements to higher-order finite elements (T6 or Q8). This feature is particularly desirable, since convergence of the results can be easily checked with a *p-refined* finite element mesh generated in this way. If this scheme is applied to the whole finite element mesh, its structure remains consistent (Fig.13). The quality of the mesh is also preserved.

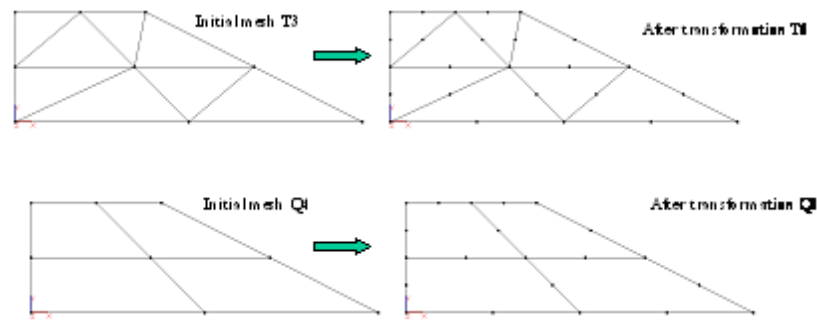


Fig. 13 Transform meshes from simple to higher-order elements (*p*-refinement).

5 Formulation of the element matrices and vectors for elasticity problem

The finite element problem consists of calculating the individual element stiffness matrices and vectors, and assembling them into the global stiffness matrix and force vectors. The set of simultaneous equations that this produces is then solved for the nodal displacements.

The stress vector σ and the strain vector ε are, respectively (Figure 14):

$$\begin{aligned} \sigma &= [\sigma_x \quad \sigma_y \quad \sigma_z \quad \tau_{xy} \quad \tau_{yz} \quad \tau_{zx}] \\ \varepsilon &= [\varepsilon_x \quad \varepsilon_y \quad \varepsilon_z \quad \gamma_{xy} \quad \gamma_{yz} \quad \gamma_{zx}] \end{aligned} \quad (5)$$

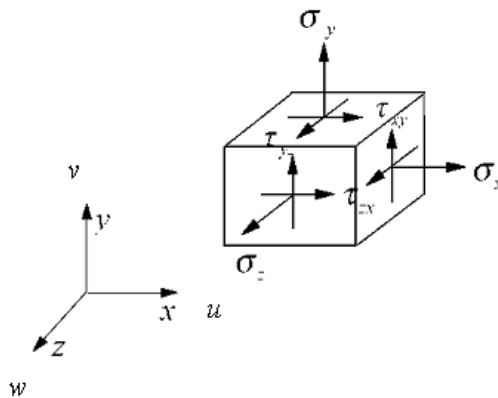


Fig. 14. Components of the stress.

The stress-strain relation is represented as:

$$\boldsymbol{\varepsilon} = \mathbf{C}\boldsymbol{\sigma} \quad (6)$$

or as:

$$\boldsymbol{\sigma} = \mathbf{E}\boldsymbol{\varepsilon} \quad (7)$$

where \mathbf{C} is a symmetric matrix of material compliances, \mathbf{E} is a symmetric matrix of material stiffness, and $\mathbf{E}=\mathbf{C}^{-1}$. The components of the displacement vector \mathbf{u} along x , y and z directions are u , v , and w respectively. The following sign convention is used: Positive y -coordinates and vertical forces are taken upward, i.e. parallel to the Y -axis. Positive x -coordinates and horizontal forces are taken to the right, i.e. parallel to the x axis. The vertical deflections are measured along the y -axis. A positive deflection therefore denotes an upward movement.

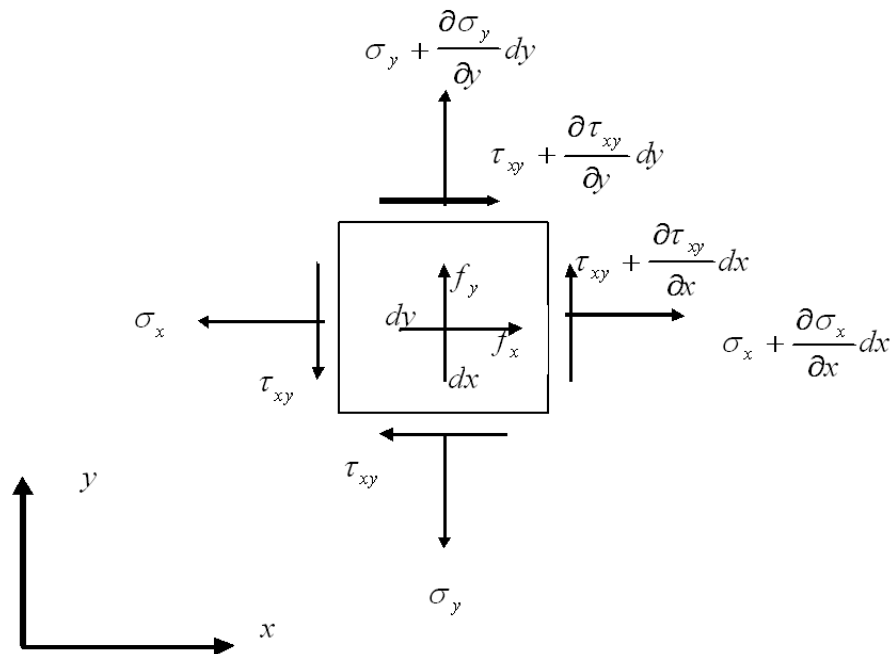


Fig. 15. Stresses and body forces that act on a plane differential element of constant thickness.

5.1 Equilibrium equations

Figure 15 shows a plane differential element. The equilibrium equations are developed stating that the differential element is in equilibrium under forces applied to it. Forces come from stresses on the edges and from body forces. In general, stresses and body forces are functions of the coordinates.

Thus, for instance, $\frac{\partial \sigma}{\partial x}$ is the rate of change of σ_x with respect to x , and $\frac{\partial \sigma}{\partial x} dx$ is the amount of change of σ_x over distance dx .

The stresses in the structure must satisfy the following equilibrium equations:

$$\begin{aligned} \frac{\partial \sigma_x}{\partial x} + \frac{\partial \tau_{xy}}{\partial y} + f_x &= 0 \\ \frac{\partial \tau_{xy}}{\partial x} + \frac{\partial \sigma_y}{\partial y} + f_y &= 0 \\ \tau_{xy} &= \tau_{yx} \end{aligned} \tag{8}$$

where f_x and f_y are body forces, such as gravity forces, per unit volume. In the finite element method, these equilibrium equations are satisfied in an approximate sense.

5.2 Boundary conditions

Boundary conditions consist of prescription of displacement and of stress. The boundary S of the body can be divided into two parts, S_u and S_f . The boundary conditions (BC's) are described as:

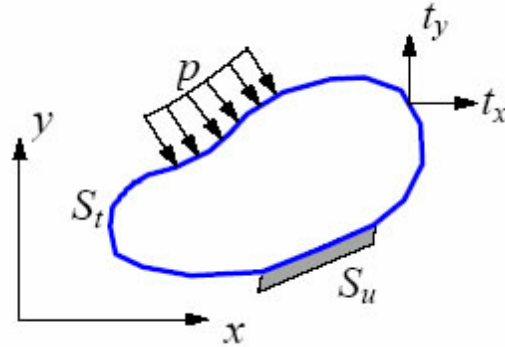


Fig. 16. Boundary conditions.

$$u = \bar{u}, \quad v = \bar{v} \quad \text{on } S_u \quad (9)$$

$$t_x = \bar{t}_x, \quad t_y = \bar{t}_y \quad \text{on } S_t \quad (10)$$

in which t_x and t_y are traction forces (stresses on the boundary) and the barred quantities are those with known values.

5.3 Strain-Displacement Relations

For plane structures, under the small strain and small rotation hypotheses we can write the following relations between deformations and displacements:

$$\varepsilon_x = \frac{\partial u}{\partial x}, \quad \varepsilon_y = \frac{\partial v}{\partial y}, \quad \gamma_{xy} = \frac{\partial u}{\partial y} + \frac{\partial v}{\partial x} \quad (11)$$

or in matrix form:

$$\begin{Bmatrix} \varepsilon_x \\ \varepsilon_y \\ \gamma_{xy} \end{Bmatrix} = \begin{bmatrix} \frac{\partial}{\partial x} & 0 \\ 0 & \frac{\partial}{\partial y} \\ \frac{\partial}{\partial y} & \frac{\partial}{\partial x} \end{bmatrix} \begin{Bmatrix} u \\ v \end{Bmatrix} \quad (12)$$

or in a condensed form:

$$\boldsymbol{\varepsilon} = \mathbf{D}\mathbf{u} \quad (13)$$

where u and v are the components of displacements in the x and y directions. If the displacement field is represented by polynomials, the strains and stresses are one order lower than the displacements.

5.4 A General Formula for the Stiffness Matrix

Consider a linearly elastic body that carries conservative load. Let its volume be V and its surface area be S . The expression for the potential energy in a linearly elastic body is:

$$W_p = \int_V \left(\frac{1}{2} \boldsymbol{\varepsilon}^T \mathbf{E} \boldsymbol{\varepsilon} - \boldsymbol{\varepsilon}^T \mathbf{E} \boldsymbol{\varepsilon}_0 + \boldsymbol{\varepsilon}^T \boldsymbol{\sigma}_0 \right) dV - \int_V \mathbf{u}^T \mathbf{F} dV - \int_S \mathbf{u}^T \boldsymbol{\Phi} dS - \mathbf{D}^T \mathbf{P} \quad (14)$$

in which

$\mathbf{u} = [u \quad v]^T$ represents the displacement field;

$\boldsymbol{\varepsilon} = [\varepsilon_x \quad \varepsilon_y \quad \gamma_{xy}]^T$ represents the strain field;

\mathbf{E} the elastic constants matrix (material property)

$\boldsymbol{\varepsilon}_0, \boldsymbol{\sigma}_0$ initial strains and initial stresses;

$\mathbf{F} = [F_x \quad F_y]^T$ body forces;

$\boldsymbol{\Phi} = [\Phi_x \quad \Phi_y]^T$ surface tractions;

\mathbf{D} represents the nodal d.o.f. displacements

\mathbf{P} loads applied directly to d.o.f.

Displacements within an element are interpolated from element nodal d.o.f. \mathbf{d} as:

$$\mathbf{u} = \mathbf{N}\mathbf{d} \quad (15)$$

where \mathbf{N} is the shape function matrix.

Strains are obtained from displacements by differentiation.

$$\boldsymbol{\varepsilon} = \partial\mathbf{u} = \partial\mathbf{N}\mathbf{d} = \mathbf{B}\mathbf{d} \quad (16)$$

where

$$\mathbf{B} = \partial\mathbf{N} \quad (17)$$

and represents the strain-displacement operator. The differential operator matrix ∂ is given in the case of the plane problems as:

$$\partial = \begin{bmatrix} \frac{\partial}{\partial x} & 0 \\ 0 & \frac{\partial}{\partial y} \\ \frac{\partial}{\partial y} & \frac{\partial}{\partial x} \end{bmatrix} \quad (18)$$

Substitution of the expressions for \mathbf{u} and $\boldsymbol{\varepsilon}$ into Eq. 14 yields:

$$W_p = \frac{1}{2} \sum_{n=1}^{N.EI} \mathbf{d}_n^T \mathbf{k}_n \mathbf{d}_n - \sum_{n=1}^{N.EI} \mathbf{d}_n^T \mathbf{r}_{en} - \mathbf{D}^T \mathbf{P} \quad (19)$$

where summation symbols indicate the we include contribution from all finite elements of the structure, and the element stiffness matrix and element equivalent nodal loads vector are defined as:

$$\mathbf{k} = \int_{V_e} \mathbf{B}^T \mathbf{E} \mathbf{B} dV_e \quad (20)$$

$$\mathbf{r}_e = \int_{V_e} \mathbf{B}^T \mathbf{E} \boldsymbol{\varepsilon}_0 dV_e - \int_{V_e} \mathbf{B}^T \boldsymbol{\sigma}_0 dV_e + \int_{V_e} \mathbf{N}^T \mathbf{F} dV_e + \int_{S_e} \mathbf{N}^T \boldsymbol{\Phi} dS_e \quad (21)$$

where V_e denotes the volume of an element and S_e its surface and in the surface integral the shape function matrix is evaluated on S_e .

Every degree of freedom in an element displacement vector \mathbf{d} also appears in the vector of global structural d.o.f. \mathbf{D} . Therefore \mathbf{D} can replace \mathbf{d} in Equation (14) if \mathbf{k} and \mathbf{r}_e of every element are conceptually expanded to structure size. Thus Eq.(14) becomes:

$$W_p = \frac{1}{2} \mathbf{D}^T \sum_{n=1}^{N.EI} \mathbf{k}_n \mathbf{D} - \mathbf{D}^T \sum_{n=1}^{N.EI} \mathbf{r}_{en} - \mathbf{D}^T \mathbf{P} = \frac{1}{2} \mathbf{D}^T \mathbf{K} \mathbf{D} - \mathbf{D}^T \mathbf{R} \quad (22)$$

where

$$\begin{aligned}\mathbf{K} &= \sum_{n=1}^{N.E.} \mathbf{k}_n \\ \mathbf{R} &= \sum_{n=1}^{N.E.} \mathbf{r}_{en} + \mathbf{P}\end{aligned}\quad (23)$$

represents the global stiffness matrix and nodal force vector expanded in global coordinates at structure level. In the Eq.(22) the summation operator indicate the assembly of element matrices and vectors.

This way the total potential W_p of the structure is represented as a function of d.o.f. \mathbf{D} . Making W_p stationary with respect to small changes in the vector \mathbf{D} we can write:

$$\frac{\partial W_p}{\partial \mathbf{D}} = 0 \quad (24)$$

or explicitly:

$$\frac{\partial W_p}{\partial D_1} = \frac{\partial W_p}{\partial D_2} = \dots = \frac{\partial W_p}{\partial D_n} = 0 \quad (25)$$

yielding the following simultaneous algebraic equations to be solved for n unknowns representing the displacements collected for each d.o.f. of vector \mathbf{D} :

$$\mathbf{KD} = \mathbf{R} \quad (26)$$

where n represents the number of total d.o.f. of structure, \mathbf{K} and \mathbf{R} represents the global stiffness matrix and nodal loads vector assembled for the entire structure.

5.4.1 Plane strain

This case is defined as a deformation state in which $w=0$ everywhere and u and v are functions of x and y but not of z . Thus, $\varepsilon_x = \gamma_{xy} = \gamma_{zx} = 0$. A typical slice of an underground tunnel that lies along the z axis might deform in essentially plane strain conditions. The constitutive matrix \mathbf{E} for isotropic plane strain is:

$$\mathbf{E} = \frac{E}{(1+\nu)(1-2\nu)} \begin{bmatrix} 1-\nu & \nu & 0 \\ \nu & 1-\nu & 0 \\ 0 & 0 & (1-2\nu)/2 \end{bmatrix} \quad (27)$$

If needed, σ_z can be obtained from the relation $\varepsilon_z = 0 = (\sigma_z - \nu\sigma_y - \nu\sigma_x)/E$ after σ_x and σ_y are known.

5.4.2 Plane stress

Thus is a condition that prevails in a flat plate in the xy plane, loaded only in its own plane and without z -direction restraint, so that \mathbf{k}_t . Then, constitutive matrix is:

$$\mathbf{E} = \frac{E}{1-\nu^2} \begin{bmatrix} 1 & \nu & 0 \\ \nu & 1 & 0 \\ 0 & 0 & (1-\nu)/2 \end{bmatrix} \quad (28)$$

where E is the Young's modulus, ν the Poisson's ratio.

5.4.3 Axisymmetric case

Axisymmetric elements are defined as having a constant value of displacement in the circumferential or θ direction. These are similar to the two-dimensional element, except that it is used in the $r-z$ plane as shown in Fig. 17.

The stress and strain components for the element are:

$$\begin{aligned} \boldsymbol{\sigma}^T &= [\sigma_r \quad \sigma_\theta \quad \sigma_z \quad \tau_{rz}] \\ \boldsymbol{\varepsilon}^T &= [\varepsilon_r \quad \varepsilon_\theta \quad \varepsilon_z \quad \gamma_{rz}] \end{aligned} \quad (29)$$

where the strains are defined as follows, with u and w being the displacements in the r and z directions respectively:

$$\varepsilon_r = \frac{\partial u}{\partial r}, \quad \varepsilon_\theta = \frac{u}{r}, \quad \varepsilon_z = \frac{\partial w}{\partial z}, \quad \gamma_{rz} = \frac{\partial u}{\partial z} + \frac{\partial w}{\partial r} \quad (30)$$

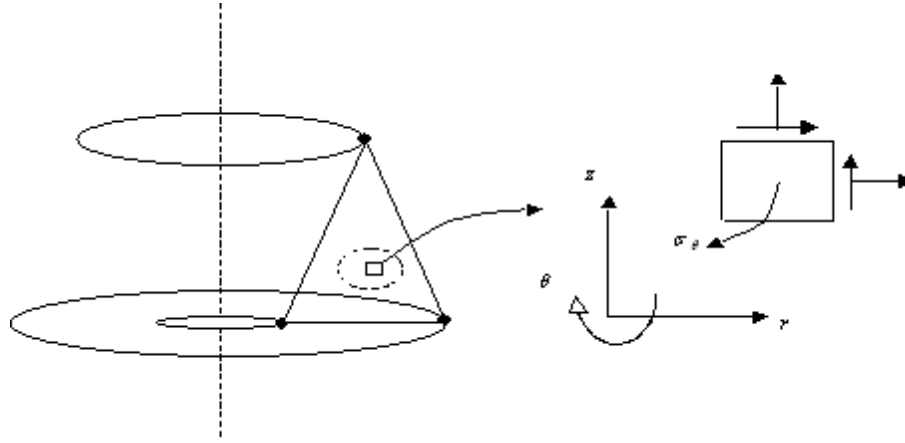


Fig. 17. Basic axisymmetric element and stress components.

The constitutive matrix that linking the stresses and strains is:

$$\mathbf{E} = \frac{E}{(1+\nu)(1-2\nu)} \begin{bmatrix} 1-\nu & \nu & \nu & 0 \\ \nu & 1-\nu & \nu & 0 \\ \nu & \nu & 1-\nu & 0 \\ 0 & 0 & 0 & \frac{1-2\nu}{2} \end{bmatrix} \quad (31)$$

where E is the Young's modulus, ν the Poisson's ratio.

The two-dimensional isoparametric finite elements employed in GFAS are linear and quadratic triangles and quadrilaterals. Isoparametric finite elements are based on the parametric definition of both coordinate and displacement functions. The same shape functions are used for specification of the element shape and for interpolation of the displacement field.

5.5 Finite element types

Displacements (u , v) in a plane element are interpolated from nodal displacements (u_i , v_i) using

shape functions N_i as follows:

$$\begin{Bmatrix} u \\ v \end{Bmatrix} = \begin{bmatrix} N_1 & 0 & N_2 & 0 & \dots \\ 0 & N_1 & 0 & N_2 & \dots \end{bmatrix} \begin{Bmatrix} u_1 \\ v_1 \\ u_2 \\ v_2 \\ \dots \end{Bmatrix} \quad (32)$$

$$\mathbf{u} = \mathbf{N}\mathbf{d} \quad (33)$$

where \mathbf{N} is the *shape function matrix*, \mathbf{u} the displacement vector and \mathbf{d} the *nodal* displacement vector. Here we have assumed that u depends on the nodal values of u only, and v on nodal values of v only.

From strain-displacement relation, the strain vector is:

$$\begin{aligned} \boldsymbol{\varepsilon} &= \mathbf{D}\mathbf{u} = \mathbf{D}\mathbf{N}\mathbf{d} \\ \boldsymbol{\varepsilon} &= \mathbf{B}\mathbf{d} \end{aligned} \quad (34)$$

where

$$\mathbf{B} = \mathbf{D}\mathbf{N} \quad (35)$$

is the strain-displacement matrix.

Consider the strain energy stored in an element:

$$\begin{aligned} U &= \frac{1}{2} \int_V \boldsymbol{\sigma}^T \boldsymbol{\varepsilon} dV = \frac{1}{2} \int_V (\sigma_x \varepsilon_x + \sigma_y \varepsilon_y + \tau_{xy} \gamma_{xy}) dV = \frac{1}{2} \int_V (\boldsymbol{\varepsilon} \boldsymbol{\sigma})^T dV = \frac{1}{2} \int_V \boldsymbol{\varepsilon}^T \mathbf{E} \boldsymbol{\varepsilon} dV \\ &= \frac{1}{2} \mathbf{d}^T \int_V \mathbf{B}^T \mathbf{E} \mathbf{B} dV \mathbf{d} \\ &= \frac{1}{2} \mathbf{d}^T \mathbf{k} \mathbf{d} \end{aligned} \quad (36)$$

From this, we obtain the general formula for the element stiffness matrix:

$$\mathbf{k} = \int_V \mathbf{B}^T \mathbf{E} \mathbf{B} dV \quad (37)$$

where the constitutive matrix \mathbf{E} is given by the stress-strain relation. The stiffness matrix \mathbf{k} defined by the above formula is symmetric since the constitutive matrix \mathbf{E} is symmetric.

5.5.1 Constant strain triangle (T3)

The two-dimensional simplex element is a triangle as shown in Fig. 18, it has two degrees of freedom at each node. It is also called *linear triangular element*.

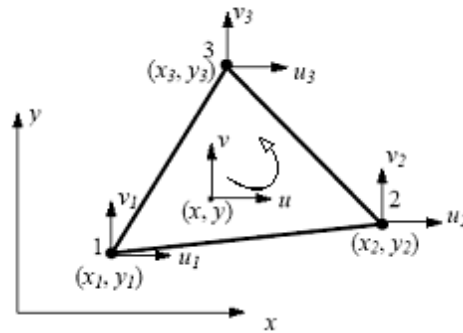


Fig. 18. Linear triangle finite element (T3)

For this element, we have three nodes at the vertices of the triangle, which are numbered around the element in the counterclockwise direction. Each node has two degrees of freedom (can move in the x and y directions). The displacements u and v are assumed to be linear functions within the element that is:

$$\begin{aligned} u &= \alpha_0 + \alpha_1 x + \alpha_2 y \\ v &= \beta_0 + \beta_1 x + \beta_2 y \end{aligned} \quad (38)$$

The constants α and β are determined imposing the nodal conditions. Solving the system of equations we can find the coefficients in terms of nodal displacements and coordinates.

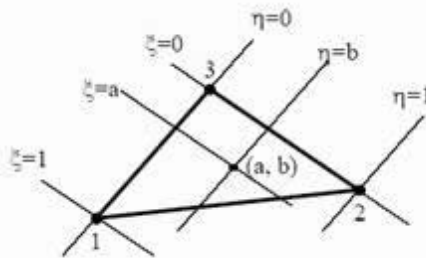


Fig. 19 The natural coordinates for linear triangle finite element

Introducing the natural coordinates (ξ, η) on the triangle (Fig.19), the shape functions can be represented by:

$$N_1 = \xi, \quad N_2 = \eta, \quad N_3 = 1 - \xi - \eta \quad (39)$$

Thus, in terms of nodal d.o.f the displacement field is:

$$\begin{Bmatrix} u \\ v \end{Bmatrix} = \begin{bmatrix} N_1 & 0 & N_2 & 0 & N_3 & 0 \\ 0 & N_1 & 0 & N_2 & 0 & N_3 \end{bmatrix} \begin{Bmatrix} u_1 \\ v_1 \\ u_2 \\ v_2 \\ u_3 \\ v_3 \end{Bmatrix} \quad (40)$$

We have two coordinate systems for the element: the global coordinates (x, y) and the natural coordinates (ξ, η) . The relation between two is given by:

$$\begin{cases} x = N_1 x_1 + N_2 x_2 + N_3 x_3 \\ y = N_1 y_1 + N_2 y_2 + N_3 y_3 \end{cases} \quad (41)$$

Displacement u or v on the element can be viewed as functions of (x, y) or (ξ, η) . Using the chain rule for derivatives, we have:

$$\begin{Bmatrix} \frac{\partial u}{\partial \xi} \\ \frac{\partial u}{\partial \eta} \end{Bmatrix} = \begin{bmatrix} \frac{\partial x}{\partial \xi} & \frac{\partial y}{\partial \xi} \\ \frac{\partial x}{\partial \eta} & \frac{\partial y}{\partial \eta} \end{bmatrix} \begin{Bmatrix} \frac{\partial u}{\partial x} \\ \frac{\partial u}{\partial y} \end{Bmatrix} = \mathbf{J} \begin{Bmatrix} \frac{\partial u}{\partial x} \\ \frac{\partial u}{\partial y} \end{Bmatrix} \quad (42)$$

where \mathbf{J} is called the Jacobian matrix of the transformation.

5.5.2 Linear Strain Triangle (T6)

This element is also called quadratic triangular element.

There are six nodes on this element: three corner nodes and three mid-side nodes (Fig.20). Each node has two degrees of freedom (DOF). The displacements (u, v) are assumed to be quadratic functions of (x, y) .

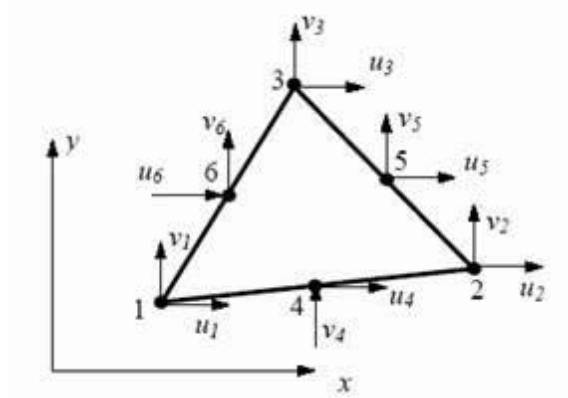


Fig.20. Quadratic triangular element.

$$\left. \begin{aligned} u &= \alpha_0 + \alpha_1 x + \alpha_2 y + \alpha_3 x^2 + \alpha_4 xy + \alpha_5 y^2 \\ v &= \beta_0 + \beta_1 x + \beta_2 y + \beta_3 x^2 + \beta_4 xy + \beta_5 y^2 \end{aligned} \right\} \quad (43)$$

From these, the strains are linear functions, thus we have the "linear strain triangle" (LST), which provides better results than the CST.

In the natural coordinate system, defined earlier, the six shape functions for the LST element are:

$$\left. \begin{aligned} N_1 &= \xi(2\xi - 1) \\ N_2 &= \eta(2\eta - 1) \\ N_3 &= \zeta(2\zeta - 1) \\ N_4 &= 4\xi\eta \\ N_5 &= 4\eta\zeta \\ N_6 &= 4\zeta\xi \end{aligned} \right\} \quad (44)$$

in which $\zeta = 1 - \xi - \eta$.

Displacements can be written as:

$$\left. \begin{aligned} u &= \sum_{i=1}^6 N_i u_i \\ v &= \sum_{i=1}^6 N_i v_i \end{aligned} \right\} \quad (45)$$

The element stiffness matrix is still given by:

$$\mathbf{k} = \int_V \mathbf{B}^T \mathbf{E} \mathbf{B} dV \quad (46)$$

but here $\mathbf{B}^T \mathbf{E} \mathbf{B}$ is quadratic in x and y . The integral is computed numerically.

5.5.3 Linear Quadrilateral Element (Q4)

There are four nodes at the corners of the quadrilateral shape (Fig.21). In the natural coordinate system (ξ, η) , the four shape functions are:

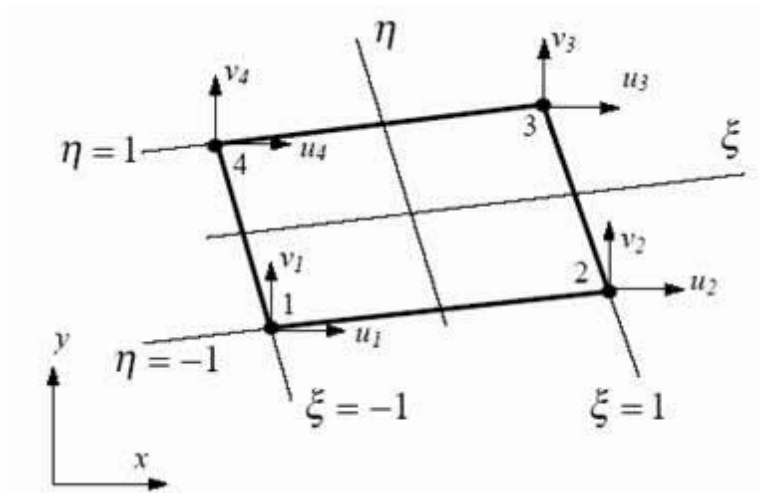


Fig. 21. Linear quadrilateral element (Q4).

$$\begin{aligned} N_1 &= \frac{1}{4}(1 - \xi)(1 - \eta) \\ N_2 &= \frac{1}{4}(1 + \xi)(1 - \eta) \\ N_3 &= \frac{1}{4}(1 + \xi)(1 + \eta) \\ N_4 &= \frac{1}{4}(1 - \xi)(1 + \eta) \end{aligned} \quad (47)$$

The displacement field is given by:

$$\begin{aligned} u &= \sum_{i=1}^4 N_i u_i \\ v &= \sum_{i=1}^4 N_i v_i \end{aligned} \quad (48)$$

which are bilinear functions over the element.

5.5.4 Quadratic Quadrilateral Element (Q8)

There are eight nodes for this element, four corner nodes and four mid-side nodes (Fig.22). In the natural coordinate system (ξ, η) , the eight shape functions are:

$$\begin{aligned} N_1 &= \frac{1}{4} (1 - \xi)(\eta - 1)(\xi + \eta + 1) \\ N_2 &= \frac{1}{4} (1 + \xi)(\eta - 1)(-\xi + \eta + 1) \\ N_3 &= \frac{1}{4} (1 + \xi)(\eta + 1)(\xi + \eta - 1) \\ N_4 &= \frac{1}{4} (\xi - 1)(\eta + 1)(\xi - \eta + 1) \\ N_5 &= \frac{1}{2} (1 - \eta)(1 - \xi^2) \\ N_6 &= \frac{1}{2} (1 + \xi)(1 - \eta^2) \\ N_7 &= \frac{1}{2} (1 + \eta)(1 - \xi^2) \\ N_8 &= \frac{1}{2} (1 - \xi)(1 - \eta^2) \end{aligned} \quad (49)$$

The displacement field is given by:

$$\begin{aligned}
 u &= \sum_{i=1}^8 N_i u_i \\
 v &= \sum_{i=1}^8 N_i v_i
 \end{aligned}
 \tag{50}$$

which are quadratic functions over the element. Strains and stresses over a quadratic quadrilateral element are linear functions that are better representations.

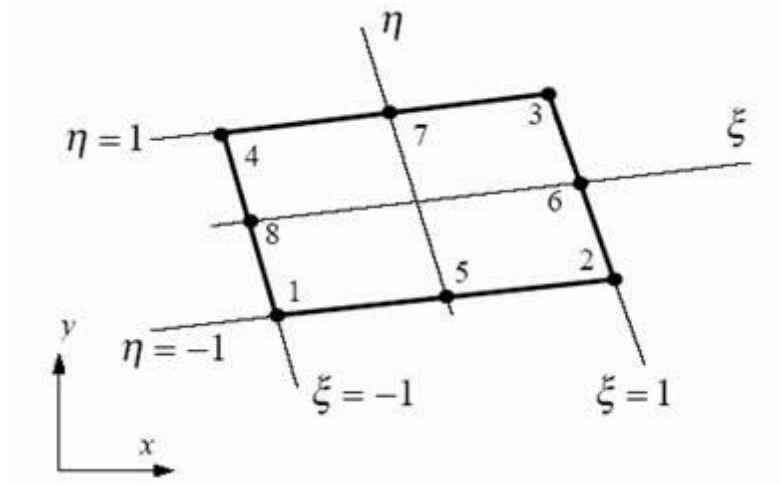


Fig.22. Quadratic quadrilateral element (Q8).

5.6 Numerical integration in finite elements

Integration of expressions for stiffness matrices and load vectors can not be performed analytically for general case of isoparametric elements. Instead, stiffness matrices and load vectors are typically evaluated numerically using Gauss quadrature rule over triangular or quadrilateral regions. The Gauss quadrature formula for the domain integral in two-dimensional case (natural coordinates) is of the form:

$$I = \int_{-1}^1 \int_{-1}^1 f(\xi, \eta) d\xi d\eta = \sum_{i=1}^n H_i f(\xi_i, \eta_i)
 \tag{51}$$

where ξ_i, η_j are abscissas and H_i are weighting functions of the Gauss integration rule.

The sampling points and weighting functions used for quadrilateral elements are shown in Table 3.

A pattern of either 2 x 2 or 3 x 3 sampling points is used, depending on the order of the function to be evaluated. Generally the four-point formula is used for the 4-noded quadrilateral, while the nine-point formula is used for the 8-noded element.

The general 8-node quadrilateral element stiffness matrix contains fourth order polynomial terms and thus requires nine sampling points for exact integration. It is often the case, however, that the use of "reduced" integration by using the four integration points improves the performance of this element. This is found to be particularly true in the plasticity applications.

Table 3. Gauss quadrature weights and sampling points for quadrilateral elements.

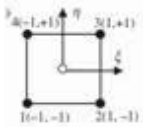
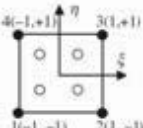
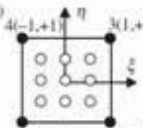
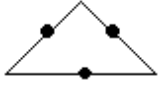
Sampling points location	Degree of polynomial	n	Coordinates		Weighting functions
			ξ	η	
	1	1	0	0	4
	3	4	-1/√3 1/√3 -1/√3 1/√3	-1/√3 -1/√3 1/√3 1/√3	1 1 1 1
	4	9	-√3/5 0 √3/5 -√3/5 0 √3/5 -√3/5 0 √3/5	-√3/5 -√3/5 -√3/5 0 0 0 √3/5 √3/5 √3/5	25/81 40/81 25/81 40/81 64/81 40/81 25/81 40/81 25/81

Table 4. Gauss quadrature weights and sampling points for triangular elements.

Sampling points location	Degree of polynomial	n	Coordinates		Weighting functions
			ξ	η	
	1	1	1/3	1/3	1/2
	2	3	1/2	1/2	1/6
			1/2	0	1/6
			0	1/2	1/6

The weights and quadrature points for triangular elements (constant strain triangle-T3 and linear strain triangle-T6) are summarized in Table 4.

5.7 Stress calculation

After computing the element matrices and vectors, the assembly process is used to compute the global equation system. Solution of the global equation system provides displacements at nodes of the finite element model. Post processing of the results is then required to calculate the strains and stresses in each element. For elasticity problems, the strains in an element are calculated from the displacements by:

$$\boldsymbol{\varepsilon} = \mathbf{B}\mathbf{U} \quad (52)$$

In simplex elements (CST-T3 for instance) the strain-displacement matrix \mathbf{B} is a constant, and the strains are constant, and therefore can be computed anywhere in the element. For the higher-order elements, however, \mathbf{B} is a function of the coordinate system (displacements) and not always explicit. Therefore the strains must be evaluated at specific positions in such elements. The most accurate locations are the sampling points used to calculate the strain-displacement matrix \mathbf{B} and the stiffness matrix \mathbf{k} .

Stresses are calculated with the Hook's law. These stresses can be computed anywhere in the

element but have best precision at the Gaussian integration points used for the stiffness element formulation. For instance for the 4-noded quadrilateral element the stresses have best precision at 2x2 integration points as shown in the Figure 23.

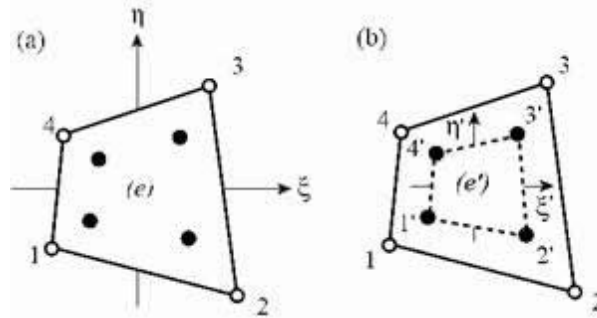


Fig.23. Extrapolation from 4-node quadrilateral sampling points; (a) 2 x 2 rule. (b) Gauss element (e')

In order to build a continuous field of stresses it is necessary to extrapolate result values from the integration points to the nodes of the finite element. The stresses of the nodes, particularly those at the corners of the element, are more useful. To calculate the nodal stresses, either the \mathbf{B} matrix must be calculated at the nodes, or the stresses must be interpolated from the values at the sampling points. A possible way to create continuous stress field with reasonable accuracy consists of: 1) extrapolation of stresses from reduced integration points to nodes; 2) averaging contributions from finite elements at all nodes of the finite element model. The interpolation-extrapolation process is described as follows.

Let's assume that stresses have been computed at the four Gauss points of a 4-noded quadrilateral plane element (points 1', 2', 3' and 4'). We now wish to interpolate or extrapolate these stresses to other points in element. In Figure 23 the coordinate ξ' is proportional with ξ and η' with η . At point 3' $\xi'=1$ and $\eta'=1$ and $\xi=\eta=1/\sqrt{3}$. That is

$$\begin{aligned}\xi' &= \xi\sqrt{3} \\ \eta' &= \eta\sqrt{3}\end{aligned}\quad (52)$$

Stresses at any point P in the element are found by the usual shape functions assumed for the displacement field interpolation:

$$\sigma_P = \sum_{i=1}^4 N_i \sigma_i \quad (53)$$

where σ is $\sigma_x, \sigma_y, \tau_{xy}$ respectively. The shape functions N_i are the bilinear shape functions:

$$N_i = \frac{1}{4} (1 \pm \xi')(1 \pm \eta') \quad (54)$$

The shape functions are evaluated at the ξ' , η' coordinates of point P . For example, let point P coincide with corner A . To calculate stress σ_x at this node from σ_x calculated at the four Gauss points we substitute $\xi' = \eta' = \sqrt{3}$ into the shape functions defined above and apply the formula given by the Eq.(53).

In the cases of triangular elements similar approach is applied. For instance for higher order 6-noded triangular finite element and three sampled Gauss points the stresses at any point in the element are computed using the shape functions as:

$$\sigma_P = \sum_{i=1}^3 N_i \sigma_i \quad (55)$$

where the shape functions N_i

$$\begin{aligned} N_1 &= \xi' \\ N_2 &= \eta' \\ N_3 &= 1 - \xi' - \eta' \end{aligned} \quad (56)$$

are computed at the ξ' , η' coordinates:

$$\begin{aligned} \xi' &= 2\xi - \frac{1}{3} \\ \eta' &= 2\eta - \frac{1}{3} \end{aligned} \quad (57)$$

As already stated these quadratures are lower order for higher order elements and represents the so called reduce integration scheme. The reduced integration scheme may be desirable for two reasons. First since the expense of generating a finite element matrix by numerical integration is proportional to the number of sampling points, using fewer sampling points means lower cost. Second, a lower-order rule tends to soften an element, thus countering the overly stiff behavior associated with an assumed displacement field. Stresses are usually averaged at nodes in FEA software to provide more accurate stress values. This option should be turned off at nodes between two materials or other discontinuity locations where discontinuity does exist. The stresses and strains at the centre of the element will be obtained through extrapolation of the stresses from the Gauss integration points.

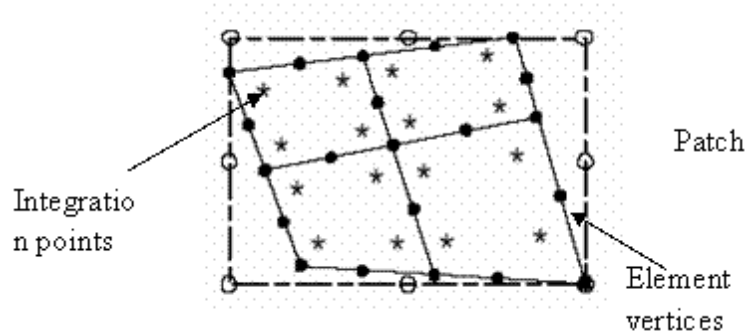


Fig. 24. Super convergent Patch Stress Recovery.

Moreover in the computer program is implemented a very efficient technique called *Super Convergent Patch Stress Recovery (SCP)*. Basically the method use the concept of the local patch of elements sampled at their integration points to yield a smooth set of least square fit nodal stresses (Fig. 24). As noted earlier, the integration points are special points where the stresses have the best values, those gradient locations match those of polynomials of one ore more degrees higher.

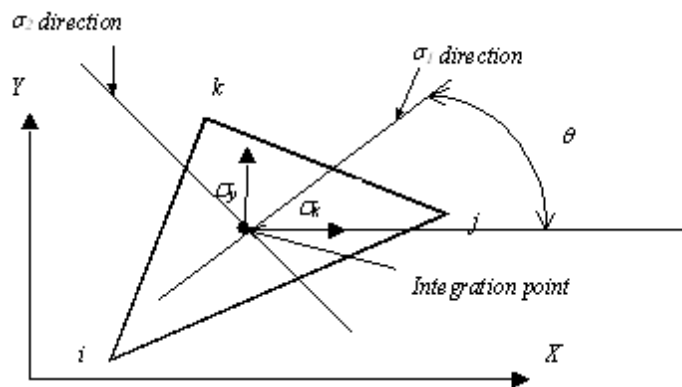


Fig. 25. Principal stresses.

The user is often interested not only in the individual stress components, but in some overall stress value such as Von-Misses stress. In case of plane stress, the Von-Misses stress is given by:

$$\sigma_v = \sqrt{\sigma_1^2 + \sigma_2^2 - 2\sigma_1 \sigma_2} \quad (58)$$

where σ_1 and σ_2 are principal stresses given by:

$$\sigma_{1,2} = \frac{\sigma_x + \sigma_y}{2} \pm \sqrt{\left(\frac{\sigma_x - \sigma_y}{2}\right)^2 + \tau_{xy}^2} \quad (59)$$

The angle formed by the principal stresses directions may be also computed (Fig. 25):

$$\tan 2\theta = \frac{2\tau_{xy}}{\sigma_y - \sigma_x}$$

The postprocessor display the stress contour, which typically are smoothed by working from nodal average stresses. These contours may be plotted as “stress bands” by designating equally spaced stress intervals, locating the areas of each element that fall into each interval, and using different colour to plot each interval.

5.8 Consistent element nodal loads

The consistent element nodal loads vector \mathbf{r}_e given by the Eq. (21) converts loads distributed throughout an element or over its surface or from initial strains or stress to discrete loads at element nodes. These loads are called consistent because they are based on the same shape functions as used to calculate the element stiffness matrix. Moreover these loads are statically equivalent to the original distributed loading; both \mathbf{r}_e and the original loading have the same resultant force and the same moment about an arbitrarily chosen point.

These loads are called work equivalent loads for the following reason: work done by nodal loads \mathbf{r}_e in going through nodal displacements \mathbf{d} is equal to work done by distributed loads \mathbf{F} and Φ in going through the displacement field associated with element shape function:

$$W = \mathbf{d}^T \mathbf{r}_e = \int_{\xi_i} \mathbf{d}^T \mathbf{N}^T \Phi dS = \int_{\xi_i} \mathbf{u}^T \Phi dS \quad (60)$$

The later integral sums the work of force increments ΦdS in going through displacements \mathbf{u} where \mathbf{u} are field displacements created by \mathbf{d} via shape functions \mathbf{N} .

5.8.1 Body forces

The forces are given by the following equation:

$$\mathbf{r}_{em} = \int_{V_e} \mathbf{N}^T \mathbf{F} dV_e \quad (61)$$

which can be detailed for a constant thickness finite element with n nodes as:

$$\mathbf{r}_{em} = \int_{V_e} \begin{bmatrix} N_1 & 0 \\ 0 & N_1 \\ N_2 & 0 \\ 0 & N_2 \\ \dots & \dots \\ N_n & 0 \\ 0 & N_n \end{bmatrix} \begin{bmatrix} F_x \\ F_y \end{bmatrix} dV_e = h \int_{V_e} \begin{bmatrix} N_1 F_x \\ N_1 F_y \\ N_2 F_x \\ N_2 F_y \\ \dots \\ N_n F_x \\ N_n F_y \end{bmatrix} dA_e \quad (62)$$

where F_x and F_y are the body forces about x and y axis such as gravity forces, inertial forces etc.

For instance the gravity-loading vector \mathbf{r}_{em} , in plane strain state ($h=1$) is accumulated element by element from integrals of the type:

$$\mathbf{r}_{em} = \sum_{i=1}^{No\ elements} \gamma \iint \mathbf{N}^T dx dy \quad (63)$$

where γ denotes the material density of the element and \mathbf{N} the shape function matrix. These calculations are performed in the same part of the program that forms the global stiffness matrix. It may be noted that only those freedoms corresponding to vertical movement are incorporated in the integrals. For instance for 3-noded finite elements the gravitational forces are computed as:

$$\mathbf{r}_{em} = -\frac{1}{3} h A_e \gamma \begin{bmatrix} 0 \\ 1 \\ 0 \\ 1 \\ 0 \\ 0 \\ 1 \end{bmatrix} \quad (64)$$

assuming that the element is referenced in the global system of coordinates such that the gravitational load acting along y axis.

5.8.2 Distributed forces

The distributed forces are given by the following equation:

$$\mathbf{r}_{es} = \int_{S_e} \mathbf{N}^T \mathbf{Q} dS_e \quad (65)$$

which can be detailed for a constant thickness n -noded isoparametric finite element as:

$$\mathbf{r}_{es} = \int_{S_e} \begin{bmatrix} N_1 & 0 \\ 0 & N_1 \\ N_2 & 0 \\ 0 & N_2 \\ \dots & \dots \\ N_n & 0 \\ 0 & N_n \end{bmatrix} \begin{bmatrix} Q_x \\ Q_y \end{bmatrix} dS_e \quad (66)$$

where Q_x and Q_y are the components of distributed load along the x and y axis, and because the thickness of the finite element is constant ($h=\text{const}$) $dS_e = h dl$ we obtain:

$$\mathbf{r}_{es} = h \int_{L_e} \begin{bmatrix} N_1 Q_x \\ N_1 Q_y \\ N_2 Q_x \\ N_2 Q_y \\ \dots \\ N_n Q_x \\ N_n Q_y \end{bmatrix} dl \quad (67)$$

5.8.3 Initial stress/strain loads

In this case the consistent equivalent nodal loads are given by the first two terms of the Eq. (21):

$$\mathbf{r}_{es} = \int_{V_e} \mathbf{B}^T \mathbf{E} \boldsymbol{\varepsilon}_0 dV_e - \int_{V_e} \mathbf{B}^T \boldsymbol{\sigma}_0 dV_e \quad (68)$$

These nodal loads are self equilibrating, produces zero resultant force and zero resultant moment. Some particular cases are given in order to illustrate the evaluation of the initial stress loads.

5.8.4 Pore pressure loads

The effect of free surface over soil massive is taken into account in two ways; the first consists in computation of the hydrostatic spectra computing the water pore pressures either through a rigorous steady state flow analysis and through an external loading due to reservoir water that act over the massive.

The pore pressures are computed at all submerged (Gauss integration samples) points and subtracted from the total normal stresses computed at the same locations following the application of surface and gravity loads. The resulting effective stresses are then used in the remaining parts of the algorithm relating to the assessment of yield functions and elasto-plastic stress redistribution.

If we denoted p the water pore pressures, meaning a potential of the volume forces, then over an infinitesimal element acting in both directions x - y of the plane the following forces:

$$p_x = -\frac{\partial p}{\partial x}, \quad p_y = -\frac{\partial p}{\partial y} \quad (69)$$

Let's assume an finite element e with nodes i,j,k and the potential of the volume forces at those nodes are p_i, p_j, p_k , then the forces potential for the considered element can be written as (stores the nodal values of the prescribed pore pressures) :

$$\mathbf{p}^e = [p_i \quad p_j \quad p_k]^T \quad (70)$$

Because for this potential we can chose the same shape functions as for the displacement field of the finite element, we can write analogous:

$$\mathbf{p} = [N_i \quad N_j \quad N_k] \mathbf{p}^e = \mathbf{N} \mathbf{p}^e \quad (71)$$

The effect of water pore pressure produce normal stresses σ'_0 , for plane strain analysis given by:

$$\sigma'_0 = \mathbf{m}\mathbf{p} \quad (72)$$

where for plane strain cases:

$$\mathbf{m} = [1 \quad 1 \quad 0]^T \quad (73)$$

The total stress vector then assumes the following form:

$$\sigma' = \sigma + \sigma'_0 = \mathbf{D}\boldsymbol{\varepsilon} + \mathbf{m}\mathbf{p} \quad (74)$$

Consequently, the general equilibrium relationship, given by the equation (21) of the finite element can be generalized, introducing the following term in the element equivalent nodal loads vector taking into account in this way the effect of the water pore pressures:

$$\mathbf{r}_{e,wp} = -\int_V \mathbf{B}^T \mathbf{m}\mathbf{p} dV = -\int_V (\mathbf{B}^T \mathbf{m}\mathbf{N} dV) \mathbf{p}^e \quad (75)$$

5.8.5 Excavation loads

When a portion of material (soil) is excavated, either in the open excavations (cuts) or in enclosed tunnels, forces must be applied along the excavated surface such that the remaining material should experience the correct stress relief effect and the new free surface is stress- free. Let us suppose that the body A is to be removed from body B as shown in Figure (26), and let us denote the stresses in the two part of the body before excavations as $\boldsymbol{\sigma}_A^0$ and $\boldsymbol{\sigma}_B^0$ respectively. Any external loads are taken into account in forming these stresses prior to removal of the body A . Since both bodies are in equilibrium forces \mathbf{F}_{AB} must be applied to body B due to body A to maintain $\boldsymbol{\sigma}_B^0$ and, similarly \mathbf{F}_{BA} must act on body A . These forces are equal in magnitude but are opposite in sign. The excavation forces acting on a boundary depend on the stress state in the excavated material and on the self-weight of that material. It can be shown that:

$$\mathbf{F}_{BA} = \int_{V_A} \mathbf{B}^T \boldsymbol{\sigma}_A^0 dV_A + \gamma \int_{V_A} \mathbf{N}^T dV_A \quad (76)$$

Where \mathbf{B} is the strain-displacement matrix, V_A the excavated volume, \mathbf{N} the element shape functions

and γ the soil unit weight.

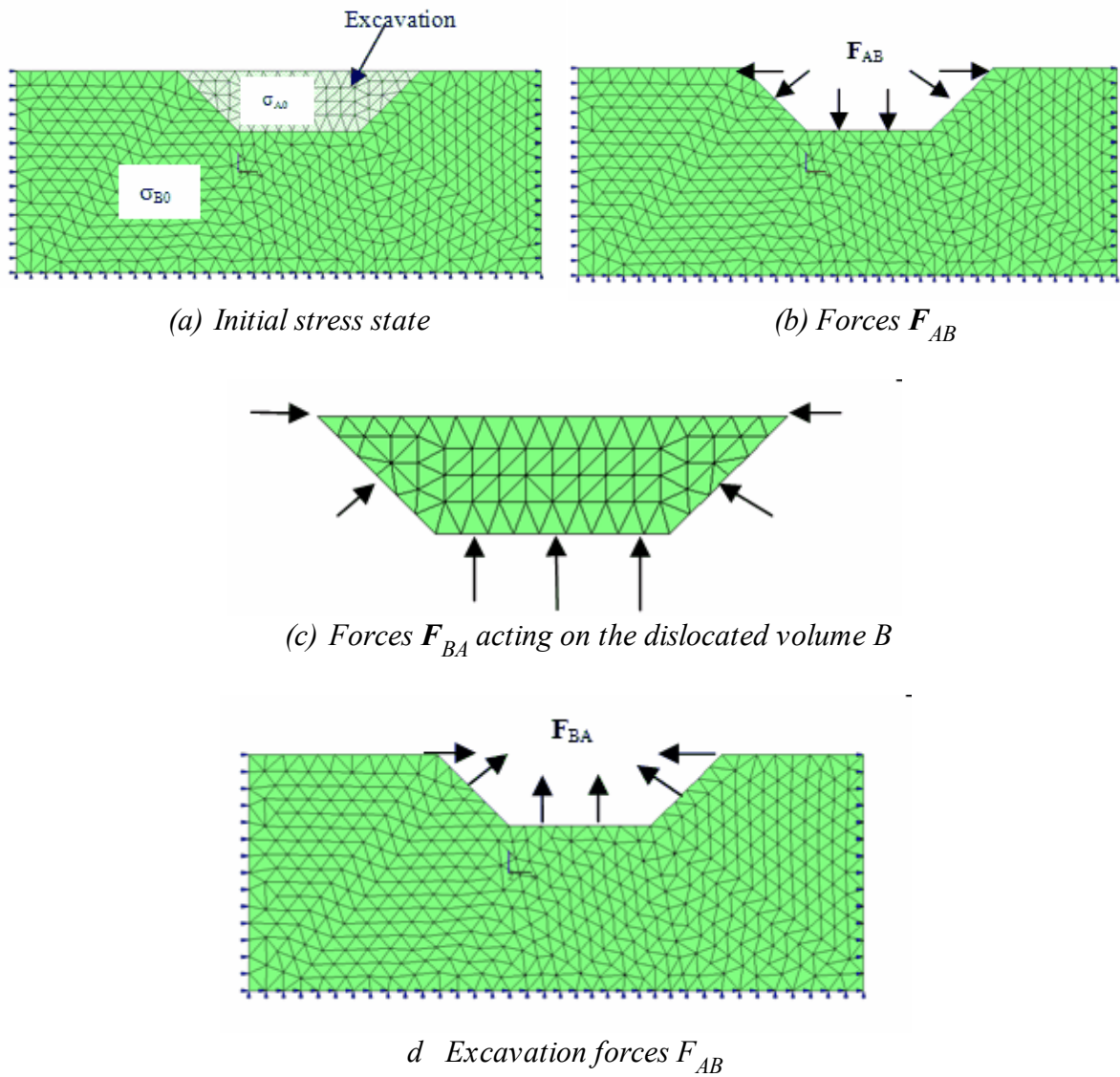


Fig. 26. Excavation loads

5.8.6 Gravity loading

The gravity-loading vector \mathbf{P}_a is accumulated element by element from integrals of the type:

$$\mathbf{P}_a = \sum_{i=1}^{\text{No. elements}} \gamma \iint \mathbf{N}^T dx dy \quad (77)$$

where γ denotes the material density of the element and \mathbf{N} the shape function matrix. These calculations are performed in the same part of the program that forms the global stiffness matrix. It may be noted that only those freedoms corresponding to vertical movement are incorporated in the integrals.

5.9 Assembly and storage strategy

The total system matrix (global stiffness matrix) is symmetrical provided its constituent matrices are symmetrical. The matrix also possesses the useful property of "bandedness" which means that the terms are concentrated around the "leading diagonal". This symmetry is also taken into account. The symmetrical half of a band matrix is stored as a rectangular array with a size equal to the number of system equations times the semi-bandwidth plus 1. In this case zeros are filled into the extra locations in the first few or last rows depending on whether the lower or upper "half" of the matrix is stored. Special storage scheme, the "skyline" technique is also implemented. To reduce storage requirements this technique is recommended. This has the effect of reducing the number of zero terms that would be stored in the stiffness matrix due to bandwidth variability using conventional (constant bandwidth) storage methods.

5.10 Incorporation of boundary conditions

Once the element equations have been assembled to give the system equations, the boundary conditions of the problem must be incorporated.

There are several ways in which the boundary conditions can be incorporated into the system equations.

5.10.1 Explicit specification of BC's

In the explicit method, the BC's conditions are incorporated through elimination of the lines and columns associated to the degree of freedoms blocked. This means that the equation components associated with these nodes are not required in the solution and information is given to the assembly routine that prevents these components from ever being assembled into the final system. Thus only the non-zero nodal values are solved for.

5.10.2 Imposing prescribed displacements (Penalty method)

This method uses the fact that computer computations have limited precision. The BC's conditions are handled by adding a "large" number, to the leading diagonal of the stiffness matrix in the row in which the prescribed value (i.e. a zero values means full fixity of degree of freedom) is required. The term in the same row of the right hand side vector is then set to the prescribed value multiplied by the augmented stiffness coefficient. Any structural degree of freedom can be prescribed in this way. Each prescription adds a large diagonal stiffness value to the stiffness matrix and also a large value to the load vector if the prescribed degree of freedom is nonzero. This procedure is successful if "small" terms are small relative to "large" terms (i.e. the stiffness matrix coefficients are indeed more small than the "large" value assumed).

5.10.3 Elastic supports

This method is very similar with the penalty method. The spring (elastic support) can be added to any structural degree of freedom. Each spring adds a prescribed value to the leading diagonal of the stiffness matrix in the row in which the prescribed value is required. Elastic supports, or springs, are

defined by entering spring constants in the X and/or Y directions. The spring constant is defined as the force or moment that will cause a unit displacement in the relevant direction. A very stiff spring (a large value, say 10^{20}) a zero displacement is enforced.

5.11 Solution of equilibrium equations

When the boundary conditions have been incorporated into the system equations, the final step is the solution for the unknown variables, the nodal displacements. Two methods have been implemented: Gaussian elimination technique with constant bandwidth storage scheme and Cholesky decomposition technique associated with a skyline storage strategy.

6 Formulation of the beam-column elements

In this section we outline the formulation of the line elements such those truss and beam elements used in the program to model the liners, bolts, anchors and geosynthetics elements.

6.1 Bar or truss elements

Figure 27 shows a straight bar whose nodal degrees of freedom are axial and transversal displacements (u_i, v_i, u_j, v_j). A linear displacement field is appropriate.

$$\begin{aligned}u_x &= \alpha_1 + \beta_1 x \\v_x &= \alpha_2 + \beta_2 x\end{aligned}\tag{78}$$

Imposing the limit conditions the displacement field can be rewritten as:

$$\begin{bmatrix} u \\ v \end{bmatrix} = \begin{bmatrix} N_1 & 0 & N_2 & 0 \\ 0 & N_1 & 0 & N_2 \end{bmatrix} \begin{bmatrix} u_i \\ v_i \\ u_j \\ v_j \end{bmatrix} \quad (79)$$

where the shape functions N_i are:

$$\begin{aligned} N_1 &= 1 - \xi \\ N_2 &= \xi \end{aligned} \quad (80)$$

and in which $\xi = x/L$

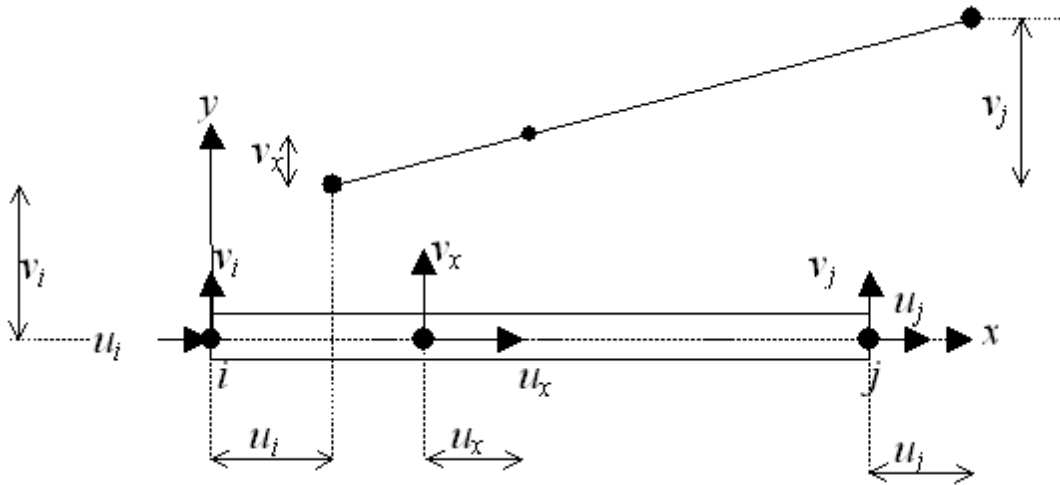


Figure.27. Truss element.

The axial strain along the element length is defined as:

$$\varepsilon_x = \frac{\partial u}{\partial x} = \begin{bmatrix} \frac{\partial}{\partial x} & 0 \end{bmatrix} \begin{bmatrix} u \\ v \end{bmatrix} = \begin{bmatrix} \frac{\partial}{\partial x} & 0 \end{bmatrix} \begin{bmatrix} N_1 & 0 & N_2 & 0 \\ 0 & N_1 & 0 & N_2 \end{bmatrix} \begin{bmatrix} u_i \\ v_i \\ u_j \\ v_j \end{bmatrix} \quad (81)$$

or in the matrix condensation form the displacements and strains relationships can be expressed as:

$$\boldsymbol{\varepsilon} = \mathbf{B}\mathbf{u} \quad (82)$$

where

$$\mathbf{B} = \partial \mathbf{N} = \begin{bmatrix} \frac{\partial N_1}{\partial x} & 0 & \frac{\partial N_2}{\partial x} & 0 \\ 0 & \frac{\partial N_1}{\partial \xi} & 0 & \frac{\partial N_2}{\partial \xi} \end{bmatrix} = \frac{1}{L} \begin{bmatrix} \frac{\partial N_1}{\partial \xi} & 0 & \frac{\partial N_2}{\partial \xi} & 0 \end{bmatrix} \quad (83)$$

and represents the strain-displacement operator.

The element stiffness matrix is computed in this case as:

$$\mathbf{k} = \frac{EA}{L} \int_0^L \mathbf{B}^T \mathbf{B} d\xi = \frac{EA}{L} \int_0^L \begin{bmatrix} -1 \\ 0 \\ 1 \\ 0 \end{bmatrix} \begin{bmatrix} 1 & 0 & -1 & 0 \\ 0 & 0 & 0 & 0 \\ -1 & 0 & 1 & 0 \\ 0 & 0 & 0 & 0 \end{bmatrix} d\xi = \frac{EA}{L} \begin{bmatrix} 1 & 0 & -1 & 0 \\ 0 & 0 & 0 & 0 \\ -1 & 0 & 1 & 0 \\ 0 & 0 & 0 & 0 \end{bmatrix} \quad (84)$$

Where EA represent the axial stiffness of the element (E is Young modulus, A cross-section area) and L the element length. The stiffness matrix \mathbf{k} defined above relates axial forces at the nodes, to the axial displacements at the nodes, and represents the stiffness

matrix in the local element system. If the bar is oriented at an angle β in the xy plane, the matrix must be transformed by a rotation matrix as:

$$\mathbf{K} = \mathbf{T}^T \mathbf{k} \mathbf{T} \quad (85)$$

where for the xy plane the rotation matrix is:

$$\mathbf{T} = \begin{bmatrix} \cos \beta & \sin \beta & 0 & 0 \\ -\sin \beta & \cos \beta & 0 & 0 \\ 0 & 0 & \cos \beta & \sin \beta \\ 0 & 0 & -\sin \beta & \cos \beta \end{bmatrix} \quad (86)$$

The element stiffness matrix in the global coordinates system becomes:

$$\mathbf{K} = \frac{EA}{L} \begin{bmatrix} \cos^2 \beta & \sin \beta \cos \beta & -\cos^2 \beta & -\sin \beta \cos \beta \\ \sin \beta \cos \beta & \sin^2 \beta & -\sin \beta \cos \beta & -\sin^2 \beta \\ -\cos^2 \beta & -\sin \beta \cos \beta & \cos^2 \beta & \sin \beta \cos \beta \\ -\sin \beta \cos \beta & -\sin^2 \beta & \sin \beta \cos \beta & \sin^2 \beta \end{bmatrix} \quad (87)$$

6.2 Two-noded beam-column element

Figure 28 shows a six degree of freedom straight beam-column element. Rotation θ is assumed to be small, so that $\theta \approx dw/dx$. The displacement field along the element is assumed to be the following shape (a linear shape for axial displacements and third degree polynomial for transversal

displacements):

$$u_x = \alpha + \alpha_1 x \quad (88)$$

$$v_x = \beta + \beta_1 x + \beta_2 x^2 + \beta_3 x^3$$

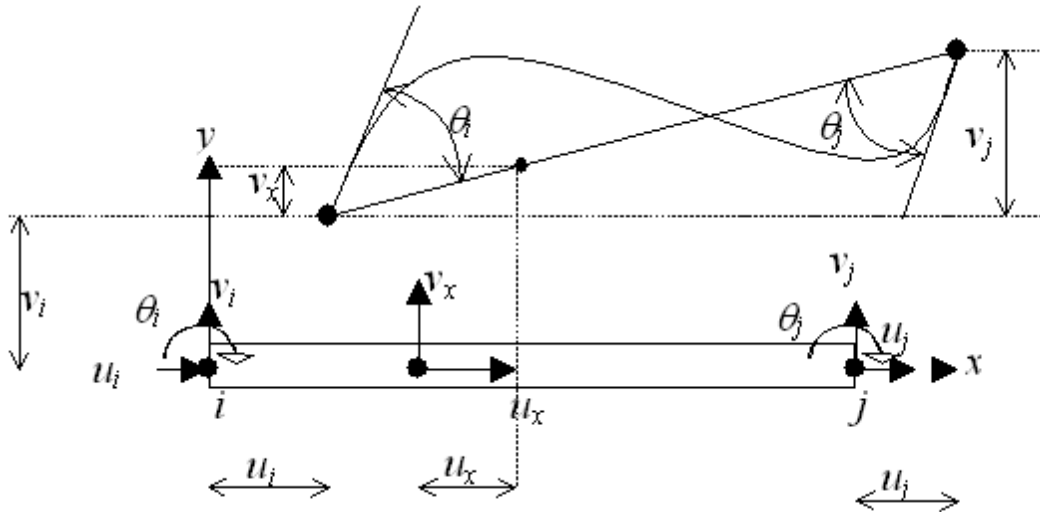


Fig. 28. Beam column element

The third degree polynomial shape has been chosen for the transverse displacements since for an element loaded only at the nodes the shear forces and bending moment variation along the element is constant and linear respectively:

$$M_x = \frac{d^2 v}{dx^2} = 2\beta_2 + 6\beta_3 x \quad (89)$$

$$T_x = \frac{d^3 v}{dx^3} = 6\beta_3$$

Imposing the limit conditions the displacement element field can be rewritten:

$$\begin{bmatrix} u \\ v \end{bmatrix} = \begin{bmatrix} N_1 & 0 & 0 & 0 & 0 & 0 \\ 0 & N_2 & 0 & 0 & 0 & 0 \\ 0 & 0 & N_3 & 0 & 0 & 0 \\ 0 & 0 & 0 & N_4 & 0 & 0 \\ 0 & 0 & 0 & 0 & N_5 & 0 \\ 0 & 0 & 0 & 0 & 0 & N_6 \end{bmatrix} \begin{bmatrix} u_i \\ v_i \\ \theta_i \\ u_j \\ v_j \\ \theta_j \end{bmatrix}$$

(90)

where the shape functions N_i in this case are:

$$\begin{aligned}
 N_1 &= 1 - \xi \\
 N_2 &= \xi \\
 N_3 &= 1 - 3\xi^2 + 2\xi^3 \\
 N_4 &= l(\xi - 2\xi^2 + \xi^3) \\
 N_5 &= 3\xi^2 - 2\xi^3 \\
 N_6 &= -l(\xi^2 - \xi^3)
 \end{aligned} \tag{91}$$

and in which $\xi = x/L$. Assuming a linear distribution of the strains along the cross-section (plain section hypothesis) the strain-displacement relationship is:

$$\varepsilon_x = \frac{\partial u}{\partial x} - y \frac{\partial^2 v}{\partial x^2} \tag{92}$$

or written in the matrix form:

$$\varepsilon_x = \begin{bmatrix} \frac{\partial}{\partial x} & -y \frac{\partial^2}{\partial x^2} \end{bmatrix} \begin{bmatrix} u \\ v \end{bmatrix} = \begin{bmatrix} \frac{\partial}{\partial x} & -y \frac{\partial^2}{\partial x^2} \\ 0 & N_3 & N_4 & 0 & N_5 & N_6 \end{bmatrix} \begin{bmatrix} u_i \\ v_i \\ \theta_i \\ u_j \\ v_j \\ \theta_j \end{bmatrix} \tag{93}$$

or in the matrix condensation form the displacements and strains relationships can be expressed as:

$$\boldsymbol{\varepsilon} = \mathbf{B}\mathbf{u} \tag{94}$$

where \mathbf{u} represents the nodal displacement vector, and \mathbf{B} represents the strain-displacement operator:

$$\boldsymbol{\varepsilon} = \mathbf{B}\mathbf{u} \tag{95}$$

$$\mathbf{u} = \begin{bmatrix} u_i & v_i & \theta_i & u_j & v_j & \theta_j \end{bmatrix}^T \tag{96}$$

$$\mathbf{B} = \begin{bmatrix} \frac{\partial}{\partial x} & -y \frac{\partial^2}{\partial x^2} & -y \frac{\partial^2}{\partial x^2} & \frac{\partial}{\partial x} & -y \frac{\partial^2}{\partial x^2} & -y \frac{\partial^2}{\partial x^2} \end{bmatrix} \tag{97}$$

or with the following relations:

$$\begin{aligned}
 \frac{\partial}{\partial x} &= \frac{1}{L} \frac{\partial}{\partial \xi} \\
 \frac{\partial^2}{\partial x^2} &= \frac{1}{L^2} \frac{\partial^2}{\partial \xi^2}
 \end{aligned} \tag{98}$$

and assuming a doubly symmetric cross-sections, the element stiffness matrix can be computed as:

$$\mathbf{k} = \begin{bmatrix} \frac{EA}{L} & 0 & 0 & -\frac{EA}{L} & 0 & 0 \\ 0 & \frac{12EI}{L^3} & \frac{6EI}{L^2} & 0 & -\frac{12EI}{L^3} & \frac{6EI}{L^2} \\ 0 & \frac{6EI}{L^2} & \frac{4EI}{L} & 0 & -\frac{6EI}{L^2} & \frac{2EI}{L} \\ -\frac{EA}{L} & 0 & 0 & \frac{EA}{L} & 0 & 0 \\ 0 & -\frac{12EI}{L^3} & -\frac{6EI}{L^2} & 0 & \frac{12EI}{L^3} & -\frac{6EI}{L^2} \\ 0 & \frac{6EI}{L^2} & \frac{2EI}{L} & 0 & -\frac{6EI}{L^2} & \frac{4EI}{L} \end{bmatrix}$$

With the definition of moment of inertia and cross-sectional area:

$$I = \int_A y^2 dA \quad (100)$$

$$A = \int_A dA$$

and for constant EI the element stiffness matrix given by the equation (99) is:

$$\mathbf{k} = \begin{bmatrix} \frac{EA}{L} & 0 & 0 & -\frac{EA}{L} & 0 & 0 \\ 0 & \frac{12EI}{L^3} & \frac{6EI}{L^2} & 0 & -\frac{12EI}{L^3} & \frac{6EI}{L^2} \\ 0 & \frac{6EI}{L^2} & \frac{4EI}{L} & 0 & -\frac{6EI}{L^2} & \frac{2EI}{L} \\ -\frac{EA}{L} & 0 & 0 & \frac{EA}{L} & 0 & 0 \\ 0 & -\frac{12EI}{L^3} & -\frac{6EI}{L^2} & 0 & \frac{12EI}{L^3} & -\frac{6EI}{L^2} \\ 0 & \frac{6EI}{L^2} & \frac{2EI}{L} & 0 & -\frac{6EI}{L^2} & \frac{4EI}{L} \end{bmatrix} \quad (101)$$

A slightly modified form of Eq. (101) is able to account for transverse shear deformation (Timoshenko beam-column).

$$\mathbf{k} = \begin{bmatrix} \frac{EA}{L} & 0 & 0 & -\frac{EA}{L} & 0 & 0 \\ 0 & \frac{12EI}{L^3(1+\Phi)} & \frac{6EI}{L^2(1+\Phi)} & 0 & -\frac{12EI}{L^3(1+\Phi)} & \frac{6EI}{L^2(1+\Phi)} \\ 0 & \frac{6EI}{L^2(1+\Phi)} & \frac{(4+\Phi)EI}{L(1+\Phi)} & 0 & -\frac{6EI}{L^2(1+\Phi)} & \frac{(2-\Phi)EI}{L(1+\Phi)} \\ -\frac{EA}{L} & 0 & 0 & \frac{EA}{L} & 0 & 0 \\ 0 & -\frac{12EI}{L^3(1+\Phi)} & -\frac{6EI}{L^2(1+\Phi)} & 0 & \frac{12EI}{L^3(1+\Phi)} & -\frac{6EI}{L^2(1+\Phi)} \\ 0 & \frac{6EI}{L^2(1+\Phi)} & \frac{(2-\Phi)EI}{L(1+\Phi)} & 0 & -\frac{6EI}{L^2(1+\Phi)} & \frac{(4+\Phi)EI}{L(1+\Phi)} \end{bmatrix} \quad (102)$$

$$\Phi = \frac{12EI}{GA_s L^2}$$

where

, G represents the shear modulus and A_s the shear area, and the product GA_s represents the shear rigidity.

The stiffness matrix if for the xy local element coordinate system oriented with the beam. If the beam is inclined at an angle β to the global coordinate axis X , the element stiffness matrix in global coordinate system is computed as:

$$\mathbf{K} = \mathbf{T}^T \mathbf{k} \mathbf{T} \quad (103)$$

where the rotation matrix \mathbf{T} has the following expression:

$$\mathbf{T} = \begin{bmatrix} \cos \beta & \sin \beta & 0 & 0 & 0 & 0 \\ -\sin \beta & \cos \beta & 0 & 0 & 0 & 0 \\ 0 & 0 & 1 & 0 & 0 & 0 \\ 0 & 0 & 0 & \cos \beta & \sin \beta & 0 \\ 0 & 0 & 0 & -\sin \beta & \cos \beta & 0 \\ 0 & 0 & 0 & 0 & 0 & 1 \end{bmatrix} \quad (104)$$

6.3 Joining beam-column elements to plane elements. Dissimilar elements.

By „*dissimilar elements*” we mean elements whose d.o.f. are of different type and/or of different location. As examples, considering the elements depicted in the Figure 29, the left end of a beam-column element is to be attached at an arbitrary location along an edge of plane four-node quadrilateral element, or we may wish to connect two force member (a truss element) to points arbitrarily located along edges (or inside) of a plane four-noded element. A way of dealing with these situations is to impose constraints that force d.o.f. of mating elements to have a prescribed relation to one another. A method of connecting these elements is briefly described in the following sections.

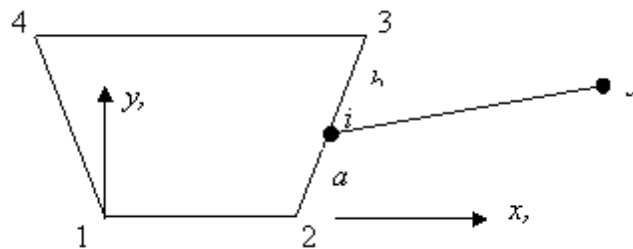


Figure 29. Dissimilar elements.

6.3.1 Beam-column element connected to a plane element

The beam-column element stiffness relation is:

$$\mathbf{k}'\mathbf{u}' = \mathbf{r}' \quad (105)$$

where the displacement and nodal load vectors are:

$$\begin{aligned} \mathbf{u}' &= [u_i \quad v_i \quad \theta_i \quad u_j \quad v_j \quad \theta_j]^T \\ \mathbf{r}' &= [f_{ix} \quad f_{iy} \quad m_i \quad f_{jx} \quad f_{jy} \quad m_j]^T \end{aligned} \quad (106)$$

We assume that the translational displacements at node i of the beam-column element are linearly interpolated along edge 2-3 from translational d.o.f at nodes 2 and 3 of plane element and that rotation θ_i is the same as the rotation of edge 2-3. In these conditions, between the beam-column displacements \mathbf{u}' and the plane element nodal displacements we can write:

$$\mathbf{u}' = \mathbf{T}\mathbf{u} \quad (107)$$

where, with $c = \cos \beta$, $s = \sin \beta$, the transformation matrix \mathbf{T} is:

$$\begin{aligned} \mathbf{T}_{[6 \times 7]} &= \begin{bmatrix} \mathbf{T}_{3[4 \times 3]} & \mathbf{0}_{[4 \times 3]} \\ \mathbf{0}_{[3 \times 3]} & \mathbf{I}_{[3 \times 3]} \end{bmatrix}, \text{ where} \\ \mathbf{T}_{3[4 \times 3]} &= \frac{1}{L} \begin{bmatrix} a & 0 & b & 0 \\ 0 & a & 0 & b \\ c & s & -c & -s \end{bmatrix} \end{aligned} \quad (108)$$

and the displacement vector \mathbf{u} contains the displacements of the plane element and displacements at the free node j of the beam-column element:

$$\mathbf{u} = [u_2 \quad v_2 \quad u_3 \quad v_3 \quad u_j \quad v_j \quad \theta_j]^T \quad (109)$$

Applying the principle of virtual displacements if between the displacement \mathbf{u} and \mathbf{u}' the relation (107) holds then for the nodal force vectors \mathbf{r} we can write a similar relation as:

$$\mathbf{r} = \mathbf{T}^T \mathbf{r}' \quad (110)$$

We can argue that since \mathbf{r} and \mathbf{r}' describe the same resultant force, and the work done by the force during a prescribed virtual displacement must be independent of the coordinate system in which the

work is computed. In this conditions, multiply the both terms of eq.(105) with \mathbf{T}^T and using the equation (107) for displacement vector \mathbf{u}' the equation (105) becomes:

$$\mathbf{T}^T \mathbf{k}' \mathbf{T} \mathbf{u} = \mathbf{T}^T \mathbf{r}' \quad (111)$$

or in matrix condensed form:

$$\mathbf{k} \mathbf{u} = \mathbf{r} \quad (112)$$

where the modified stiffness matrix of the beam-column element is:

$$\mathbf{k} = \mathbf{T}^T \mathbf{k}' \mathbf{T} \quad (113)$$

and the modified nodal load vector \mathbf{r} is given in equation (111). In this way for the new element the stiffness relation is given by the eq.(113) and the plane element and beam-column element can now be assembled to one another or assembled into the rest of the structure. Node i and its degrees of freedom do not appear in the assembled structures. Node i may be called a “slave” node because its d.o.f. are completely determined by d.o.f. of “master” nodes 2 and 3. Similar relations can be obtained in the case when the beam-column element is mapped in to the higher order plane elements. In this case the nodal displacements of the beam element are quadratically interpolated from translational d.o.f of plane element nodes.

6.3.2 Truss element connected to a plane element

Let us consider the truss element connected to points arbitrarily located along edges of a plane four-noded element (Fig.30).

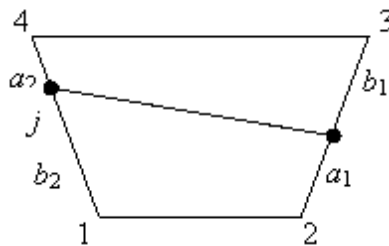


Figure 30.

The deformational-stiffness relation for the truss element is written as:

$$\mathbf{k}' \mathbf{u}' = \mathbf{r}' \quad (114)$$

where \mathbf{k}' , \mathbf{u}' and \mathbf{r}' represents the stiffness matrix, displacement vector and nodal force vector associated with the degrees of freedom of nodes i and j of the truss element:

$$\mathbf{u}' = \begin{bmatrix} u_i & v_i & u_j & v_j \end{bmatrix}^T \quad (115)$$

With displacements linearly interpolated along edges of the quadrilateral the displacement transformation for d.o.f. of the truss element can be written in function of the displacements of the plane element nodes (\mathbf{u}), via transformation matrix \mathbf{T} as:

$$\mathbf{u}' = \mathbf{T} \mathbf{u} \quad (116)$$

Where the transformation matrix \mathbf{T} contains terms like those in the eq. (108). For the case depicted in the Figure 30 the displacement transformation relation can be detailed in the matrix form as:

$$\begin{bmatrix} u_i \\ v_i \\ u_j \\ v_j \end{bmatrix} = \begin{bmatrix} 0 & 0 & b_1/l1 & 0 & a_1/l1 & 0 & 0 & 0 \\ 0 & 0 & 0 & b_1/l1 & 0 & a_1/l1 & 0 & 0 \\ a_2/l2 & 0 & 0 & 0 & 0 & 0 & b_2/l2 & 0 \\ 0 & a_2/l2 & 0 & 0 & 0 & 0 & 0 & b_2/l2 \end{bmatrix} \begin{bmatrix} u_1 \\ v_1 \\ u_2 \\ v_2 \\ u_3 \\ v_3 \\ u_4 \\ v_4 \end{bmatrix} \quad (117)$$

By transformation, \mathbf{k}' and \mathbf{r}' of the truss element are to be converted to \mathbf{k} and \mathbf{r} which are associated with the degrees of freedom of the four corner nodes of the quadrilateral. Thus, $\mathbf{r}'_{[4 \times 1]}$ becomes $\mathbf{r}_{[8 \times 1]}$ and $\mathbf{k}'_{[4 \times 4]}$ becomes $\mathbf{k}_{[8 \times 8]}$:

$$\begin{aligned} \mathbf{k}_{[8 \times 8]} &= \mathbf{T}_{[8 \times 4]}^T \mathbf{k}'_{[4 \times 4]} \mathbf{T}_{[4 \times 8]} \\ \mathbf{r}_{[8 \times 1]} &= \mathbf{T}_{[8 \times 4]}^T \mathbf{r}'_{[4 \times 1]} \end{aligned} \quad (118)$$

After this transformations the nodal force vector and stiffness matrix can be directly added to the corresponding arrays of the quadrilateral or assembled into the structure. The nodes i and j of the truss element and their d.o.f. are not explicitly present, we can say that d.o.f. of the bar element are constrained to follow d.o.f. of the quadrilateral. Similar relations can be obtained in the case when the truss element is mapped into the higher order plane elements. In this case the nodal displacements of the truss element are quadratically interpolated from translational d.o.f of plane element nodes. For instance assuming the six-noded higher order element crossed by the truss element the displacement transformation relation is:

$$\mathbf{u}'_{[4 \times 1]} = \mathbf{T}_{[4 \times 12]} \mathbf{u}_{[12 \times 1]} \quad (119)$$

and in which

$$\mathbf{u}^i_{[4 \times 1]} = \begin{bmatrix} u_i & v_i & u_j & v_j \end{bmatrix}^T \quad (120)$$

$$\mathbf{u}_{[12 \times 1]} = [u_1 \ v_1 \ u_2 \ v_2 \ u_3 \ v_3 \ u_4 \ v_4 \ u_5 \ v_5 \ u_6 \ v_6]^T \quad (121)$$

$$\mathbf{T}_{[12 \times 12]} = \begin{bmatrix} \alpha_i & 0 & \beta_i & 0 & \gamma_i & 0 & 0 & 0 & 0 & 0 & 0 & 0 \\ 0 & \alpha_i & 0 & \beta_i & 0 & \gamma_i & 0 & 0 & 0 & 0 & 0 & 0 \\ 0 & 0 & 0 & 0 & 0 & 0 & \alpha_j & 0 & \beta_j & 0 & \gamma_j & 0 \\ 0 & 0 & 0 & 0 & 0 & 0 & 0 & \alpha_j & 0 & \beta_j & 0 & \gamma_j \end{bmatrix} \quad (122)$$

where:

$$\begin{aligned} \alpha_i &= 2 \left(\frac{b_i}{l_i} \right)^2 - 3 \left(\frac{b_i}{l_i} \right) + 1 \\ \beta_i &= 4 \left(\frac{b_i}{l_i} \right) - 4 \left(\frac{b_i}{l_i} \right)^2 \\ \gamma_i &= 2 \left(\frac{b_i}{l_i} \right)^2 - \left(\frac{b_i}{l_i} \right) \end{aligned} \quad (123)$$

This approach can be applied even when the truss element nodes fall inside the plane element. For instance considering the truss element with nodes i and j within the triangular 3-noded element like in the Figure 31.

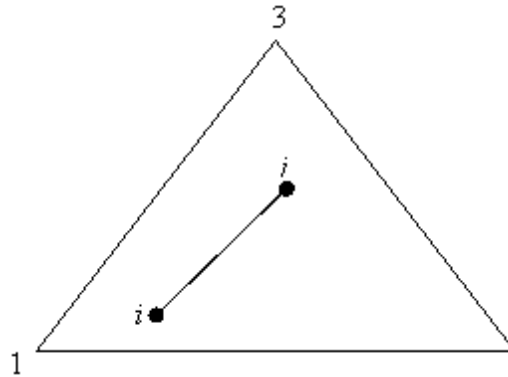


Figure 31.

The displacements of the element nodes can be obtained throughout shape functions of the “parent element” as:

$$\begin{bmatrix} u_i \\ v_i \\ u_j \\ v_j \end{bmatrix} = \begin{bmatrix} N_1^i & 0 & N_2^i & 0 & N_3^i & 0 \\ 0 & N_1^i & 0 & N_2^i & 0 & N_3^i \\ N_1^j & 0 & N_2^j & 0 & N_3^j & 0 \\ 0 & N_1^j & 0 & N_2^j & 0 & N_3^j \end{bmatrix} \begin{bmatrix} u_1 \\ v_1 \\ u_2 \\ v_2 \\ u_3 \\ v_3 \end{bmatrix} \quad (124)$$

where $N_k^{i(j)}$, $k=1,2,3$ represents the shape functions for the triangular element computed for each node coordinates of the truss element. Hence the stiffness matrix and nodal force vector are obtained in this case:

$$\begin{aligned} \mathbf{k}_{[6 \times 6]} &= \mathbf{T}_{[6 \times 4]}^T \mathbf{k}'_{[4 \times 4]} \mathbf{T}_{[4 \times 6]} \\ \mathbf{r}_{[6 \times 1]} &= \mathbf{T}_{[6 \times 4]}^T \mathbf{r}'_{[4 \times 1]} \end{aligned} \quad (125)$$

Where the transformation matrix in this case is:

$$\mathbf{T}_{[4 \times 6]} = \begin{bmatrix} N_1^i & 0 & N_2^i & 0 & N_3^i & 0 \\ 0 & N_1^i & 0 & N_2^i & 0 & N_3^i \\ N_1^j & 0 & N_2^j & 0 & N_3^j & 0 \\ 0 & N_1^j & 0 & N_2^j & 0 & N_3^j \end{bmatrix} \quad (126)$$

Similar transformation matrices can be obtained when quadrilateral or higher order plane elements are used. The shape functions are computed in truss element nodes with known coordinates. Usually these coordinates are given in the global coordinates whereas the shape functions of the plane elements are given in the natural coordinate systems. Therefore some transformations are also necessary to obtain the coordinates of the truss element nodes in the natural coordinates. These transformations are based on the isotropic character of the plane element used. For triangular elements the global coordinates (x, y) and the natural coordinates (ξ, η) . are related as:

$$\begin{cases} x = N_1 x_1 + N_2 x_2 + N_3 x_3 \\ y = N_1 y_1 + N_2 y_2 + N_3 y_3 \end{cases} \quad (127)$$

in which x_i, y_i ($i=1,2,3$) represents the coordinates of the triangular element nodes and the shape functions N_i have the following expressions represented in the natural coordinate system as:

$$N_1 = \xi, \quad N_2 = \eta, \quad N_3 = 1 - \xi - \eta \quad (128)$$

For the known x, y coordinates we can obtain the corresponding natural coordinates by solving the following system of equations:

$$\begin{bmatrix} x_1 - x_3 & x_2 - x_3 \\ y_1 - y_3 & y_2 - y_3 \end{bmatrix} \begin{bmatrix} \xi \\ \eta \end{bmatrix} = \begin{bmatrix} x - x_3 \\ y - y_3 \end{bmatrix} \quad (129)$$

Similarly we can obtain the natural coordinates in the case when the plane element is quadrilateral.

6.3.3 Bolts elements

The bolts pass through the elements in the mesh, and are modelled by one or a series of truss elements. Two different bolt models are available: end anchored and fully bonded.

6.3.3.1 End anchored bolts

The end-anchored bolt is represented by a truss deformable element (Figure 32). This element behaves as a single element and the interaction with the finite element mesh is through the endpoints only. These nodes can be assigned anywhere in the structural mesh, the nodes are mapped in the finite element mesh elements. The stiffness matrix of the anchor is added to the global stiffness matrix of the structure in this way.

The d.o.f displacements of the anchored element are computed in functions of the plane element nodal displacements in which the ended anchor nodes fall:

$$\begin{bmatrix} u_i \\ v_i \\ u_j \\ v_j \end{bmatrix} = \begin{bmatrix} N_1^i & 0 & N_2^i & 0 & N_3^i & 0 & 0 & 0 & 0 & 0 & 0 & 0 \\ 0 & N_1^i & 0 & N_2^i & 0 & N_3^i & 0 & 0 & 0 & 0 & 0 & 0 \\ 0 & 0 & 0 & 0 & 0 & 0 & N_1^j & 0 & N_2^j & 0 & N_3^j & 0 \\ 0 & 0 & 0 & 0 & 0 & 0 & 0 & N_1^j & 0 & N_2^j & 0 & N_3^j \end{bmatrix} \begin{bmatrix} u_1 \\ v_1 \\ u_2 \\ v_2 \\ u_3 \\ v_3 \\ u_4 \\ v_4 \\ u_5 \\ v_5 \\ u_6 \\ v_6 \end{bmatrix} \quad (130)$$

or in the condensed form:

$$\mathbf{u}_{\text{anchor}[4 \times 1]} = \mathbf{T}_{[4 \times 12]} \mathbf{u}_{\text{plane elements}[12 \times 1]} \quad (131)$$

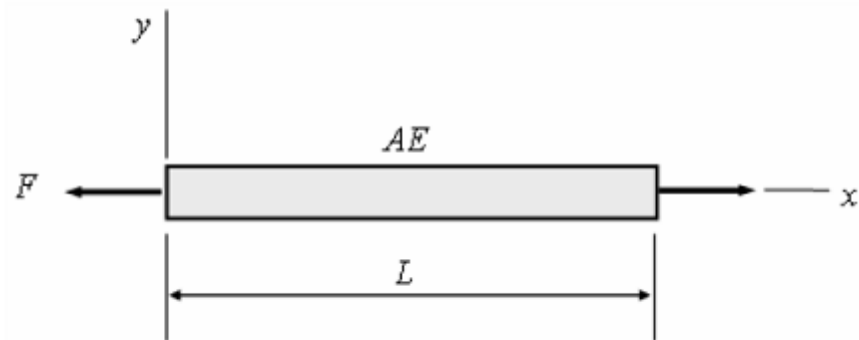
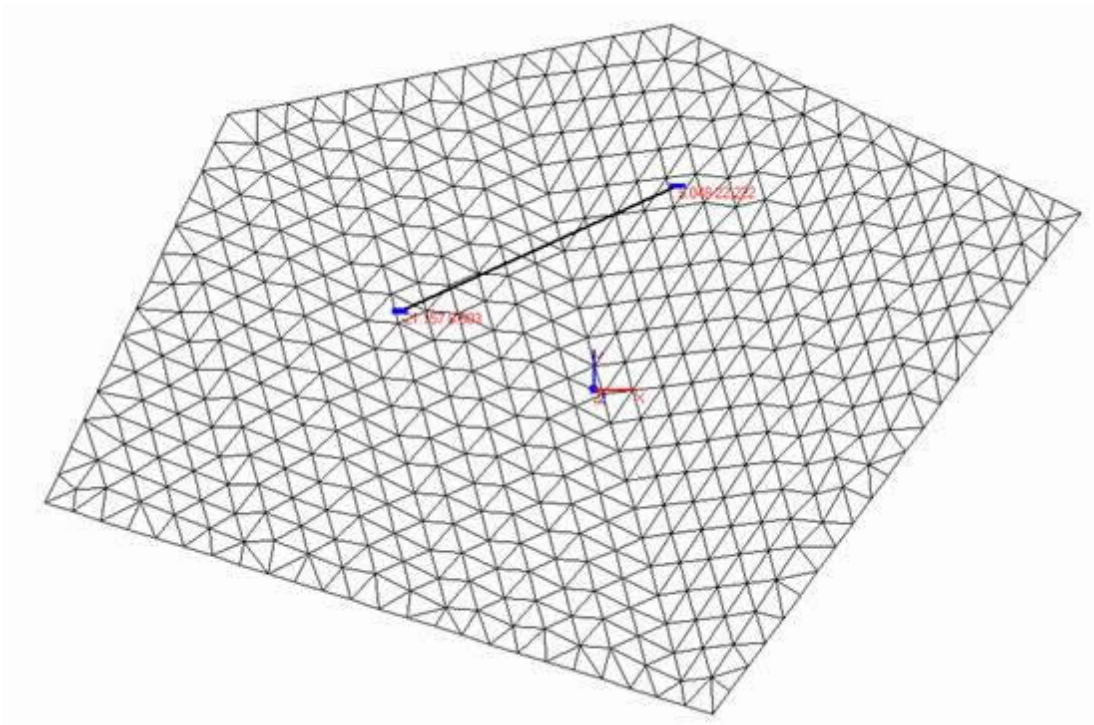


Fig. 32. Bolt element



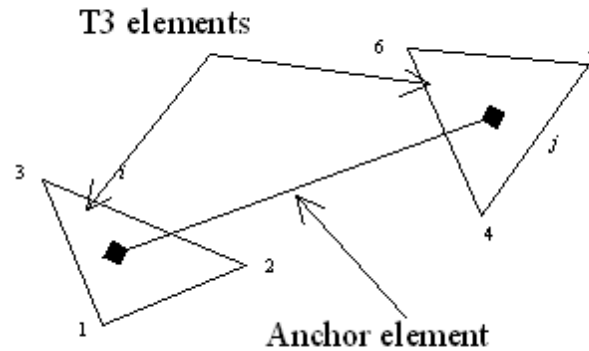


Figure 33. End anchored bolts.

Then the anchor stiffness matrix and nodal forces vector are computed as:

$$\begin{aligned} \mathbf{k}_{[12 \times 12]} &= \mathbf{T}_{[12 \times 4]}^T \mathbf{k}'_{[4 \times 4]} \mathbf{T}_{[4 \times 12]} \\ \mathbf{r}_{[12 \times 1]} &= \mathbf{T}_{[12 \times 4]}^T \mathbf{r}'_{[4 \times 1]} \end{aligned} \quad (132)$$

After this transformations the nodal force vector and stiffness matrix can be directly added to the corresponding arrays of the „parent” plane elements or assembled into the structure. The nodes i and j of the truss element and their d.o.f. are not explicitly present, we can say that d.o.f. of the bar element are constrained to follow d.o.f. of the „parent” plane elements. Other situations, associated with higher order or quadrilateral elements are taken into account in the same way.

The axial force F in the anchor is calculated from the stiffness-displacement relation expressed in the local element system as:

$$\begin{bmatrix} F_{xi} \\ F_{xj} \end{bmatrix} = \frac{EA}{L} \begin{bmatrix} 1 & -1 \\ -1 & 1 \end{bmatrix} \begin{bmatrix} u_i \\ u_j \end{bmatrix} \quad (133)$$

in which the displacements at nodes i and j are computed in function of the nodal displacements of the parent plane elements throughout the shape functions. For instance, considering the 3-noded triangular element (Fig. 33) the displacements at each node, in the global coordinate system are expressed as:

$$\begin{aligned} {}_g u_i &= N_1^1 u_1 + N_2^1 u_2 + N_3^1 u_3 \\ {}_g v_i &= N_1^1 v_1 + N_2^1 v_2 + N_3^1 v_3 \\ {}_g u_j &= N_1^2 u_4 + N_2^2 u_5 + N_3^2 u_6 \\ {}_g v_j &= N_1^2 v_4 + N_2^2 v_5 + N_3^2 v_6 \end{aligned} \quad (134)$$

where N_i^k represents the shape functions computed for each plane element in the points associated with end anchored element. These displacements are transformed in the local coordinate system via transformation matrix (131) as:

$$\begin{bmatrix} u_i \\ v_i \\ u_j \\ v_j \end{bmatrix} = \mathbf{T}^T \begin{bmatrix} g^u u_i \\ g^v v_i \\ g^u u_j \\ g^v v_j \end{bmatrix} \quad (135)$$

Finally, with the local axial displacements computed using the above equation, the axial force along the anchor element is computed using the equation (133).

In the program have been implemented fully linear and elasto-plastic anchors. In the first case the anchor have an elastic behaviour, the failure do not occur. In the second case, failure of an anchor element occurs due to tensile yielding of the bolt material. The failure is controlled by the tensile yield strength F_y (Figure 34). When the axial force in the element reach the yield strength, that element is considered failed and no residual resistance is assumed to carryout further.

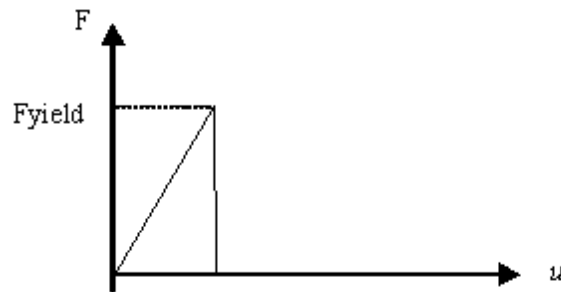


Fig. 34. Failure criteria.

6.3.3.2 Fully bonded bolts

Fully bonded bolts are divided into “bolt elements” according to where the bolts cross the finite element mesh. It is assumed a “perfect bond” between the truss element (bolt) and crossed plane

elements. These bolt elements act independently of each other. Neighbouring fully bonded bolt elements do not influence each other directly, but only indirectly through their effect on the plane elements (Fig. 35).

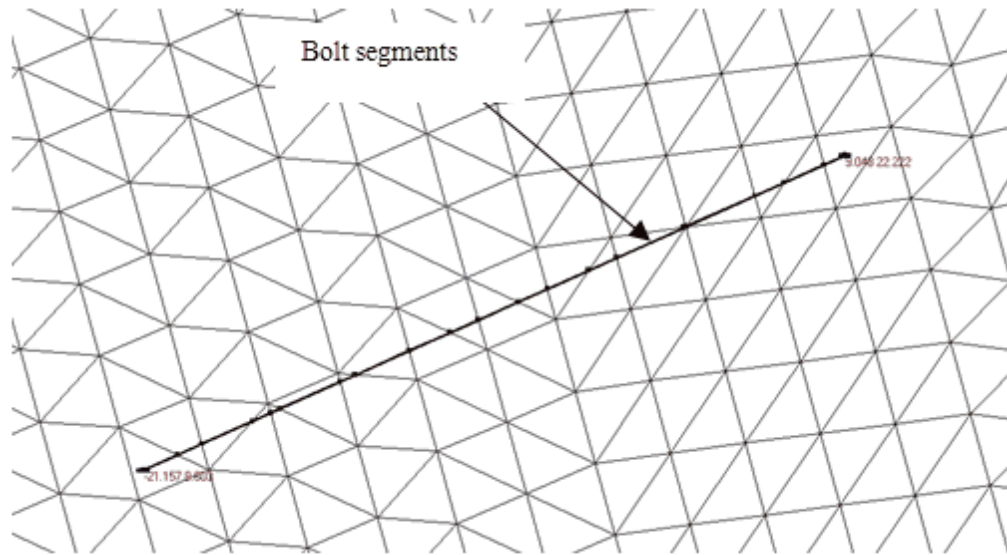


Figure 35. Fully bonded bolts.

The bolt stiffness matrix and nodal force vector are determined as in section 4.3.2, in function of the transformation matrix that depends of the shape functions of the crossed plane element.

The axial force along the bolt is determined from the relative axial displacements of the bolt element.

$$F_{\text{bolt}} = \frac{EA}{L}(u_j - u_i) \quad (136)$$

where u_j and u_i represents the axial local displacements at ended nodes determined as in section 4.3.2.

When a plastic behaviour is selected for the fully bonded bolts, the failure of the bolt is assumed to occur if the axial force F_{bolt} exceeds the yield strength of the bolt material. No residual force is allowed in this case (Fig. 34).

6.3.3.3 Liner elements

The liner elements are composed of beam-column elements with three degrees of freedom per node: two translational degrees of freedom (u, v) and one rotational degree of freedom (rotation in the x - y plane θ) in each node. The liners are based on Bernoulli or Timoshenko beam theory, deflections are due to shearing as well as bending. Bending moments, shear forces and axial forces in the elements are evaluated in function of the nodal displacements and rotations determined at the ended nodes assigned in the finite plane element nodes (mesh). The liners nodes coincide with the nodes of the general structural mesh. In this way between the translations of the liner elements and the displacements in the finite element mesh exist a perfect compatibility. Translational d.o.f are shared by plane elements and beam elements at nodes. Rotational d.o.f at these nodes are associated with only the beam elements (liners).

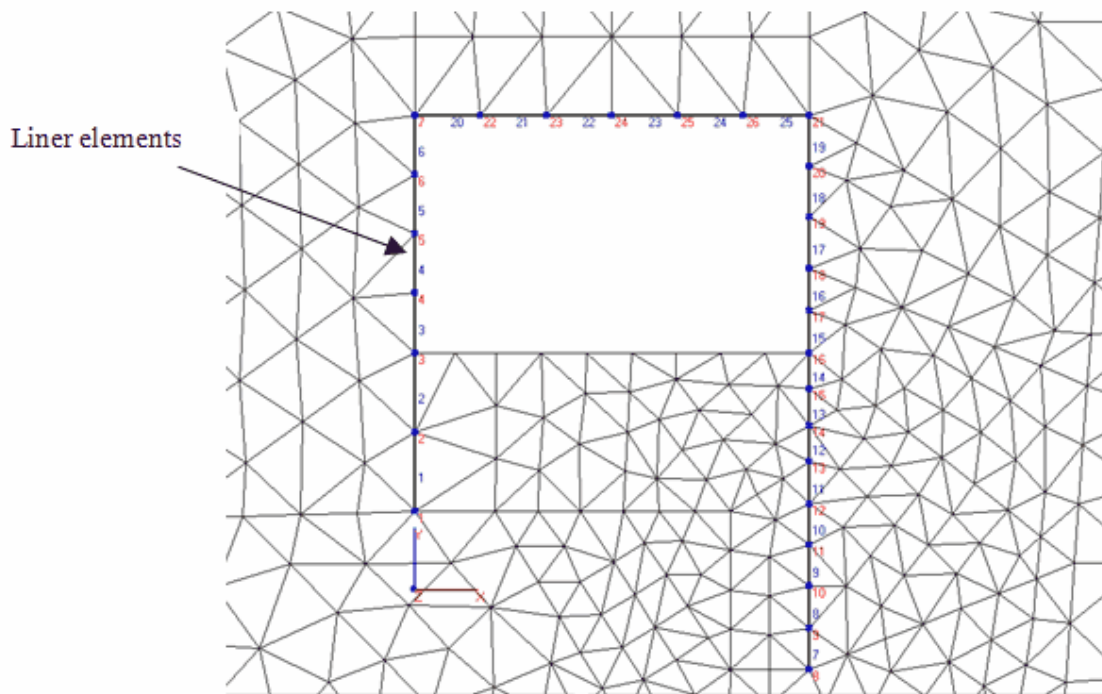


Fig.36. Liner elements

6.3.3.4 Geogrid elements

Geogrids are slender structures with normal stiffness but with no bending stiffness (truss elements) used to model soil reinforcements. Geogrids are composed of truss elements with two translational degrees of freedom in each node (u, v). These translational d.o.f. are shared by plane elements and truss elements at nodes. The axial forces in the geogrids are determined in function of the relative axial displacements at the nodes. The formulation of the geogrid element is similar with fully bonded bolt, but because the plane element nodes and geogrid nodes coincide it is not necessary to make constraint transformations like in the case of bolt elements. The elements may have a plastic behaviour and in this case an element is say to be yielded when the axial force over passed the axial yield strength of the element.

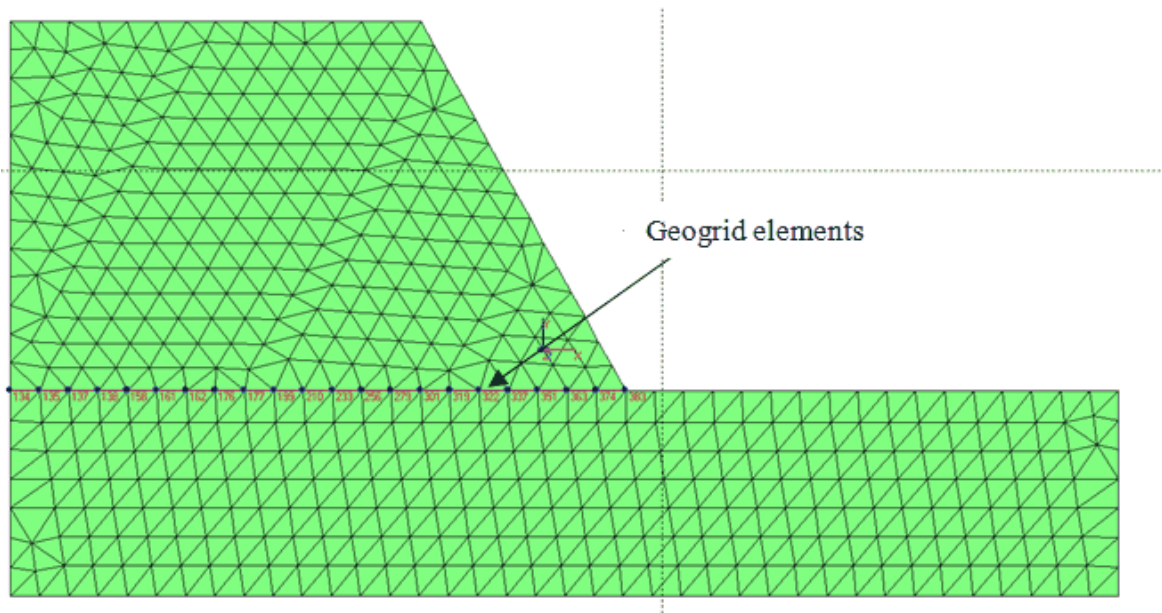


Fig.37. Geogrid elements (Geotextile).

7 Nonlinear analysis formulation

7.1 Inelastic stress-strain behavior

A material is called nonlinear if a strain-dependent matrix rather than a matrix of constants relate stresses and strains. Plastic flow is a cause of material non-linearity. During plastic straining, the material may flow in an "associated" manner, that the vector of plastic strain increment may be normal to the yield or failure surface. Alternatively, normality may not exist and the flow may be "non-associated". For frictional materials, whose ultimate state is described by the Mohr-Coulomb criterion, non-associated flow rules may be preferred in which plastic straining is described by a plastic potential function.

In order to formulate a theoretical description, three requirements have to be addressed, yield criterion, flow rule and hardening rule.

7.1.1 Yield criterion

Yield criterion or yield function, defines the state of stresses at which material response changes from elastic to plastic. We define a yield function F , which is a function of stresses σ and quantities α and \mathbf{W}_p which control the hardening (i.e. how a given yield surface in space is modified due to a plastic strain response:

$$F = F(\sigma, \alpha, \mathbf{W}_p) \quad (137)$$

If we evaluate F the possible results are:

$F < 0$, *elastic conditions*

$F = 0$, *yielding is beginning or is in progress*

$F > 0$, *not physical possible*

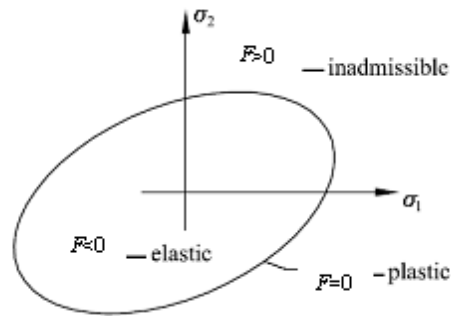


Fig. 38. Yield surface.

7.1.2 Flow rule

Flow rule relates plastic strain increments to stress increments after onset of initial yielding. We define a plastic potential Q , which has units of stress and is a function of stresses, $Q = Q(\boldsymbol{\sigma}, \boldsymbol{\alpha}, W_p)$. The plastic strain increments (flow rule) are given by:

$$d\boldsymbol{\varepsilon}^p = \frac{\partial Q}{\partial \boldsymbol{\sigma}} d\lambda \quad (138)$$

where $d\lambda$ represents a scalar that may be called a "plastic multiplier". Thus:

$$\begin{aligned} d\varepsilon_x^p &= \frac{\partial Q}{\partial \sigma_x} d\lambda \\ d\varepsilon_y^p &= \frac{\partial Q}{\partial \sigma_y} d\lambda \\ &\dots \\ d\gamma_{xz}^p &= \frac{\partial Q}{\partial \sigma_{xz}} d\lambda \end{aligned} \quad (139)$$

This rule is known as the normality principle because the above relations can be interpreted as requiring the normality of the plastic strain increment vector to the yield surface in the hyper-space of stress dimensions.

The flow rule is called "associated" if $Q=F$ and "non-associated" otherwise. Associated flow rules are commonly used for ductile metals, but non-associated rules are better suited to model soil and

granular materials.

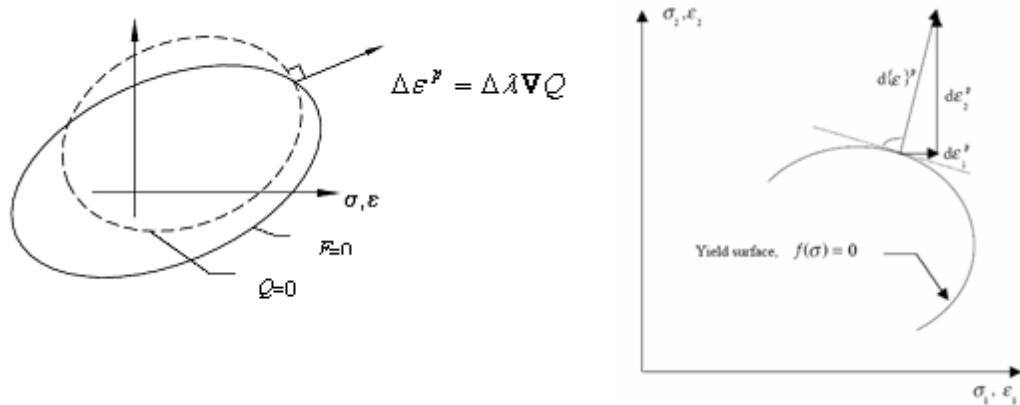


Fig. 39. (a) Geometrical representation of the plastic strain increment; (b) normality rule in 2D stress-space.

7.1.3 Hardening rule

Hardening rule predicts the change in the yield surface due to plastic strains. Two hardening rules can be formulated:

- Isotropic hardening: Bauschinger effect is ignored but the elastic range expands.
- Kinematic hardening: Bauschniger effect is included but elastic range remains constant.

Isotropic hardening can be represented by the plastic work per unit volume W_p thus:

$$W_p = \int d\boldsymbol{\sigma}^T d\boldsymbol{\varepsilon}^p \quad (140)$$

Kinematic hardening is given by vector determining the translation of the yield surface in general stress state.

7.2 Incremental stress-strain relations

We will assume that strain increments include elastic components and plastic components and they are small. An incremental stress-strain relation, analogous to the relation $\boldsymbol{\sigma} = \mathbf{E}\boldsymbol{\varepsilon}$ of elasticity can be formulated.

During an increment of plastic straining $dF=0$ thus:

$$\frac{\partial F}{\partial \boldsymbol{\sigma}} d\boldsymbol{\sigma} + \frac{\partial F}{\partial \mathbf{a}} d\mathbf{a} + \frac{\partial F}{\partial W_p} dW_p = 0 \quad (141)$$

By substitution:

$$d\boldsymbol{\sigma} = \mathbf{E} d\boldsymbol{\varepsilon}^e = \mathbf{E}(d\boldsymbol{\varepsilon} - d\boldsymbol{\varepsilon}^p) = \mathbf{E} \left(d\boldsymbol{\varepsilon} - \frac{\partial \mathbf{Q}}{\partial \boldsymbol{\sigma}} d\lambda \right) \quad (142)$$

The resulting equation to solve for the plastic multiplier $d\lambda$ is:

$$d\lambda = \mathbf{P}_\lambda d\boldsymbol{\varepsilon} \quad (143)$$

where \mathbf{P}_λ is the row matrix in which both work hardening and strain hardening are included in this expression:

$$\mathbf{P}_\lambda = \frac{\frac{\partial F}{\partial \boldsymbol{\sigma}} \mathbf{E}}{\frac{\partial F}{\partial \boldsymbol{\sigma}} \mathbf{E} \frac{\partial \mathbf{Q}}{\partial \boldsymbol{\sigma}} - \frac{\partial F}{\partial \boldsymbol{\sigma}} \mathbf{C} \frac{\partial \mathbf{Q}}{\partial \boldsymbol{\sigma}} - \frac{\partial F}{\partial W_p} \boldsymbol{\sigma}^r \frac{\partial \mathbf{Q}}{\partial \boldsymbol{\sigma}}} \quad (144)$$

Rearranging the terms yield:

$$\begin{aligned} d\boldsymbol{\sigma} &= \mathbf{E}_{ep} d\boldsymbol{\varepsilon} \\ \mathbf{E}_{ep} &= \mathbf{E} \left(\mathbf{I} - \frac{\partial \mathbf{Q}}{\partial \boldsymbol{\sigma}} \mathbf{P}_\lambda \right) \end{aligned} \quad (145)$$

where \mathbf{I} is a unit matrix and \mathbf{E}_{ep} is the generalized tangent constitutive matrix. If $Q=F$ (associated flow rule) this matrix \mathbf{E}_{ep} is symmetric. For $F < 0$ (yield has not occur) or $F=0$ and $dF < 0$ (unloading from plastic state) then $\mathbf{E}_{ep} = \mathbf{E}$.

The tangent stiffness matrix \mathbf{k}_t is now given by:

$$\mathbf{k}_t = \int_V \mathbf{B}^T \mathbf{E}_{ep} \mathbf{B} dV \quad (146)$$

7.3 Failure criteria

Several failure criteria have been incorporated as suitable for representing the strength of soils as engineering materials.

7.3.1 The Von-Mises criterion

This criterion taking into accounts the all three principal shear stress into account. In this case the yield function is given by:

$$F(J_2) = \sqrt{J_2} - k \quad (147)$$

or in terms of the so-called equivalent stress $\bar{\sigma}$ as

$$F(\sigma) = \bar{\sigma} - \sigma_0 \quad (148)$$

where

$$\begin{aligned} \bar{\sigma} &= (\tau_{xy}^2 + \tau_{yz}^2 + \tau_{zx}^2)^{1/2} = \left[\frac{1}{2}(\sigma_1 - \sigma_2)^2 + \frac{1}{2}(\sigma_2 - \sigma_3)^2 + \frac{1}{2}(\sigma_3 - \sigma_1)^2 \right]^{1/2} = \\ &= \left[\frac{1}{2}(\sigma_x - \sigma_y)^2 + \frac{1}{2}(\sigma_y - \sigma_z)^2 + \frac{1}{2}(\sigma_z - \sigma_x)^2 + 3\tau_{xy}^2 + 3\tau_{yz}^2 + 3\tau_{zx}^2 \right]^{1/2} \end{aligned} \quad (149)$$

For plane strain applications assuming no plastic volume change:

$$\sigma_0 = \sqrt{3}c_u \quad (150)$$

whereas under triaxial conditions:

$$\sigma_0 = 2c_u \quad (151)$$

where c_u is the undrained "cohesion" or shear strength of the soil.

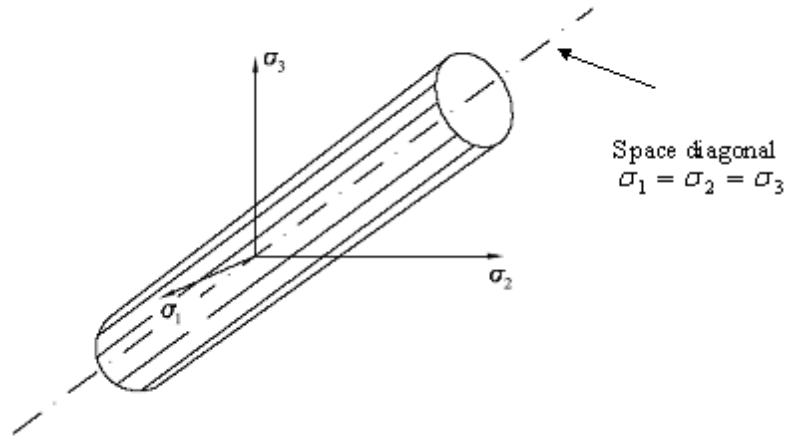


Fig.40. von Mises criterion in principal stress space

When plotted in three-dimensional principal stress space the yield surface depicts a cylinder parallel to the hydrostatic axis $\sigma_1 = \sigma_2 = \sigma_3$ as shown in Figure 40.

7.3.2 Mohr-Coulomb and Tresca criteria

In principal stress space, this criterion takes the form of an irregular hexagonal cone. This criterion can be written in principal stresses as:

$$F_{mc} = \frac{\sigma_1 + \sigma_2}{2} \sin \Phi - \frac{\sigma_1 - \sigma_3}{2} - c \cos \Phi \quad (152)$$

where the principal stresses are given by:

$$\begin{aligned} \sigma_1 &= \sigma_m + \frac{2}{3} \bar{\sigma} \sin \left(\theta - \frac{2\pi}{3} \right) \\ \sigma_3 &= \sigma_m + \frac{2}{3} \bar{\sigma} \sin \left(\theta + \frac{2\pi}{3} \right) \end{aligned} \quad (153)$$

and where the "mean" and "deviator" stresses are

$$\left. \begin{aligned} \sigma_m &= \frac{1}{\sqrt{3}} s \\ \bar{\sigma} &= \sqrt{\frac{3}{2}} t \end{aligned} \right| \quad (154)$$

The invariants s and t are:

$$s = \frac{1}{\sqrt{3}} (\sigma_x + \sigma_y + \sigma_z) \quad (155)$$

$$t = \frac{1}{\sqrt{3}} \sqrt{(\sigma_x - \sigma_y)^2 + (\sigma_y - \sigma_z)^2 + (\sigma_z - \sigma_x)^2 + 6\tau_{xy}^2 + 6\tau_{yz}^2 + 6\tau_{zx}^2} \quad (156)$$

Substituting for σ_1 and σ_3 from (59) gives the function:

$$F_{mc} = \sigma_m \sin \phi + \bar{\sigma} \left(\frac{\cos \theta}{\sqrt{3}} - \frac{\sin \theta \sin \phi}{3} \right) - c \cos \phi \quad (157)$$

The Tresca criterion is obtained from (63) by putting $\phi_u = 0$ to give:

$$F_t = \frac{\bar{\sigma} \cos \theta}{\sqrt{3}} - c_u \quad (158)$$

7.4 Elastic-plastic procedures

When the material behavior is nonlinear, material properties in an element are dictated by material properties at a finite number of sampling points in each element. Typically these points are quadrature stations of a numerical integration rule. At each point one must keep a record of strains and update the record in each computational cycle.

The number of points must be small to reduce computational expense. However, to accurately capture the spread of yielding in individual elements many sampling points are needed. The choice is between many simple elements and a smaller number of more sophisticated elements.

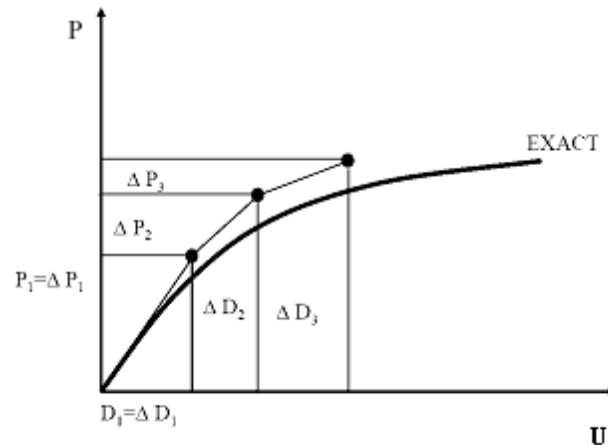


Fig. 41. Nonlinear analysis procedure

The implementation of the elasto-plastic constitutive relations in a finite element context requires the consideration of two different levels, the global level and the material level respectively. On the global level equilibrium must be satisfied as in any other linear or nonlinear finite element computation, whereas on the material level the plasticity relations must be satisfied. Performing the finite element discretization in the usual way, one ends up with the following equation system:

$$\mathbf{K}\mathbf{U} = \mathbf{F} \quad (159)$$

where \mathbf{F} represents the applied load vector, \mathbf{U} the displacement vector and \mathbf{K} the stiffness matrix. Since the stress-strain relations are non-linear, the constitutive matrix depends on the current state of stress the stiffness matrix is non-linear. Two main types of solution procedure can be adopted to model material non-linearity. With either solution method, the load is incremented in several steps and the solution is obtained through a series of linearized steps.

7.4.1 Constant-stiffness method

The first approach involves "constant stiffness" iterations in which non-linearity is introduced by iteratively modifying the right hand side "loads" vector. The global stiffness matrix, usually kept

elastic, in such an analysis is formed once only. Each iteration thus represents an elastic analysis. Convergence is said to occur when stresses generated by the loads satisfy some stress-strain law or yield or failure criterion within prescribed tolerances. The loads vector at each iteration consists of externally applied loads and self-equilibrating "body loads". The body loads have the effect of redistributing stresses within the system, but they do not alter the net loading on the system. The method is shown in Figure 42. For load-controlled problems, many iterations may be required as failure approached, because the elastic global stiffness matrix starts to seriously overestimate the actual material stiffness.

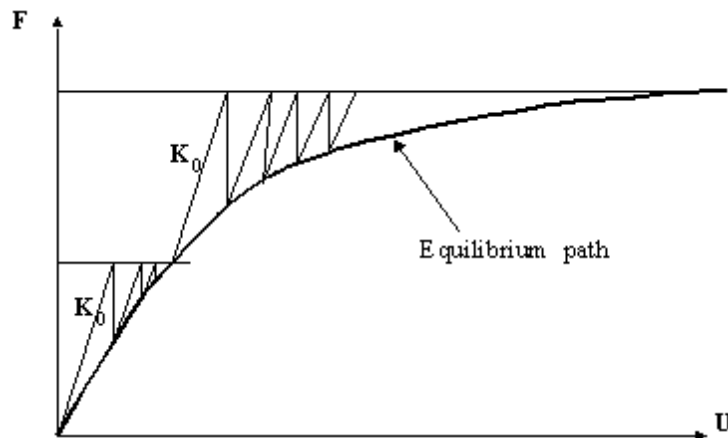


Fig. 42. Constant stiffness method.

The effects of plastic action are regarded as initial stresses that produce fictitious loads, which are combined with the load actually applied. This procedure avoids the expense of repeatedly forming and factoring a tangent-stiffness matrix, but may converge slowly if plastic strains are large or widespread.

7.4.1.1 Generation of self-equilibrating body loads

During each computational cycle, assuming the material is yielding, the strains will contain both elastic and plastic components, thus:

$$\Delta \boldsymbol{\varepsilon} = \Delta \boldsymbol{\varepsilon}^e + \Delta \boldsymbol{\varepsilon}^p \quad (160)$$

Only the elastic strain increments $\Delta \boldsymbol{\varepsilon}^e$ generate stresses:

$$\Delta \boldsymbol{\sigma} = \mathbf{E} \Delta \boldsymbol{\varepsilon} \quad (161)$$

These stress increments are added to stresses already existing from the previous load step and the updated stresses substituted into the failure criterion. If stress redistribution is necessary, yield criterion is violated ($F > 0$), this is done by altering the load increment vector \mathbf{F}^i in the global system of equations, corresponding to the load cycle i :

$$\mathbf{K} \mathbf{U}^i = \mathbf{F}^i \quad (161)$$

where \mathbf{K} represents the elastic (initial) global stiffness matrix and \mathbf{U}^i represents the global displacements increments. This vector holds two types of load, as given by:

$$\mathbf{F} = \mathbf{F}_a + \mathbf{F}_b^i \quad (162)$$

where \mathbf{F}_a is the actual applied external load increment and \mathbf{F}_b^i is the body loads vector that varies from one iteration to the next and must be self-equilibrating so that the net loading on the system is not affected by it.

7.4.1.2 Initial strain method

In this method the material is allowed to sustain stresses outside the failure criterion for finite "periods". Instead of plastic strains, we refer to viscoplastic strains and are generated as a rate that is related to the amount by which yield has been violated by:

$$\dot{\boldsymbol{\varepsilon}}^{\text{vp}} = F \frac{\partial Q}{\partial \boldsymbol{\sigma}} \quad (163)$$

where F is the yield function and Q is the plastic potential function.

The increment of viscoplastic strain, which is accumulated from one iteration to the next, is obtained through multiplication the strain rate by a pseudo time step as:

$$\delta \boldsymbol{\varepsilon}^{\text{vp},i} = \Delta t \dot{\boldsymbol{\varepsilon}}^{\text{vp},i} \quad (164)$$

and

$$\Delta \mathbf{\epsilon}^{vp,i} = \Delta \mathbf{\epsilon}^{vp,i-1} + \delta \mathbf{\epsilon}^{vp,i} \quad (165)$$

where the time step for numerical stability depends on the assumed failure criterion as:

$$\Delta t = \frac{4(1+\nu)}{3E} \quad (166)$$

for Von-Mises materials

$$\Delta t = \frac{4(1+\nu)(1-2\nu)}{E(1-2\nu + \sin^2 \phi)} \quad (167)$$

for Mohr-Coulomb materials

The derivatives of the plastic potential function Q with respect to stresses are expressed as:

$$\frac{\partial Q}{\partial \sigma} = \frac{\partial Q}{\partial \sigma_m} \frac{\partial \sigma_m}{\partial \sigma} + \frac{\partial Q}{\partial J_2} \frac{\partial J_2}{\partial \sigma} + \frac{\partial Q}{\partial J_3} \frac{\partial J_3}{\partial \sigma} \quad (168)$$

where $J_2 = \frac{t^2}{2}$ where t represents the second deviatoric stress invariant:

$$t = \frac{1}{\sqrt{3}} \sqrt{(\sigma_x - \sigma_y)^2 + (\sigma_y - \sigma_z)^2 + (\sigma_x - \sigma_z)^2 + 6\tau_{xy}^2 + 6\tau_{yz}^2 + 6\tau_{zx}^2} \quad (169)$$

and

$$J_3 = s_x s_y s_z - s_x \tau_{yz}^2 - s_y \tau_{zx}^2 - s_z \tau_{xy}^2 + 2\tau_{xy} \tau_{yz} \tau_{zx} \quad (170)$$

$$s_x = \frac{(2\sigma_x - \sigma_y - \sigma_z)}{3}, \text{ etc.} \quad (171)$$

$$\sigma_m = \frac{1}{\sqrt{3}} s \quad (179)$$

where the first invariant (mean stress invariant) s is given by the relation:

$$s = (\sigma_x + \sigma_y + \sigma_z) \quad (180)$$

It may be noted that in geotechnical applications, plane strain conditions are enforced and in the above equations $\tau_{yz} = \tau_{zx} = 0$.

The viscoplastic strain rate is evaluated numerically by the expression:

$$\dot{\boldsymbol{\varepsilon}}^{vp} = F \left(\frac{\partial Q}{\partial \sigma_x} \mathbf{M}^1 + \frac{\partial Q}{\partial J_2} \mathbf{M}^2 + \frac{\partial Q}{\partial J_3} \mathbf{M}^3 \right) \boldsymbol{\sigma} \quad (181)$$

where

$$\mathbf{M}^1 = \frac{1}{3(\sigma_x + \sigma_y + \sigma_z)} \begin{bmatrix} 1 & 1 & 1 & 0 & 0 & 0 \\ & 1 & 1 & 0 & 0 & 0 \\ & & 1 & 0 & 0 & 0 \\ & & & sym. & 0 & 0 \\ & & & & 0 & 0 \\ & & & & & 0 \end{bmatrix} \quad (182)$$

$$\mathbf{M}^2 = \frac{1}{3} \begin{bmatrix} 2 & -1 & -1 & 0 & 0 & 0 \\ & 2 & -1 & 0 & 0 & 0 \\ & & 2 & 0 & 0 & 0 \\ & & & sym. & 6 & 0 \\ & & & & 6 & 0 \\ & & & & & 6 \end{bmatrix} \quad (183)$$

$$\mathbf{M}^3 = \frac{1}{3} \begin{bmatrix} s_x & s_y & s_z & \tau_{xy} & -2\tau_{yz} & \tau_{zx} \\ & s_y & s_x & \tau_{xy} & \tau_{yz} & -2\tau_{zx} \\ & & s_z & -2\tau_{xy} & \tau_{yz} & \tau_{zx} \\ & & & sym. & -3s_z & 3\tau_{yz} \\ & & & & -3s_x & 3\tau_{xy} \\ & & & & & -3s_y \end{bmatrix} \quad (184)$$

$$\boldsymbol{\sigma} = [\sigma_x \quad \sigma_y \quad \sigma_z \quad \tau_{xy} \quad \tau_{yz} \quad \tau_{zx}]^T \quad (185)$$

The self-equilibrating body loads are accumulated at each time step within each load step by summing the following integrals for all yielded elements ($F > 0$ at Gauss points):

$$\mathbf{F}_b^i = \mathbf{F}_b^{i-1} + \sum_{elements} \iiint \mathbf{B}^T \mathbf{E} \Delta \boldsymbol{\varepsilon}^{vp,i} dx dy \quad (186)$$

This process is repeated at each time step iteration until no integration point stresses violate the failure criterion within a given tolerance. The convergence criterion is based on a dimensionless measure of the amount by which the displacement increment vector \mathbf{U}^i changes from one iteration to other.

7.4.1.3 Initial stress method

This method involve an explicit relationship between increments of stress and strains. Thus, elasto-plasticity is described by:

$$\Delta\sigma = (\mathbf{E} - \mathbf{E}^{ep})\Delta\epsilon^e \quad (187)$$

where \mathbf{E}^{ep} represents the generalized tangent constitutive matrix.

For perfect plasticity in the absence of hardening or softening the tangent constitutive matrix can be obtained particularizing the equation 51:

$$\mathbf{E}^{ep} = \frac{\mathbf{E} \frac{\partial \mathbf{Q}}{\partial \sigma} \frac{\partial \mathbf{F}^T}{\partial \sigma} \mathbf{E}}{\frac{\partial \mathbf{F}^T}{\partial \sigma} \mathbf{E} \frac{\partial \mathbf{Q}}{\partial \sigma}} \quad (188)$$

The body loads \mathbf{F}_b^i in the stress redistribution process are reformed at each iteration by summing the following integral for all elements that posses yielding Gauss integration points:

$$\mathbf{F}_b^i = \sum_{elements} \iint \mathbf{B}^T \mathbf{E}^{ep} \Delta\epsilon^i d\kappa dy \quad (189)$$

This method is used in conjunction with the forward Euler approach to integrating the elasto-plastic rate equation, extrapolating from the point at which the yield surface is crossed.

7.4.1.4 Solution procedure

Loads \mathbf{F}_a on the structure are applied in increments $\Delta\mathbf{F}_{a1}$, $\Delta\mathbf{F}_{a2}$, and so on, so that $\mathbf{F}_a = \sum \Delta\mathbf{F}_{ai}$. The graphical interpretation of the method for a problem with one displacement variable is shown in Figure

1. For the first computational cycle ($i=1$) assume $\mathbf{E}_{ep} = \mathbf{E}$ for all elements. Apply the first load

increment $\Delta \mathbf{F}_1$.

2. Using the current strains, determine the current \mathbf{E}_{ep} or viscoplastic strain increment $\Delta \boldsymbol{\varepsilon}^{vp,i}$ in each element. Obtain the self-equilibration body loads for each element. Obtain the current structure (global) self-equilibrating body loads \mathbf{F}_b^i and solve $\mathbf{K} \Delta \mathbf{U}_i = \mathbf{F}_a^i - \mathbf{F}_b^i$, $\mathbf{m} = \rho \int_A \mathbf{N}^T \mathbf{N} dx dy$ where \mathbf{F}_a is the actual applied external load increment. From $\Delta \mathbf{U}_i$ obtain the current strain increment $\Delta \boldsymbol{\varepsilon}_i$ for each element.
3. If any element makes the elasto to plastic transition revise \mathbf{E}_{ep} return to previous step 2 and repeat the steps 2 and 3 until convergence.
4. Update the displacement vector $\mathbf{U}_i = \mathbf{U}_{i-1} + \Delta \mathbf{U}_i$, the strains $\boldsymbol{\varepsilon}_i = \boldsymbol{\varepsilon}_{i-1} + \Delta \boldsymbol{\varepsilon}_i$ and the stress $\boldsymbol{\sigma}_i = \boldsymbol{\sigma}_{i-1} + \Delta \boldsymbol{\sigma}_i$.
5. Apply the next load increment and return to step 2.
6. Stop when sum of incremental loads equals the total load or the structure collapse.

During the iteration process the nodal displacements caused by the actual applied external load increments and the body loads vector at successive iterations are compared. The convergence criterion is based on a dimensionless measure of the amount by which the displacement increment vector changes from one iteration to other. Convergence is said to have occurred, if the absolute change in all components of displacement vector, as a fraction of the maximum absolute component of displacement vector is less than a predefined tolerance.

7.4.2 Tangent (variable)-stiffness method

The second approach, shown in Figure 43, takes account of the reduction in stiffness of the material as failure is approached. If small enough load steps are taken, the method can become equivalent to a simple Euler "explicit" method. In this approach the global stiffness matrix may be updated periodically and "residual body-loads" iterations employed to achieve convergence. In contrasting with "constant stiffness approach" the extra cost of reforming and re-factorization the global stiffness matrix in the variable stiffness method is offset by reduced numbers of iteration, especially as failure is approached.

The algorithm requires that representation of the stress-strain relation must be stored, so that tensions and elastic constants can be obtained for any given deformation. We also have to store and update at any sampling point of each element after each computational cycle, element strains and stresses and the nodal displacements.

An incremental relationship between displacement and force is needed:

$$\mathbf{K}_t \Delta \mathbf{u} = \Delta \mathbf{F} \quad (190)$$

where \mathbf{K}_t is the tangent stiffness matrix and the above equations represent the linearized equation of the nonlinear equation 191:

$$\mathbf{K}_t = \int_V \mathbf{B}^T \mathbf{E}^{pl} \mathbf{B} dV \quad (191)$$

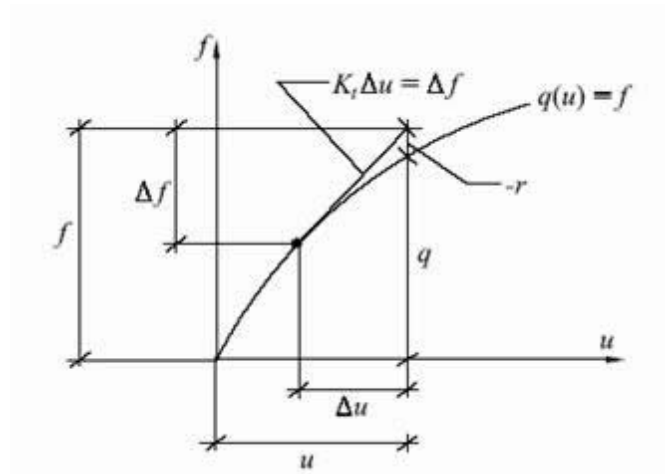


Fig. 43. Load step in tangent stiffness method.

The computation proceeds by applying a load increment $\Delta \mathbf{F}$ and computing the corresponding displacement increment from equation (190) (Fig.43).

The strain increment is computed in the usual way as:

$$\Delta \boldsymbol{\varepsilon} = \mathbf{B} \Delta \mathbf{u}_i \quad (192)$$

Next the stresses are computed via the elasto-plastic constitutive relation:

$$\Delta \boldsymbol{\sigma} = (\mathbf{E} - \mathbf{E}^{ep}) \Delta \boldsymbol{\varepsilon} = \mathbf{E}^{pl} \Delta \boldsymbol{\varepsilon} \quad (193)$$

This is a nonlinear relation since the constitutive matrix \mathbf{E}^{ep} depends on the current stress state and generally iterative procedures must thus be used. Assuming that the stresses have been computed the internal force vector can then be found as:

$$\mathbf{Q} = \int_V \mathbf{B}^T \boldsymbol{\sigma} dV \quad (194)$$

this must be balanced by the total applied load, therefore the residual force must vanish:

$$\mathbf{R} = \mathbf{Q} - \mathbf{F} \quad (195)$$

If the residual is different from a given tolerance it is applied as an external load following the well-known Newton-Raphson procedure. This then gives a new strain increment and a corresponding new stress increment, which must be determined via the nonlinear elasto-plastic constitutive relation, a new residual is computed and so on until the residual becomes sufficiently small. The procedure can be outlined as follows:

1. Apply load increment $\Delta \mathbf{F}$ and find displacement and strain increments $\Delta \mathbf{u}$ and $\Delta \boldsymbol{\varepsilon}$
2. Determine stress increment $\Delta \boldsymbol{\sigma}$ from equation (193)
3. Compute residual \mathbf{R} .
4. If $\|\mathbf{R}\| < TOL$ set \mathbf{k}_t and goto 1

Thus, the computation of a load step requires a global iterative procedure where the out of balance force, or residual, must vanish, as well as a procedure to compute the stress increments (step 2). The stress update is performed in each integration points. In order to compute the stress increment given a strain increment the backward integration scheme is implemented in the code. Essentially the method consists of an elastic predictor, followed by a plastic corrector to ensure the final stress is nearly on the yield surface.

7.4.2.1 Integration of the constitutive relations. Consistent tangent matrix

Referring to Figure 44 from a point A lying inside or on the yield surface an elastic predictor is applied. This leads to a state of stress outside the yield surface, increments end up at point B . To fulfill the yield condition a plastic corrector is applied, thus returning the stresses to the yield surface at point C . The plastic corrector is determined by two quantities, the scalar $\Delta \lambda$ giving the magnitude,

and the gradient of the loading surface $\left(\frac{\partial Q}{\partial \boldsymbol{\sigma}}\right)_C$ giving the direction. The magnitude $\Delta \lambda$ is determined such that the yield condition is fulfilled:

$$F(\boldsymbol{\sigma}_C - \Delta \boldsymbol{\sigma}^P) = 0 \quad (196)$$

where $\Delta \boldsymbol{\sigma}^P$ is given by

$$\Delta \sigma^p = \Delta \lambda \mathbf{E} \left(\frac{\partial \mathbf{Q}}{\partial \boldsymbol{\sigma}} \right)_C \quad (197)$$

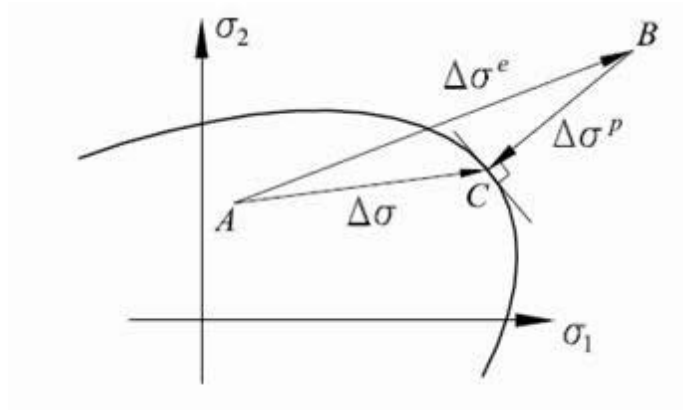


Fig. 44. Stress correction.

A first order Taylor expansion of the yield function at B gives:

$$F(\boldsymbol{\sigma}_C) = F(\boldsymbol{\sigma}_B - \Delta \boldsymbol{\sigma}^p) \approx F(\boldsymbol{\sigma}_B) - \left(\frac{\partial F}{\partial \boldsymbol{\sigma}} \right)_B^T \Delta \boldsymbol{\sigma}^p \quad (198)$$

Inserting the expression for $\Delta \boldsymbol{\sigma}^p$ into the above relation and enforcing consistency of the yield function at point C gives a step size of:

$$\Delta \lambda = \frac{F(\boldsymbol{\sigma}_B)}{\left(\frac{\partial F}{\partial \boldsymbol{\sigma}} \right)_B^T \mathbf{E} \left(\frac{\partial \mathbf{Q}}{\partial \boldsymbol{\sigma}} \right)_C} \quad (199)$$

With the backward Euler integration scheme, a consistent tangent modular matrix can be formed.

$$\Delta \boldsymbol{\sigma} = \Delta \boldsymbol{\sigma}_B - \Delta \lambda \mathbf{E} \left(\frac{\partial \mathbf{F}}{\partial \boldsymbol{\sigma}} \right)_C = (\boldsymbol{\sigma}_A + \mathbf{E} \Delta \boldsymbol{\varepsilon}) - \Delta \lambda \mathbf{E} \left(\frac{\partial \mathbf{Q}}{\partial \boldsymbol{\sigma}} \right)_C \quad (200)$$

On differentiation we get:

$$d(\Delta \boldsymbol{\sigma}) = \mathbf{E}_C^{cp} d(\Delta \boldsymbol{\varepsilon}) \quad (201)$$

where \mathbf{E}_C^{cp} is known as the "consistent tangent matrix and is given by:

$$\mathbf{E}_c^{ep} = \mathbf{E}_c - \frac{\mathbf{E}_c \frac{\partial \mathbf{Q}}{\partial \boldsymbol{\sigma}} \left(\frac{\partial \mathbf{F}}{\partial \boldsymbol{\sigma}} \right)^T \mathbf{E}_c}{\left(\frac{\partial \mathbf{F}}{\partial \boldsymbol{\sigma}} \right)^T \mathbf{E}_c \frac{\partial \mathbf{Q}}{\partial \boldsymbol{\sigma}}} \quad (202)$$

and

$$\mathbf{E}_c^{-1} = \mathbf{E}^{-1} + \Delta \lambda \nabla^2 \mathcal{Q}(\boldsymbol{\sigma}) \quad (203)$$

7.4.2.2 Solution procedure

Loads \mathbf{F} on the structure are applied in increments $\Delta \mathbf{F}_1$, $\Delta \mathbf{F}_2$, and so on, so that $\mathbf{F} = \sum \Delta \mathbf{F}_i$. The graphical interpretation of the method for a problem with one displacement variable is shown in Figure 45 where the subscripts i indicating the load step number have been dropped. Procedural steps are outlined as follows.

1. For the first computational cycle ($i=1$) assume $\mathbf{E}_{ep} = \mathbf{E}$ for all elements. Apply the first load increment $\Delta \mathbf{F}_1$.
2. Using the current strains, determine the current \mathbf{E}_{ep} in each element. Obtain the \mathbf{k}_t for each element. Determine the residual force if any. Obtain the current structure (global) tangent stiffness $\mathbf{K}_{t,i}$ and solve $\mathbf{K}_{t,i} \Delta \mathbf{U}_i = \Delta \mathbf{R}_i$. From $\Delta \mathbf{U}_i$ obtain the current strain increment $\Delta \boldsymbol{\varepsilon}_i$ for each element.
3. If any element makes the elasto to plastic transition revise \mathbf{E}_{ep} return to previous step 2 and repeat the steps 2 and 3 until convergence.
4. Update the displacement vector $\mathbf{U}_i = \mathbf{U}_{i-1} + \Delta \mathbf{U}_i$, the strains $\boldsymbol{\varepsilon}_i = \boldsymbol{\varepsilon}_{i-1} + \Delta \boldsymbol{\varepsilon}_i$ and the stress $\boldsymbol{\sigma}_i = \boldsymbol{\sigma}_{i-1} + \Delta \boldsymbol{\sigma}_i$.
5. Apply the next load increment and return to step 2.
6. Stop when sum of incremental loads equals the total load or the structure collapse.

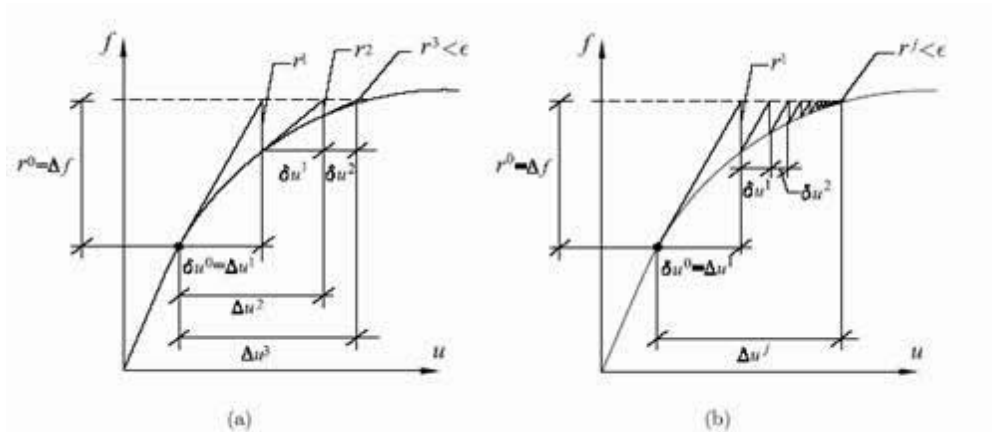


Fig. 45. Solution procedure (a) Full Newton-Raphson procedure (b) Modified Newton-Raphson procedure.

Usually the so-called modified Newton-Raphson method is used. The modification consists of computing the tangent stiffness only once in the beginning of each load step rather than in each iteration as shown in Figure 45(b). Therefore, in step 2 of the above algorithm the tangent stiffness matrix is formed and factorized only once at the beginning of the load increment.

During the iteration process the residual forces are computed. Convergence is said to have occurred, if the absolute change in all components of residual force vector, as a fraction of the maximum absolute component of force vector is less than a predefined tolerance.

8 Steady state analysis

The governing partial differential equation for a confined aquifer with flow in the horizontal (x,y) plane is:

$$k_x \frac{\partial^2 \phi}{\partial x^2} + k_y \frac{\partial^2 \phi}{\partial y^2} + Q = 0 \quad (204)$$

Where ϕ is the fluid potential or total head measured from the bottom of the aquifer, k_x and k_y are the coefficients of the permeability in the x and y directions and Q is the recharge. Pumping is a negative Q . The finite element discretization process reduces the differential equation to a set of equilibrium type equations of the form:

$$\mathbf{k}_e \Phi = \mathbf{q} \quad (205)$$

Where \mathbf{k}_e is the symmetrical conductivity matrix, Φ is a vector of nodal potential (total head) values, and \mathbf{q} is a vector of nodal inflows/outflows. The element matrices are calculated using:

$$\mathbf{k}_e = \iint \mathbf{T}^T \mathbf{K} \mathbf{T} dx dy \quad (206)$$

Assuming that the principal axes of the permeability tensor coincide with x and y , the property matrix \mathbf{K} is:

$$\mathbf{K} = \begin{bmatrix} k_x & 0 \\ 0 & k_y \end{bmatrix} \quad (207)$$

and the \mathbf{T} matrix is similar with the strain-displacement matrix \mathbf{B} in the stress analysis. For instance for 4 noded quadrilateral element the matrix \mathbf{T} is given by:

$$\mathbf{T} = \begin{bmatrix} \frac{\partial N_1}{\partial x} & \frac{\partial N_2}{\partial x} & \frac{\partial N_3}{\partial x} & \frac{\partial N_4}{\partial x} \\ \frac{\partial N_1}{\partial y} & \frac{\partial N_2}{\partial y} & \frac{\partial N_3}{\partial y} & \frac{\partial N_4}{\partial y} \end{bmatrix} \quad (208)$$

9 Initial conditions

Once the staged construction and mesh have been generated, the finite element model is complete. The initial conditions consists in the initial groundwater conditions, the initial geometry configuration and the initial effective stress state.

9.1 Initial groundwater conditions

Pore pressures and external water pressures can be generated on the basis of phreatic levels (water table). A phreatic level represents a series of points where the water pressure is zero. Using the input of phreatic level, the water pressure will increase linearly with the depth according to the specified water weight, the pressure variation is assumed to be hydrostatic. The external loading due to the reservoir is modelled by applying a normal stress to the face of the slope equal to the water pressure. Thus as shown in the Figure 47 the applied stress increases linearly with water depth and remains constant along the horizontal foundation level. These stresses are then converted into equivalent nodal loads on the finite element mesh.

Phreatic levels are defined by two or more points and do not interact with the geometrical model. Above the phreatic level the pore pressures will be zero, whereas below the phreatic level there will be a hydrostatic pore pressure distribution at each Gauss integration points.

Steady state pore pressures and external water pressures are generated in the water conditions mode. Water pore pressures can be generated on the basis of phreatic levels or alternatively, water pressures may be generated by means of a steady-state groundwater flow. The initial groundwater conditions can be generated in two different modes: the first consists in the definition of the phreatic levels and generation the water pore pressures and second through an explicit steady state flow analysis, that require a definition of the total heads on the finite element mesh boundaries.

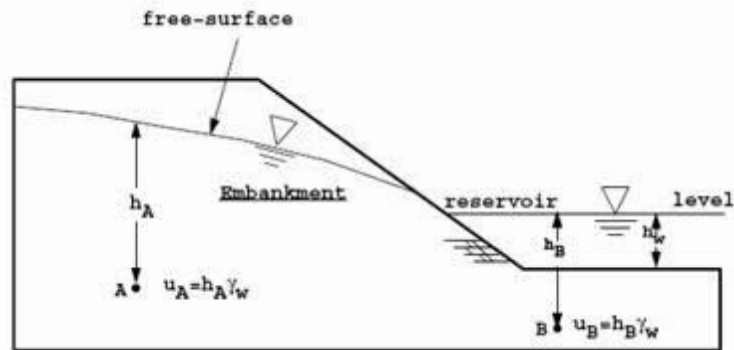


Fig.46. Free surface modelling.

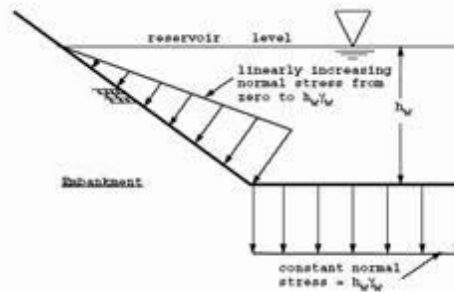


Fig.47. Reservoir loading.

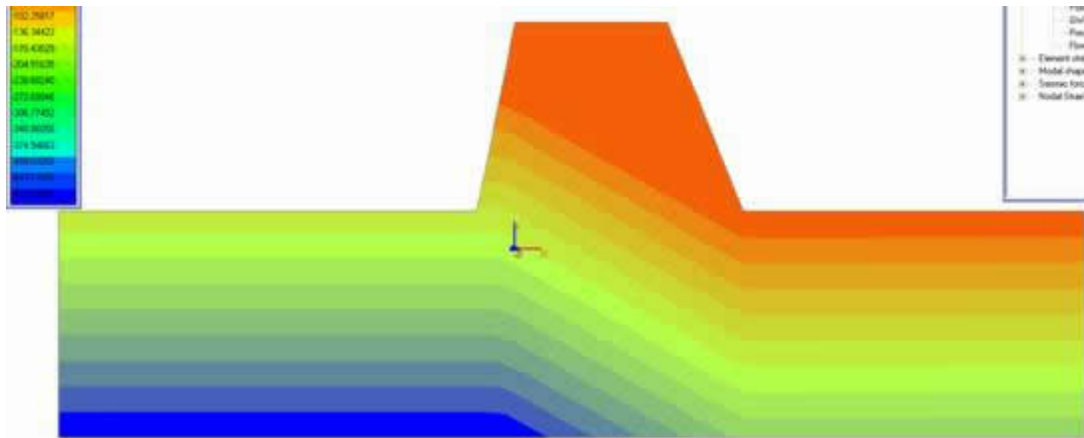
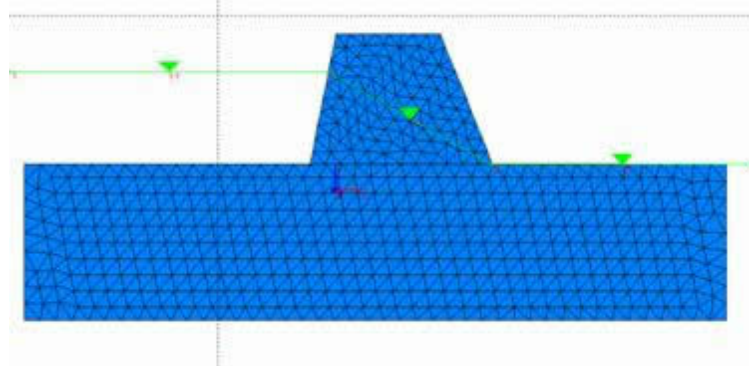


Fig. 48. Pore pressure distribution.

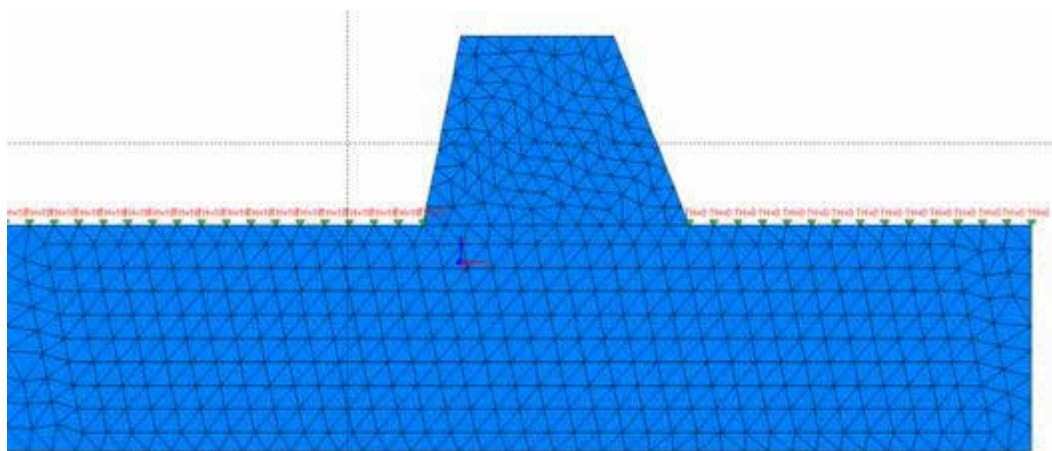


Fig.49. Hydraulic boundary conditions.

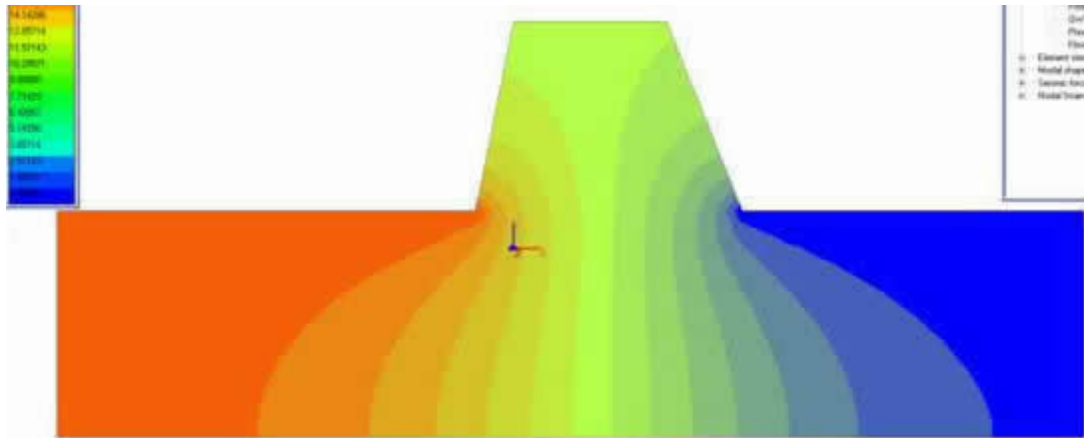


Fig.50. Steady state flow analysis. Total heads distribution.

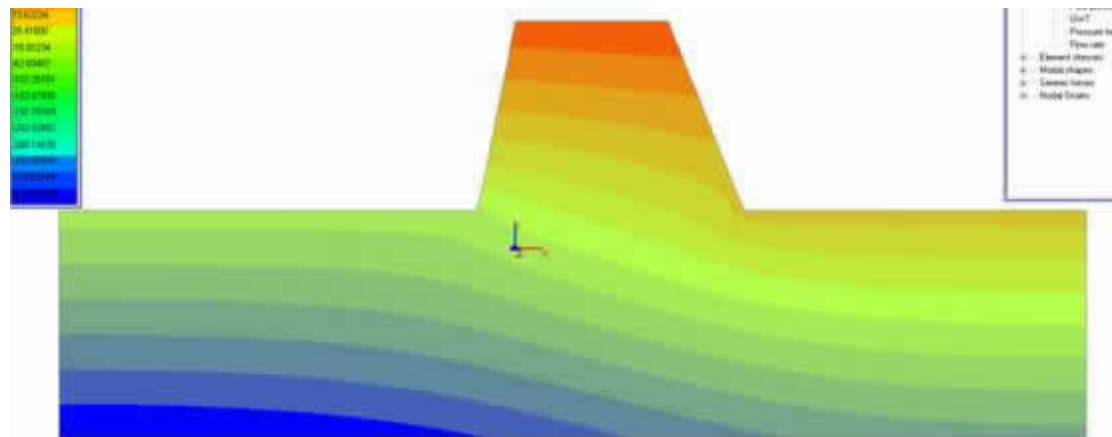


Fig.51. Steady state flow analysis. Pore pressure distribution.

9.2 Initial geostatic stresses

The initial stress conditions can be generated also in two different modes: the first consists in an explicit finite element stress analysis taking into account the gravitational loads of the massive and second through the simplified K_0 procedure. The K_0 procedure may only be used for horizontally layered geometries with horizontal ground surface and, if applicable, a horizontal phreatic level. In the case of linear elasticity we have the following relationship between normal stresses:

$$\sigma_x = \frac{\nu}{1-\nu} \sigma_y \quad (209)$$

where σ_x and σ_y represents the lateral and vertical normal stresses, respectively and ν is the Poisson ratio. This equation can be rewritten as:

$$\sigma_x = K_0 \sigma_y \quad (210)$$

where K_0 represents the coefficient of lateral earth pressure at rest. The third principal stress follows from the geometrical symmetry as:

$$\sigma_z = \sigma_x = K_0 \sigma_y \quad (211)$$

and the shear stresses are zero. The K_0 variable in general ranging from 0 to 1. GFAS offers possibility for selection of arbitrary values for this coefficient when generating an initial geostatic stress state prior to any construction stage.

In contrast to the simplified K_0 procedure, the calculation of initial stresses by means of explicit finite element stress analysis based on gravity loading can be conducted on any shape geometry and determine the initial stresses in the massive using either a linear analysis or elasto-plastic analysis. This analysis is performed in the first stage of construction prior to any staged constructions or loads. However when choose this option to generate the initial stresses results displacements, these displacements are not realistic because the soil is modelled as it appears in reality and the calculation of the initial stress should not influence the displacements computed later in the next stages of the analysis. These unrealistic displacements can be reset to zero at the start of the next calculation stage.

10 Dynamic and seismic analysis

Equations that govern the dynamic response of massive will be derived by requiring the work of external forces to be absorbed by the work of internal, inertial and viscous forces for any small kinematically admissible motion. For a single element we can write:

$$\int_V \delta \mathbf{u}^T \mathbf{F} dV + \int_S \delta \mathbf{u}^T \mathbf{Q} dS + \sum_{i=1}^n \delta \mathbf{u}_i^T \mathbf{p}_i = \int_V (\delta \boldsymbol{\varepsilon}^T \boldsymbol{\sigma} + \delta \mathbf{u}^T \rho \ddot{\mathbf{u}} + \delta \mathbf{u}^T \boldsymbol{\varepsilon}_d \dot{\mathbf{u}}) dV \quad (212)$$

where:

$\delta \mathbf{u}$ - small arbitrary displacements

$\delta \boldsymbol{\varepsilon}$ small arbitrary strains vector

\mathbf{F} - body forces vector

Φ - prescribed surface tractions

\mathbf{p}_i concentrated loads vector

$\delta \mathbf{u}^T$ - the displacement of the point at which load \mathbf{p}_i is applied.

ρ - mass density of the material

κ_d material damping parameter

Denoting with \mathbf{N} the shape functions of the finite elements, we have for the displacement field \mathbf{u} and its two first time derivatives (velocities and acceleration fields):

$$\mathbf{u} = \mathbf{N} \mathbf{d} \quad (213)$$

$$\dot{\mathbf{u}} = \mathbf{N} \dot{\mathbf{d}}$$

$$\ddot{\mathbf{u}} = \mathbf{N} \ddot{\mathbf{d}}$$

Where the vector \mathbf{d} contains the displacements at nodes of the finite element that are functions of time only.

Combining the equations (212) and (213) and since the displacements $\delta \mathbf{u}$ are arbitrary we obtain the following coupled, second-order, ordinary differential equations in time:

$$\mathbf{M} \ddot{\mathbf{d}} + \mathbf{C} \dot{\mathbf{d}} + \mathbf{R}^{\text{int}} = \mathbf{R}^{\text{ext}} \quad (214)$$

where the element mass and damping matrices are defined as:

$$\mathbf{M} = \int_{V_e} \rho \mathbf{N}^T \mathbf{N} dV \quad (215)$$

$$\mathbf{C} = \int_{V_e} \kappa_d \mathbf{N}^T \mathbf{N} dV$$

and the element internal force and external load vectors are defined as:

$$\mathbf{R}^{\text{int}} = \int_{V_e} \mathbf{B}^T \boldsymbol{\sigma} dV \quad (216)$$

$$\mathbf{R}^{\text{ext}} = \int_{V_e} \mathbf{N}^T \mathbf{F} dV + \int_{S_e} \mathbf{N}^T \Phi dS + \sum_{i=1}^n \mathbf{p}_i$$

An undamped structure, with no external loads applied to unrestrained d.o.f, undergoes harmonic motion in which each d.o.f. moves in phase with all other d.o.f. This way:

$$\mathbf{d} = \bar{\mathbf{d}} \sin \omega t \quad (217)$$

Combining Eq.(214) and Eq.(217) and setting $\mathbf{C}=0$ and $\mathbf{R}_{\text{ext}}=0$ we obtain:

$$(\mathbf{K} - \omega^2 \mathbf{M})\bar{\mathbf{d}} = \mathbf{0} \quad (218)$$

Which represents the basic statement of the vibration problems and where \mathbf{K} represents the stiffness matrix of the structure and \mathbf{M} the global mass matrix that may be „lumped” or „consistent”.

The consistent element mass matrix is defined by the following relation:

$$\mathbf{m} = \rho \int_A \mathbf{N}^T \mathbf{N} dx dy \quad (219)$$

Where \mathbf{N} represents the shape functions matrix. The lumped mass matrix is obtained by placing particle masses m_i at nodes of an element such that $\sum m_i$ is the total element mass. A lumped mass matrix is diagonal but a consistent mass matrix is not. For a 4 noded quadrilateral, for example, the lumped mass matrix is given by:

$$\mathbf{m} = \rho A / 4 \mathbf{I} \quad (220)$$

where A is the element area and \mathbf{I} the unit matrix.

11 Staged constructions

GFAS allows to construct complex geometries and analysis can be runned in different stages associated to different phases of construction. In fact the entire analysis procedure is developed under this philosophy allowing the users to create multiple staged constructions in the model. In this way complex analyses such as: excavations, embankments or constructions can be conducted. Moreover during these phases the user has the possibility to change the water pressure, boundary conditions activate or deactivate several regions from the massive, anchors, liners, geogrids or to improve the accuracy of the previous computational results. Staged construction enables the activation or deactivation of weight (gravitational loads) and selected components of the model such as anchors, liners, geogrids, loads, etc. During the Staged construction analysis, the loads are increased from 0 to 1. As soon as the load parameter reaches the value of 1.0, the constructions stage is completed and the analysis of the current phase is completed, and go the the next phase of the construction. If a staged construction calculations finishes while the load factor is smaller than 1.0, the program will stop the analysis. The most likely reason for not finishing a construction stage is that a failure mechanism has occurred.

12 Analysis types

12.1 Slope stability analysis

The method, based on finite element formulation as described earlier, can be applied with complex slope configurations in two dimensions to model virtually all types of mechanisms. General soil material models that include Mohr-Coulomb and others can be employed. The equilibrium stress, strains, and the associated shear strengths in the soil mass can be computed very accurately.

During the analysis the program gradually reduces the basic strength characteristics of the soil mass until failure occurs. The factor of safety (FS) is to be assessed, and this quantity is defined as the proportion by which $\tan \Phi$ (friction angle) and c (cohesion) must be reduced in order to cause failure with the gravity loading kept constant. This is in contrast to the bearing capacity analysis in which failure is induced by increasing the loads with the material properties remaining constant.

12.1.1 Factor of Safety (FOS) and Strength reduction factor (SRF)

Gravity loads are generated automatically in manner described in section 3.8 of the present documentation. This load is applied to the slope in a single increment. A trial strength reduction factor loops gradually weakness the soil parameters until the algorithm fails to converge. The factored soil strength parameters that go into the elasto-plastic analysis are obtained from:

$$\begin{aligned}\Phi_f &= \arctan(\tan \Phi / SRF) \\ c_f &= c / SRF\end{aligned}\tag{221}$$

where SRF is strength reduction factor. Several increasing values of the SRF factor are attempted until the algorithm fails to converge, at which point SRF is then interpreted as the factor of safety FOS . This actually means that no stress distribution can be achieved to satisfy the failure criterion and global equilibrium.

12.1.2 Material properties

The Mohr-Coulomb constitutive model is used to describe the soil material behavior. The Mohr-Coulomb criterion relates the shear strength of the material to the cohesion, normal stress and angle of internal friction of the material. The failure surface of the material has been already presented and is given by the equation (63). For Mohr-Coulomb material model, six material properties are required. These properties are:

- The friction angle ϕ
- Cohesion C
- Dilation angle ψ
- Young's modulus E
- Poisson's ratio ν
- Unit weight of soil γ

Young's modulus and Poisson's ratio have a important influence on the computed deformations prior to slope failure, but they have little influence on the predicted factor of safety in slope stability analysis. Dilation angle ψ affects directly the volume change during soil yielding. If $\psi=\phi$ the plasticity flow rule is known as "associated", and if $\psi\neq\phi$ non-associated plastic flow rule is assumed. The change in the volume during the failure is taken into account through the coefficient ψ .

12.1.3 Slope collapse

Non-convergence within a user-specified number of iterations in finite element program is taken as a suitable indicator of slope failure and is joined by an increase in the displacements. Usually the value of the maximum nodal displacement just after slope failure has a big jump compared to the one before failure.

12.1.4 Computational example

The problem to be analyzed is a slope of Mohr-Coulomb material subjected to gravity loading. The factor of safety (FOS) of the slope is to be assessed, and this quantity is defined as the proportion by which friction angle and cohesion must be reduced in order to cause failure with the gravity loading held constant. Figure 52 shows the data for an analysis of a homogenous slope with the following material properties given in Table 5. The change in the volume during the failure is not considered in this study and therefore the dilation angle ψ is taken as zero.

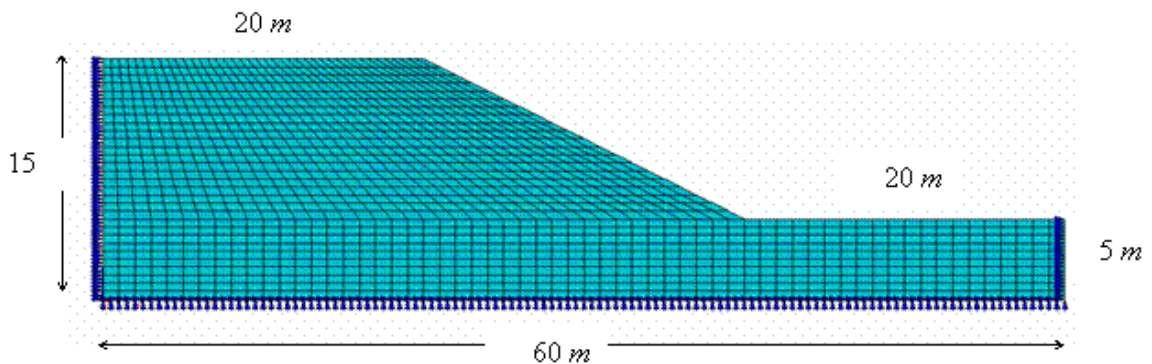


Fig. 52. Mesh and data for slope-stability example.

Table 5. Material properties

E [kN/m ²]	ν	γ [kN/m ³]	ϕ [degree]	C [kN/m ²]	ψ [degree]
1×10^5	0.3	20	20	15	0

Gravity load is applied to the model and the strength reduction factor (SRF) gradually increased affecting the equation (104) until convergence could not be achieved.

The output in Table 6 gives the strength reduction factors and the associated maximum nodal displacement at convergence, and the number of iterations to achieve convergence.

Table 6. Summarized results of slope stability analysis.

SRF	Number of iterations	Maximum displacement [cm]	Convergence
1	10	1.710982	OK
1.1	13	1.789119	OK
1.2	17	1.889358	OK
1.3	22	1.996587	OK
1.4	35	2.116528	OK

1.5	82	2.29019	OK
1.6	600	4.118373	FAILED

It can be seen that when *SRF* factor is equal with 1.6 the iteration ceiling of 600 was reached. Figure 53 shows a plot of these results and it can be seen that the displacements increase rapidly at this level of strength reduction, indicating a factor of safety of about 1.6. Bishop and Morgenstern charts give a factor of safety of 1.593 for the slope under consideration. Figure 54 shows the deformed mesh and displacement vectors corresponding to slope failure; the mechanism of failure is clearly shown to be of the "toe" type.

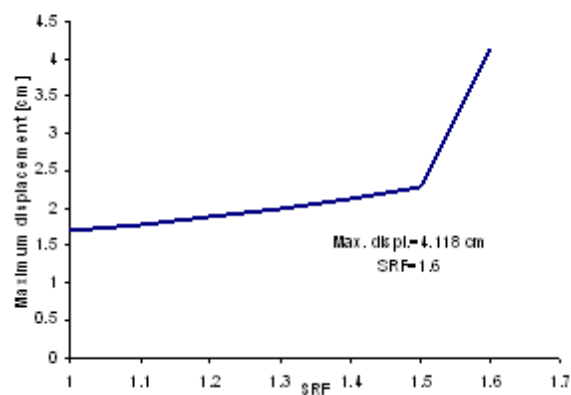


Fig. 53. Maximum displacement versus Strength Reduction Factor.

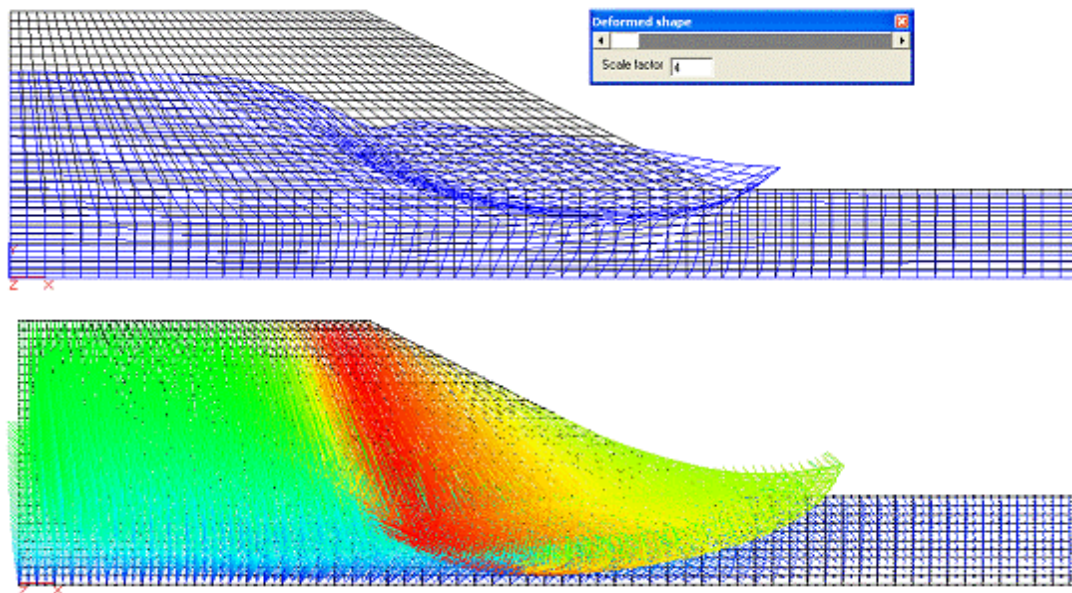


Fig. 54. Deformed mesh and displacement vectors at failure.

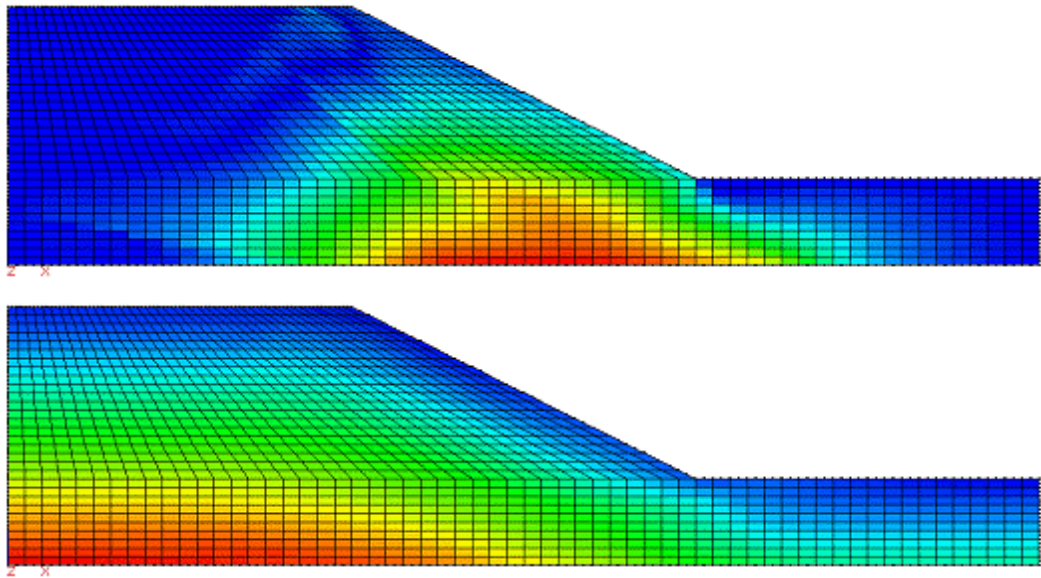


Fig. 55. Maximum Shear Stresses and Von-Misses Stresses.

12.2 Bearing capacity analysis

Plane strain conditions are enforced and in order to monitor the elasto-plastic behavior, the loads are increased incrementally until the collapse occur. The method uses constant stiffness iterations, thus the relatively time consuming stiffness matrix factorization process is called just once, while the backward substitution phase is called at each iteration. Several failure criteria have been implemented for representing the strength of soils as engineering materials. For soils with both frictional and cohesive components of shear strength *Mohr-Coulomb* failure criteria is appropriate. For undrained clays, which behave in a "frictionless" manner, *Von-Misses* failure criteria may be used.

The example shown in Figure 56 is of a flexible strip footing at the surface of a layer of uniform undrained clay. The footing supports a uniform stress q , which is increased incrementally to failure. The elasto-plastic soil is described by the Von-Misses failure criteria and is described by three parameters, namely the undrained "cohesion" c_u , followed by the elastic properties E and ν . The loads in this case are the nodal forces which would deliver a uniform stress of 1kN/m^2 ($q=1\text{kN/m}^2$)

across the footing semi-width of 2 m.

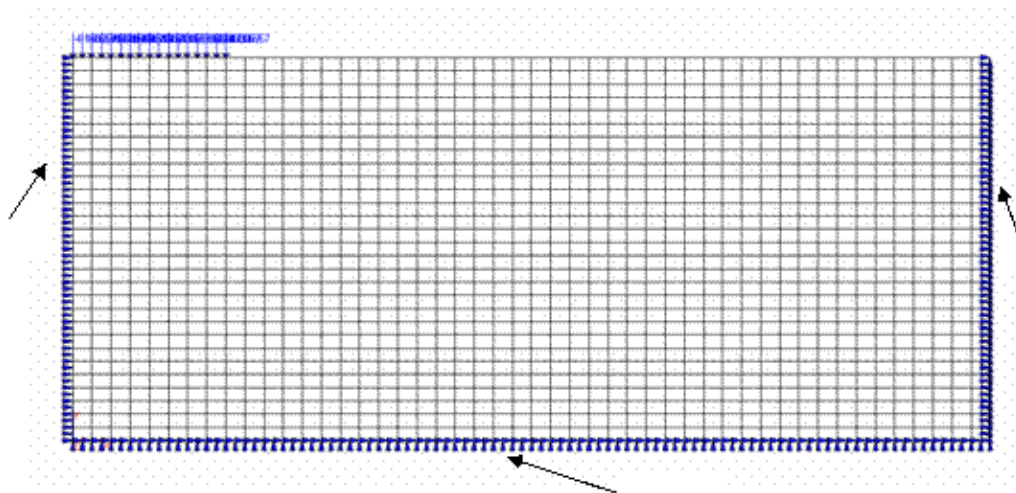


Fig.56. Mesh and data for bearing capacity example.



Fig.57. Nodal forces

Table 7. Material properties

E [kN/m ²]	v	C_u [kN/m ²]
1x10 ⁵	0.3	100

Table 8. Summarized results of bearing capacity analysis.

Applied load factor	Number of iterations	Convergence
0.2	2	OK
0.8	2	OK

1.0	2	OK
2.0	2	OK
2.8	17	OK
3.0	26	OK
3.6	41	OK
4.0	50	OK
4.4	66	OK
5.0	123	OK
5.2	300	FAILED

Figure 58 show the deformed mesh and displacement vector corresponding to unconverged solution at collapse.

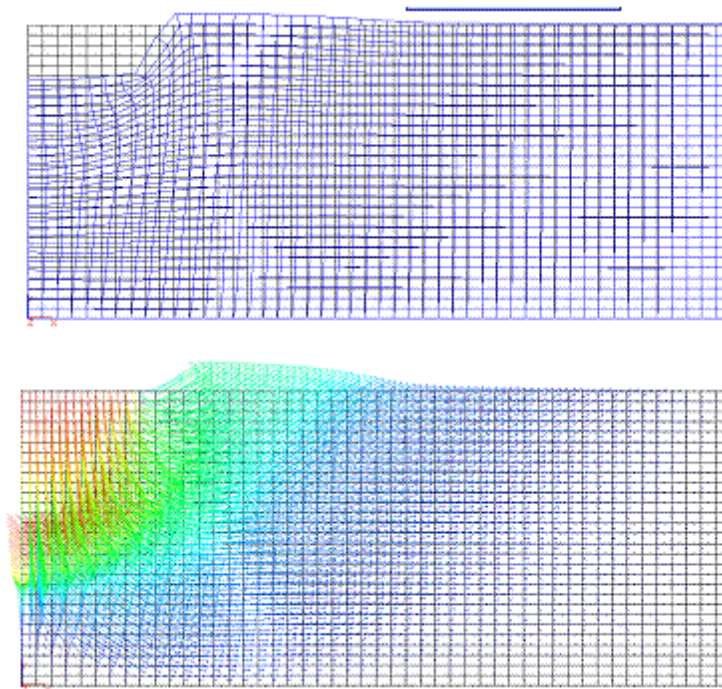


Fig. 58. Deformed mesh and displacement vectors at failure.

These loads are "factorized" by the increasing load factors from 0.1 till ultimate load factor corresponding to collapse. At load levels below failure convergence should occur in relatively few iterations. As failure is approached the algorithm has to work harder and requires more iterations to convergence. The output in Table 8 gives the applied load factors and the associated and the number of iterations to achieve convergence.

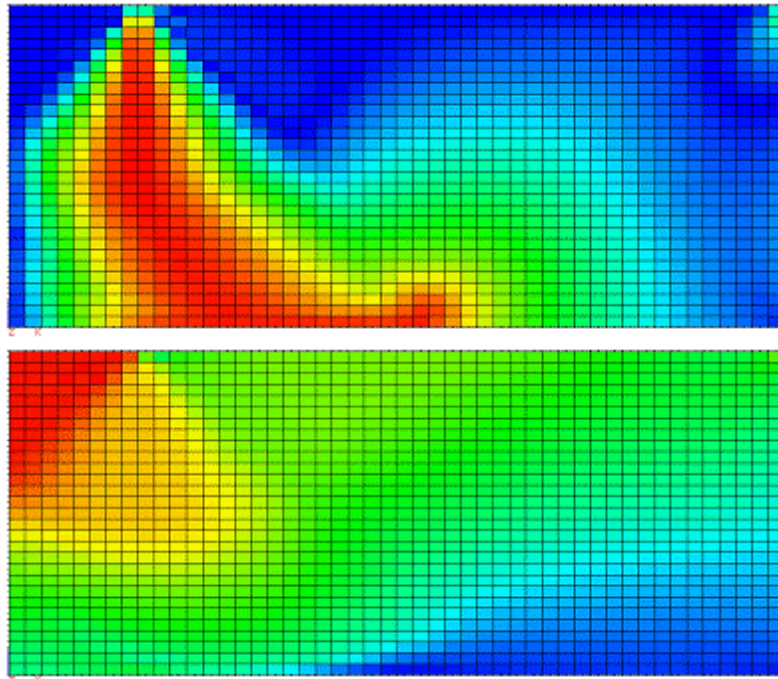


Fig.59. Maximum Shear Stresses and Sigma-X Stresses at failure.

12.3 Staged construction analysis

GFAS allows to construct complex geometries and analysis can be runned in different stages associated to different phases of construction. During the Staged construction analysis, the loads are increased from 0 to 1. As soon as the load parameter reaches the value of 1.0, the constructions stage is completed and the analysis of the current phase is completed, and go the the next phase of the construction. If a staged construction calculations finishes while the load factor is smaller than 1.0, the program will stop the analysis. The most likely reason for not finishing a construction stage is that a failure mechanism has occurred.

Table 9. Staged construction. Geometry and stages.

Stage 1	Stage 2
---------	---------

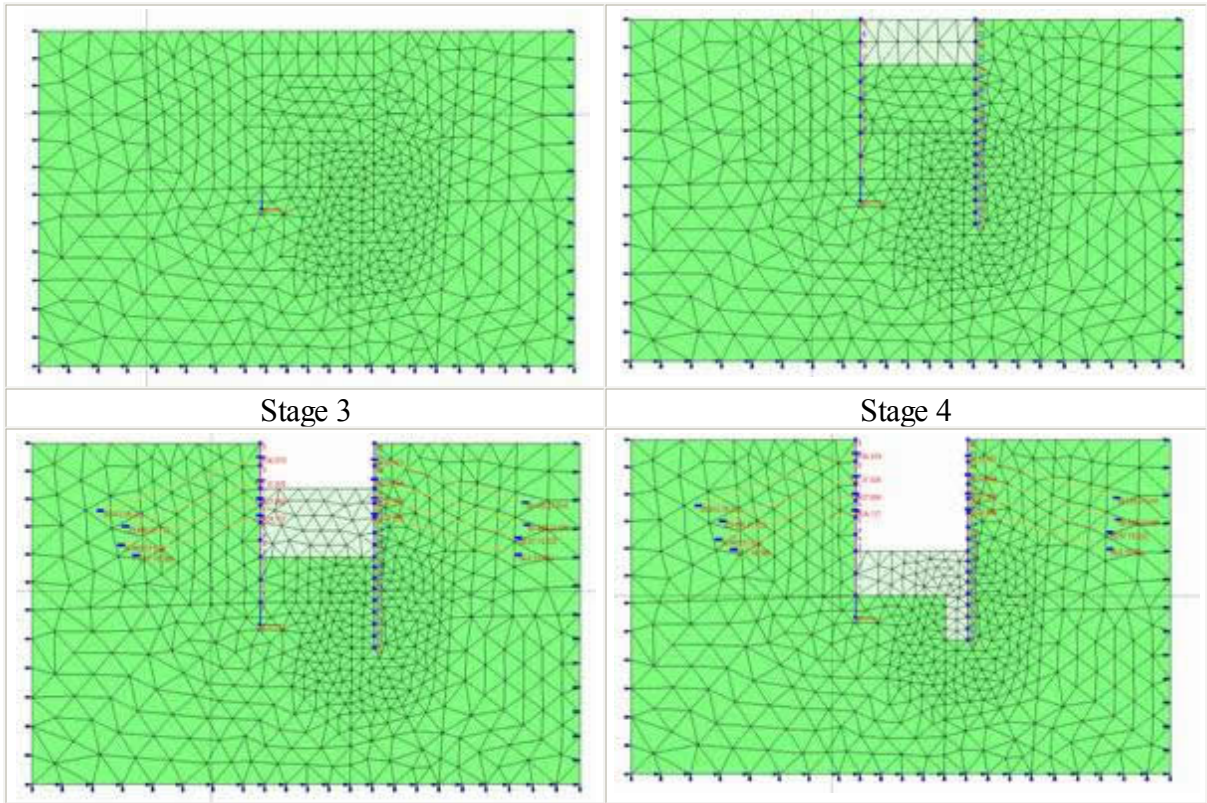
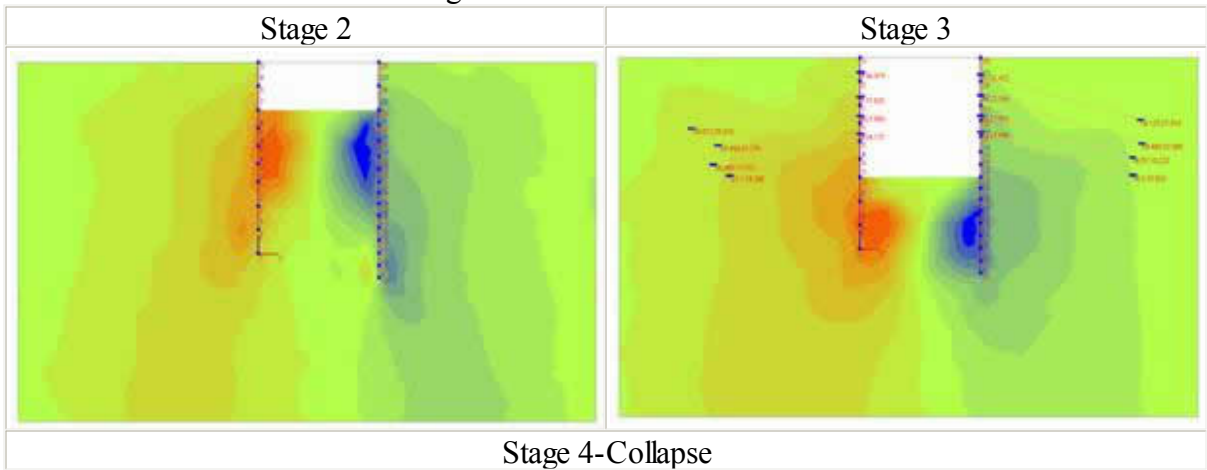
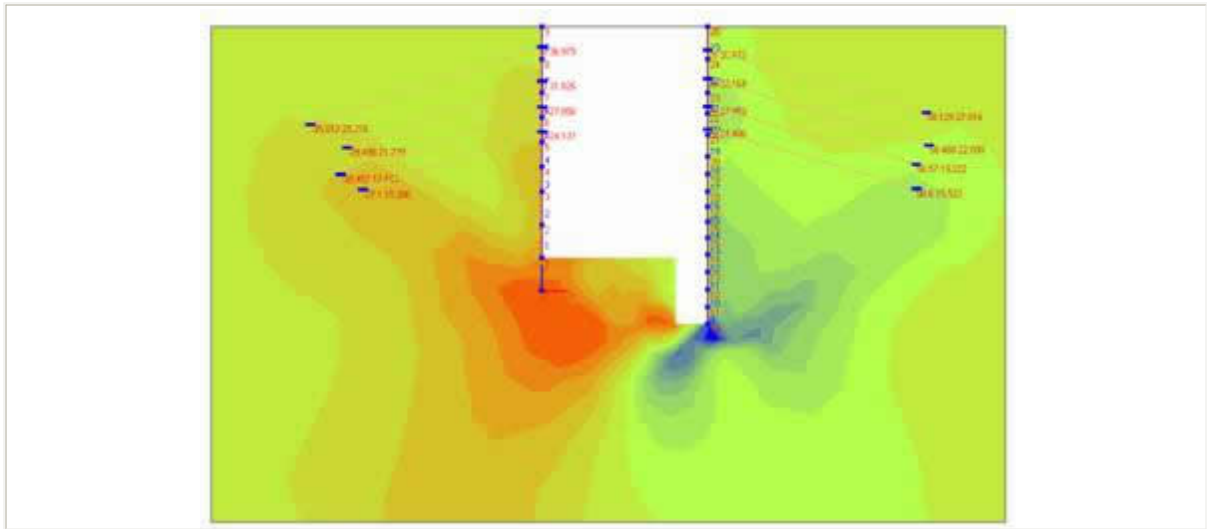


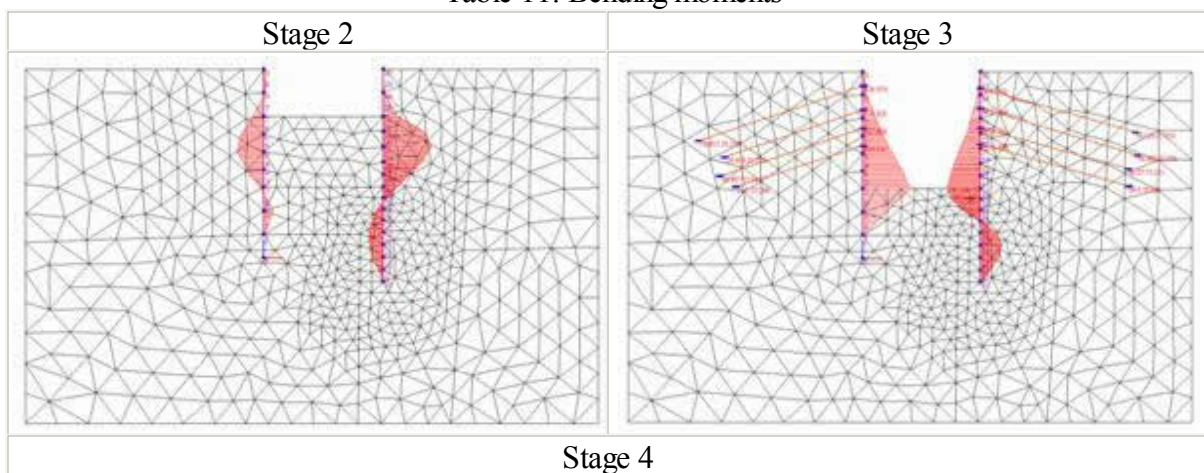
Table 10. Staged construction. Results: Shear stresses





The computational example presented here describe an open excavation constructed in four stages. During the excavation process the soil is reinforced with walls and anchors as can be seen in table 9. The soil is modeled using the Mohr-Coulomb failure criteria and the elasto-plastic behavior is assumed for anchors. Only the gravitational loads and the excavation loads are taken into account during the construction process. Table 10 shows the distribution of the shear stresses for the stages 2 to 4 whereas in table 11 are depicted for each stage the variation of the bending moments in the walls. The collapse of the construction occurs at stage 4 as it can be seen on the Load-displacement graph depicted in Fig. 60. The deformation configuration at collapse of the construction is depicted in Fig. 61. At this stage also the anchors failed as it can be seen in Table 12.

Table 11. Bending moments



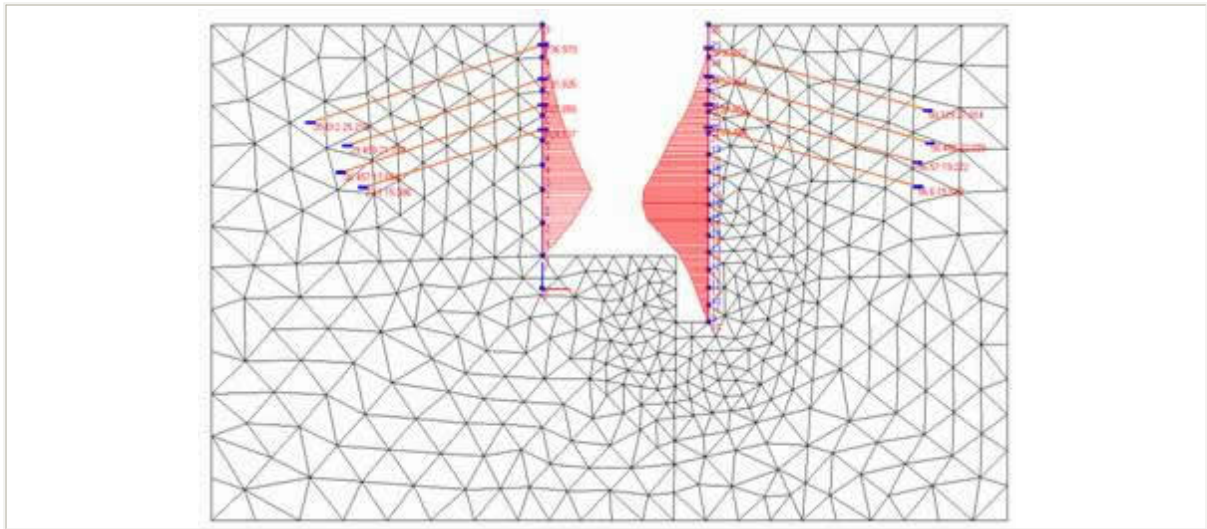
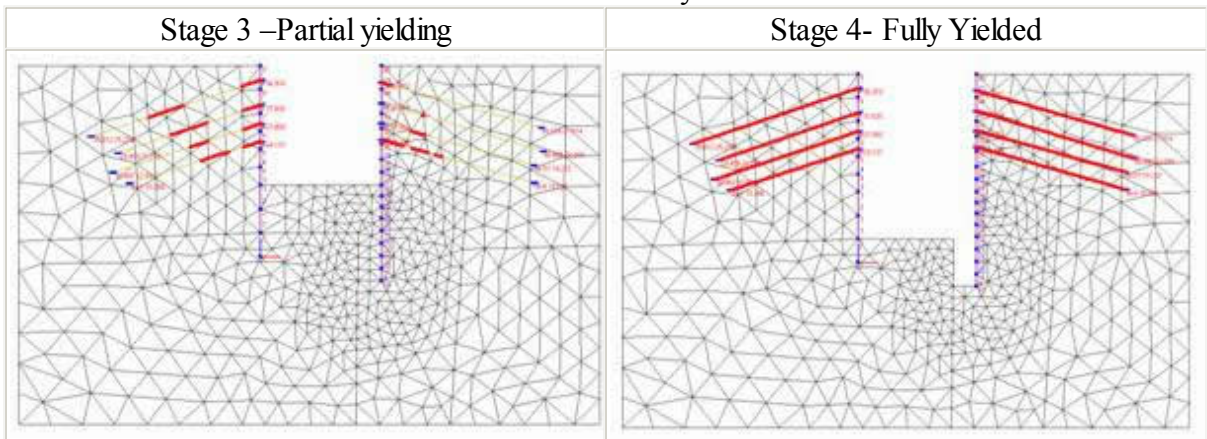


Table 12. Anchors yielded



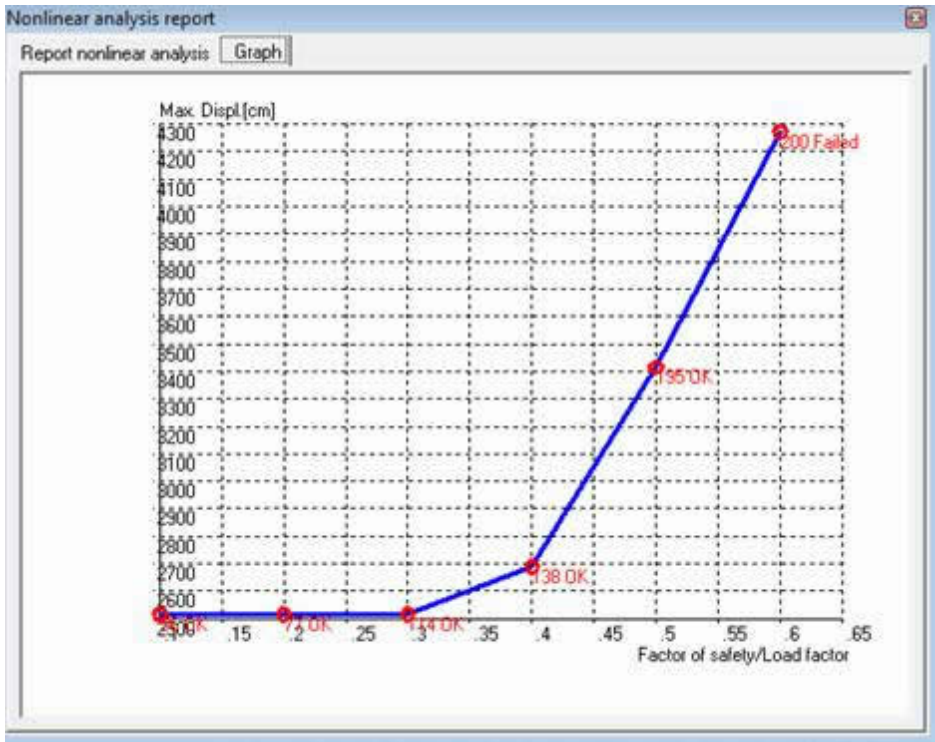


Fig. 60

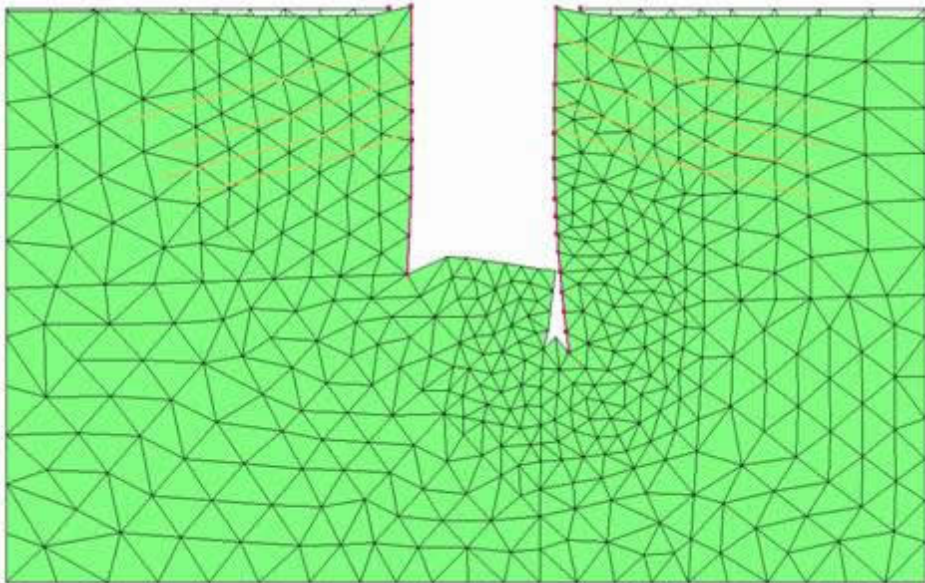


Fig.61. Deformed configuration at collapse.

13 Bibliography

1. Smith, I.M., Griffiths, D.V., *Programming the Finite Element Method*, John Wiley & Sons, 2004.
2. Akin, J.E., *Finite Element Analysis with Error Estimators*, Elsevier, 2005.
3. Zienkiewicz, O.C., Taylor, R.L., *The Finite Element Method*, McGraw-Hill, 2000.
4. Cook, R.D, Malkus, D.S., Plesha, M.E., *Concepts and Applications of Finite Element Analysis*, John Wiley & Sons, 1996.

14 Contact

GeoStru Software

Via Lungomare snc
89032 - Bianco (RC) - Italy
Tel. +39 0964911624 Fax. +39 0964992341

Skype Nick: [geostru_support_it-eng-spa](#)

Web: www.geostru.com

E-mail: geostru@geostru.com